Vehicle Dynamics Performance Optimization of a New Generation Multi-Axle Truck

A thesis submitted in partial fulfilment of the requirement for the award of the degree of

Master of Engineering

in

Thermal Engineering

Submitted by

Rishi Shah
Registration No. 801783011

Under the Supervision of

Dr. Gautam Setia
(Assistant Professor, Mechanical Engineering Department)

Dr. Devender Kumar
(Assistant Professor, Mechanical Engineering Department)

&

Mr. Amit Gupta
(General Manager, Vehicle Integration (MHCV), ERC, Tata Motors Ltd., Pune)

Department of Mechanical Engineering
Thapar Institute of Engineering & Technology, Patiala, Punjab
(Deemed to be University)
June, 2019

CERTIFICATION

This is to certify that the work down in this thesis title **"Vehicle Dynamics Performance Optimization of a New Generation Multi-Axle Truck"** submitted in partial fulfillment of requirement for the award of Master of Engineering Degree in Thermal Engineering in the Mechanical Engineering Department of Thapar Institute of Engineering & Technology, is an authentic record of work carried out by me under the guidance of **Dr. Gautam Setia,** Assistant Professor, Mechanical Engineering Department, Thapar Institute of Engineering & Technology, Patiala, **Dr. Devender Kumar,** Assistant Professor, Mechanical Engineering Department, Thapar Institute of Engineering & Technology, Patiala, and **Mr. Amit Gupta,** General Manager, Vehicle Integration, MHCV, ERC, Tata Motors Ltd., Pune. The matter embodied in this report has not been submitted in any part or full to any university or institute for the award of any degree.

Date: 28.05.2019

Rishi Shah
Roll No. 801783011

This is to certify that above declaration made by the student concerned is correct to the best of my knowledge & belief.

Amit Gupta
General Manager - M&HCV
Engineering Research Centre
TATA Motors Limited

Date: 28.05.2019

Amit Gupta
General Manager, VIG-MHCV,
ERC, Tata Motors Ltd.,
Pune, Maharashtra.

Date: 18/06/19

Dr. Gautam Setia
Assistant Professor, MED,
T.I.E.T., Patiala, Punjab.

Date: 18-06-19

Dr. Devender Kumar
Assistant Professor, MED,
T.I.E.T., Patiala, Punjab.

ABSTRACT

The main objective of this thesis work is to study the vehicle dynamics of a new generation heavy-duty commercial vehicle i.e. Truck by optimizing steering and suspension kinematics characteristics of the vehicle. Initial stage of present project was to define the problem so that critical attention could be paid on important points. Due to implementation of Increased Axle Load (IAL) regulation, major changes in the design of steering and suspension system is required to be made. Simulations were carried out based on existing suspension and steering system hardpoints. It was found that for the new vehicle development, improvements have to be made in the suspension and steering kinematics linkages in order to meet defined target values of brake steer, bump steer, Ackerman error, pitman arm & drag link toggle, caster & camber change with wheel travel etc. in order to fulfill drivers expectations of ride and comfort. In second step, model of front suspension and steering system is created in ADAMS/View and using rule of thumb improvements and sensitivity analysis method, number of hardpoints is decreased which are then used to optimize its linkages. In next step, vehicle handling behavior is studied in ADAMS/Car where full vehicle model is made and constant circular test is done. New design is released on the basis of hardpoints obtained from the optimization study. Prototype vehicle is made and various physical tests are performed whose results are compared with the results obtained through simulations. Results are in good agreement with the simulated results and shows that there is significant improvement on the steering performance of the vehicle. Some of the major other problems which were not identified during simulations but appeared on prototype vehicle were identified and their corrective actions without bringing any changes in steering or suspension linkages are proposed. Steer by brake technique didn't solve the problem completely. Use of electronic control of lift axle helped in achieving TCD target. Concept of caster steer axle was evaluated through simulation in ADAMS/Car. It is proposed that the vehicles highly understeer behavior and problem of not meeting TCD requirement will be resolved using caster steer lift axle instead of non-steerable lift axle.

ACKNOWLEDGEMENT

I would like to specially acknowledge and extent my heartfelt gratitude to all those who have helped me in completion of this thesis. I especially would like to thank **Mr. Amit Gupta,** General Manager, Vehicle Integration-MHCV, Tata Motors Ltd., **Dr. Gautam Setia,** Assistant Professor, MED, T.I.E.T. & **Dr. Devender Kumar,** Assistant Professor, MED, T.I.E.T. for their full support and guidance.

Furthermore, I am grateful to **Mr. Santosh Kumar,** Senior Manager, Vehicle Integration, Tata Motors Ltd. & **Mr. Vrushabh Sahare**, Senior Manager, CoC-Driveline Integration, Tata Motors Ltd. for their support at every step. I would also like to thank my parents for their years of love, support and encouragement in every step of my life. They have always wanted the best for me and I admire their determination and sacrifice. Besides, I would like to gratefully acknowledge my institute i.e**. Thapar Institute of Engineering & Technology** & I would also like to acknowledge **Tata Motors Ltd.** for providing the best platform for research.

Last but not the least; I would like to thank the God for all their good benevolence.

DATE: 28/05/2019

(Rishi Shah)
M.E. (Thermal)
(801783011)

TABLE OF CONTENTS

Page No.

LIST OF FIGURES

Page No.

LIST OF TABLES

Page No.

NOMENCLATURE

Symbols

$C_{i,0}$	Nominal side force coefficient on i^{th} axle [KN/*rad*]
N*i*	Actual normal load on i^{th} axle [KN]
l	Geometric wheelbase [m]
t	Tandem spread [m]
d	Distance between 2nd axle and 3rd axle [m]
g	Acceleration due to gravity [ms^{-2}]
δ	Steering angle [*deg*]

Subscripts

deg	Degree
deg/m	Degree/meter
Frt	Front
Lft	Left
Rgt	Right
Stg	Steering
ip	Input
Latac	Lateral acceleration
Max.	Maximum
a_{req}	Required/desired acceleration

Abbreviations

VD	Vehicle Dynamics
HMI	Human Machine Interface
TASE	Thermal Aerodynamics & System Engineering
NVH	Noise, Vibration & Harshness
IAL	Increased Axle Load
MoRTH	Ministry of Road Transportation & Highway
3D	Three Dimensional
CAD	Computer Aided Drawing
ARAI	Automotive Research Association of India
DMU	Digital Mock-Up

ADAMS	Automatic Dynamics Analysis of Mechanical Systems
MBD	Multi-Body Dynamics
ARB	Anti-Roll Bar
ECU	Electronic Control Unit
TCD	Turning Circle Diameter
SUV	Sport Utility Vehicle
SAI	Angle Inclination
RH/LH	Right Hand/Left Hand
HCV	Heavy Commercial Vehicle
PADL	Pitman Arm-Drag Link
U-Joints	Universal Joints
NVD	New Vehicle Development
C.G.	Centre of Gravity
GB	Gear Box
BJ	Ball Joint
SPCD	Spring Points Center Distance
HWA/SWA	Hand Wheel Angle/Steering Wheel Angle
DVG	Desired Value Generator
PID	Proportional-Integral-Derivative
LQG	Linear Quadratic Generator
TDU	Torque Distribution Unit
ATC	Automatic Traction Controller
PED	Performance, Economic & Drivability
ATC	Automatic Traction Control

CHAPTER 1

ORIGIN OF DISSERTATION PROPOSAL

INTRODUCTION

The project entitled, **"Vehicle Dynamics Performance Optimization of a New Generation Multi-Axle Truck"** basically focuses on the study of vehicle dynamics of a new concept vehicle and its development process to make it market ready for production by reducing time-to-market. During the development of any new vehicle, some of the critical parameters that have to be evaluated are highlighted below:

1. Weight Distribution & Payload,
2. Vehicle Dynamics (VD),
3. Durability,
4. Thermal, Aerodynamics & System Engineering (TASE),
5. Vehicle NVH & Sound Quality,
6. Performance, Economic & Drivability,
7. Utility & Usage,
8. Safety & Security,
9. Vehicle HMI & Audio-Visual Performance,
10. Mileage Accumulation etc.

In order to minimize the number of unique components in the development of concept vehicle, reduction in development lead time and minimize physical test iterations, modular design principle is followed. Maximum possible off the shelf proven components has been used which resulted in minimizing cost and design and validation time saving.

1.1 Current Scenario

Before the implementation of Increased axle load (IAL) regulation on 16th July, 2018 by Ministry of Road Transport and Highways (MoRTH), the maximum safe axle weight on single axle with four tires was 10.2 tonnes. MoRTH issued S.O. 3467 (E) in supersession of S.O. 728 (E), dated 18th October, 1996 & further amended S.O. 3467 (E) on 6th August 2018 issuing a notification S.O. 3881 (E) based on which the maximum safe axle weight on single axle with four tires is revised to 11.5 tonnes with the provision of 1 tonne extra load if it is fitted with pneumatic suspension[1]. Therefore, a concept of developing single axle having four tires with pneumatic suspension came into the importance in the automobile industry of India.

Table 1.1: Maximum safe axle weight limit in India [1]

Sr. No.	Axle Type	Maximum Safe Axle Weight
1.	Single Axle	
1.1	Single Axle with single Tyre	3.0 tonnes
1.2	Single Axle with two Tyres	7.0 tonnes**
1.3	Single Axle with four Tyres	11.5* tonnes
2.	Tandem axles (Two axles) (where the distance between two axles is less than 1.8 m)	
2.1	Tandem axle for rigid vehicles, trailers and semi-trailers	21 tonnes*
2.2	Tandem axle for Puller tractors for hydraulic and pneumatic trailers	28.5 tonnes
3.	Tri-axles (Three axles) (where the distance between outer axles is less than 3 m)	
3.1	Tri-axle for rigid vehicles, trailers and semi-trailers:	27 tonnes*
4.	Axle Row (two axles with four Tyres each) in Modular Hydraulic Trailers (9 tonnes load shall be permissible for single axle)	18 tonnes

* Note: If the vehicle is fitted with pneumatic suspension, 1 tonne extra load is permitted for each axle.

1.2 Motivation

The competition in automotive industries has increased with time. With the increasing demand of the customer and less availability of time it has become very difficult for the industry to provide the new vehicle based on the customer requirements in the short duration as different tests mentioned earlier above have to be performed on the vehicle prototype vehicle (proto vehicle) before freezing the final design and configuration of the vehicle for automating it in the production. Therefore, the use of multi-body simulation software has played a vital role in saving time and money of the industry. Simulation of the 3D model predicts the critical problems that may arise and thus saves time and money. With the implementation of Increased Axle Load (IAL) regulation in mid of July, 2018, the major changes in the design of axle, suspension, steering system, driveline integration, load body design etc. have been made which has direct effect on the vehicle dynamics behavior of the vehicle. Thus, vehicle dynamics performance evaluation to meet the Automotive Research Association of India (ARAI) norms is important in which mainly steering, brakes, tire & ride of the vehicle will be evaluated under vehicle dynamics test.

Improper steering design leads driver to continuously correct steering input for running the vehicle in straight ahead direction which is a handling issue. Bump & brake steer are the parameters that plays key role in handling of vehicle in uneven road. Steering design optimization will lead to better comfortable riding and eliminates the chances of accidents in

uneven roads or during breaking. Therefore, the above title for the project is proposed where the focus will be on vehicle dynamics performance evaluation.

1.3 Objectives

"Vehicle Dynamics Performance Optimization of a New Generation Multi-Axle Truck", has two major aspects to be focused on. First is the development of new concept vehicle (8X2 rigid truck with four tires lift axle) & secondly vehicle dynamics analysis of the new concept vehicle. Study of vehicle dynamics will be done in two ways: one with analysis of 3D model of vehicle in software (simulation) & secondly with experimental trials on vehicle prototype. The main objectives of this project are highlighted below:

i. Creating a virtual prototype of the vehicle (Digital Mock Up) in order to check the aggregates packaging feasibility.
ii. Steering system & suspension system optimization using ADAMS/View (a Multibody Dynamic Analysis Software) in order to provide appropriate controlling of vehicle.
iii. Simulation of full vehicle model in ADAMS/Car (a Multibody Dynamic Analysis Software) for handling trials to check whether the actual prototype which will be made will meet defined standard target result of handling trials.
iv. Testing of real proto vehicle in actual environmental condition.
v. Difficulty/Issues identified on prototype vehicle and working out solution for it.
vi. Comparison of simulated results with actual test results.

1.4 Rewards

Rewards/Benefits that are associated with this project are mentioned below:

i. This new vehicle concept will provide the provision of higher payload than the existing vehicle of same configuration. Thus, it will help to attract the customers who always prefer to invest in the vehicle which provides higher payload.
ii. Optimization of the steering system will help in reducing chances of accidents by minimizing unwanted steer of the vehicle during braking and bump.
iii. Cost & lead time for design and development of the prototype will be reduced by cutting down time & expenses of improper designed part.

iv. It has higher roll stiffness lift axle due to stiff pivot bushing which results in lower roll gradient. Thereby, eliminates the need of anti-roll bar (ARB) which cut down the cost.

v. In unloaded condition it will provide the better fuel economy compared to the existing same configuration vehicle without lift axle.

vi. During sharp turning since the truck length being long and it has single steerable front axle, use of lift axle with electronic control logic will prevent excessive wear of tires at lift axle by lifting and dropping it based on logic feed in ECU.

1.5 Risk Elements

Similarly, the risk elements of the project are

i. Under lift axle grounded, the load distribution is uniform and within the permissible range but sometimes in unfavorable conditions like puncture in lift axle tire, it may lead the driver to run the vehicle by lifting up lift axle in loaded condition. Under that situation, all the loads will be distributed among front and rear axle which will lead design challenges for chassis, suspensions, steering and axles.

ii. Since only one drive axle (rear axle) will be there thus traction provided might be less as compared to 8X4 vehicle. Hence, driving will be difficult during off road condition.

iii. Generally, for longer vehicle having multiple axles, twin steering system is used which provides better turning of the vehicle. Use of single front steerable axle will provide design challenges for steering team in meeting TCD norms of ARAI.

iv. The design of the frame should be paid special attention during designing for standing abuse loading conditions.

1.6 Project Location

This is an industrial project which was done at Tata Motors Ltd., Pune & Jamshedpur Plant. Virtual 3D model of full vehicle (DMU) was made in Creo Parametric 3.0, modeling and simulations was done using ADAMS software at Engineering Research Centre, Pune while the actual prototype and real vehicle testing was carried out in Jamshedpur plant.

CHAPTER 2
LITERATURE REVIEW

Various studies on vehicle dynamics were made in the past by many researchers. Present chapter reviews various published literatures of the researchers which puts foundation for our present work. Literature reviews provide a better understanding about the technical aspects of our topic, gap finding, latest technologies being used etc. and therefore works as a guideline for the thesis. The main focus of study is the vehicle dynamics performance optimization of a new concept vehicle being developed. Investigations has mostly been on the technique to optimize steering linkages in order to have better steering performance[2]–[11]. Work to achieve better handling characteristics has also been focused[12]–[18]. Better steering performance depends on the optimized value of break steer, bump steer, Ackerman error, toggle between pitman arm and drag link ball joint etc. while better handling depends on the slip angles of different tires, linear roll gradient and hand wheel angle gradient. Steering system with brake steer value less than 10 deg, bump steer less than 0.5 deg/m is said to be an optimized steering system (acceptable criteria of the steering system design in our thesis). Lesser the value better is the steering system performance. Packaging constraint is one of the key factor on which design of the steering system is dependent[5], [6]. Similarly, the use of auxiliary axles in between front and rear axle has its own effect on the handling behavior depending on whether the auxiliary axles are steerable, self-steerable or non-steerable[16]–[19]. Making non-steerable axle a caster steer axle, the handling behavior changes and vehicle becomes lesser understeer. Some of the papers that has been referred in the present thesis has been highlighted below:

Simple cost-effective method to evaluate brake and bump steer of the vehicle has been proposed in which using the values obtained after outdoor testing of a vehicle and the values obtained through simulation using ADAMS, a correlation has been developed[2]. Proposed method in by the author helps in providing quick investigation of vehicle system and also provides a best solution with minimum number of iterations.

The effect of wheel geometry parameters of a SUV on vehicle steering has been studied by some authors where a vehicle model was made and simulations was carried in ADAMS/Car that provided following below mentioned conclusions[3]. Increasing positive caster angle improves

returnability of steering wheel and increases steering effort while negative caster improves steering effort but causes wheel wandering. SAI improves both steering effort and steering wheel returnability. Similarly, positive camber increases vehicle tendency of understeering and negative camber enables sharp cornering. Toe-in angle increase promotes better straight-line stability of a vehicle while toe out increase promotes cornerability. Negative scrub radius provides lesser steering disturbance with a stabilizing effect.

One of the author studied the method for reducing the vehicle drift keeping in the mind the packaging constraints of the vehicle[4]. The vehicle was modelled in ADAMS and an analysis for brake and bump steer in a multi body dynamics (MBD) environment was performed considering an actual vehicle data. Different steering linkages concept for vehicle drift were proposed and using Pugh concept selection these concepts were evaluated. Finally, he proposed that for brake and bump steer, drag link ball joint plays a key role.

The effects of variation of length of tie rod on bump steer has been studied by the authors where it is concluded that when tie rod length is varied it will have an effect on bump steer as it will affect both on toe and camber of the vehicle[5]. An ideal steering system design to get zero bump steer was created. Tie rod length was varied by 5% & 10% where for 5% variation the result showed that the bump steer was lower and also have lesser steer assist within the acceptable range while for 10% variation both steer assist and bump steer was at higher.

One author modeled the front suspension and steering system in ADAMS and analyzed the bump and brake steer of the vehicle[6]. The simulated result was very closely related with the subjective results which provides inference that the simulated result could be trusted. Using various optimized concept, the vehicle steering and suspension system was optimized for brake and bump steer where steering arm and pitman draglink ball joint hardpoint is identified as the key hardpoint that must be taken care of during optimization.

Optimization technique using ADAMS/Car for off-road vehicle was studied by the authors[7]. According to which suspension hardpoint optimization should be given priority was proposed. Various effect of wheel travel on vehicle kinematics such as camber angle, caster angle, toe angle, roll & center has been presented.

One of the author also studied and analyzed the probable reasons for a vehicle drift when the brakes are applied using a simple unique methodology[8]. Problematic commercial vehicle was chosen and a methodology using which they tried to approach the solution was discussed. Conferring about the root sources of brake steer an improvement on the problematic vehicle was made where by bringing about changes in the kinematic hardpoints of steering and suspension linkages, brake steer problem was minimized. They used MBD simulation to reduce brake steer by matching draglink path with axle path during braking and suggested final changes in the kinematic hardpoints of suspension and steering system.

Leaf spring windup and brake steer has been thoroughly studied and the authors have provided the testing methodology with consideration and testing being thoroughly explained[9]. Detailed explanation has been made regarding things to be done to reduce brake steer as well as its worse effects. When steering arm ball joint is in line with center of rotation of spring windup this avoids movement of drag link and prevents brake steer. To avoid spring wind off he suggested to place damper 100mm offset in front of spring. Suspension stiffness increase will reduce brake steer. Other additional devices can also be used to reduce brake steer such as use of ABS technology, providing bell crank mechanism at spring end etc.

A method to estimate and reduce brake pulling of vehicles due to difference in force at Right Hand (RH) and Left Hand (LH) side during straight ahead braking has been explained in previous research[10]. A mathematically model has been developed which estimates amount of brake pulling. Brake pulling taking place, during bump and brake steer, due to spring wind off has been considered. When pulling due to brake and bump steer takes place in same direction as pulling due to difference in brake force, then vehicle deviation is more and vice versa. The model also helps in the identification of most sensitive parameters which results in brake pulling and thereby helps in its optimization.

One researcher also applied his systems concept in order to interrelate his knowledge of steering and vehicle development and design of a CV steering system[11]. It explains CV power and manual steering system design and development. It discusses with an interrelationship of tires, cab package and front suspension on truck steering system. It provides comprehensive knowledge of a steering system of truck starting from the steering wheel to road wheel.

Authors have also studied vehicle dynamics of a 6x2 HCV using MSC TruckSim and SuspensionSim that focused on building full vehicle model to examine its dynamic behavior using MBS methods[12]. Suspension was modelled using SuspensionSim and result from it was feed into TruckSim for full vehicle modeling. Simulations for different speed during double lane change was done and results obtained from the simulation of modelled vehicle were presented.

How simulation can be used for evaluating concept vehicle during its development has been studied by few researchers where a 9 tons 4x2 vehicle (rigid truck) has been used to perform smooth bump (15km/h), constant speed (60km/h), steep steer (45 km/h) and double lane change (60 km/h) test for evaluating selection of antiroll bars (from two different sets of front and four different sets of rear) and dampers (from three different sets) [13]. Based on simulations, shock absorbers with low vertical acceleration response and better damping energy were chosen while considering safety antiroll bar was selected.

The authors have also studied non-linear MBD model of a 3 axle HCV tractor unit for rollover stability[14]. A constant radius test showing vehicle understeer behavior and single lane change showing vehicle transient behavior were evaluated. Constant radius test predicted the value of critical lateral acceleration where rollover could take place while unstable behavior has been predicted in single lane change simulation.

A method has been proposed by an author which states equivalent action of tandem axle bogie can be achieved using single equivalent axle placed midway between tandem spread with an assumption that shared load is equal between tandem axles and the cornering stiffness of all the tires being same[15].

Earlier work has extended two axle bicycle model to three axle model by bringing minor changes in convention[16]**,** [17]. A generalized model has been developed which produces dynamic equation of motion having arbitrary number of non-steerable and steerable axles. Understeer and equivalent wheelbase expression to state vehicle handling behavior for any arbitrary vehicle configurations has been derived.

Handling behavior of the vehicle with and without steerable auxiliary axle and its comparison has been made which explains how a caster steer axles will be affecting the understeer behavior and equivalent wheelbase for a three-axle vehicle[18]. For 2nd axle caster steered, effective as

wheelbase will be defined by distance between first and last axle while for 3rd axle caster steered effective wheelbase will be decreased. Making non-steerable axle a caster steer axle, the handling behavior changes and vehicle becomes lesser understeer.

It is also very important to study the effect of tire wear in non-steerable lift axle having twin tire on each side of the axle[19]. First identification of the operating zone taking into consideration where tire wear is maximum and then an attempt to reduce tire wear was made. Comparison between new designs of non-steerable lift axle is made with self-steerable lift axle. Tire wear in self-steerable lift axle was found lesser but non-steerable lift axle at high helps in countering centrifugal force making vehicle design more yaw stable. Alternatives to reduce tire lateral scuffing is also explained.

Whole kinematics, design and analysis of lifting mechanism of dual tire lift axle having 10T load carrying capacity has been studied[20]. Design of lower mounting bracket and control arm has been focused for less packaging value so that higher load carrying capacity at varying loading conditions can be achieved. It explains lifting mechanism so as to improve vehicle performance.

One author has also studied the method to reduce turning center diameter of a commercial vehicle without bringing any changes in the vehicle geometry[21]. It explained a method where braking system and steering system works in synchronization in order to improve turn ability of the vehicle at low speed. Torque vectoring concept is utilized using a system that comprises a pneumatic, an electronic and a torque distribution unit that reduced TCD without compromising with other performances of the vehicle.

A methodology in order to bring an improvement in steering effort of commercial vehicles has also been presented by authors[22]. Factors which affects steering effort has been identified and its detailed analysis has been done both in isolation and in combination to find out its effect on steering effort. Three case studies viz. steering gear ratio, steering wheel diameter & linkages lengths and off-set, has been made. Using Ishikawa diagram, steering effort dependency on various parameters has been presented. Following the methodology, they achieved the reduction of steering efforts by 37%.

CHAPTER 3
TECHNICAL BACKGROUND

3.1 Details of Steering System of a Heavy Commercial Vehicle

Steering system helps to steer front wheels of the vehicle (either left or right). Driver inputs through steering wheel (rotational torque) helps to provide directional control to the vehicle. Steering system transmits the motions and forces to the wheels from the steering wheel using number of parts. Following mentioned are the parts of a recirculating ball steering system that transmits motion and forces from steering wheel to front wheels;

- Steering Wheel,
- Steering Column Assembly,
- Steering Gear Box,
- Pitman Arm,
- Drag Link,
- Upper Steering Arm,
- Knuckles,
- Lower Steering Arms,
- Tie rod

Figure 3.1 shown below illustrates the part of a recirculating ball steering system used in commercial vehicle.

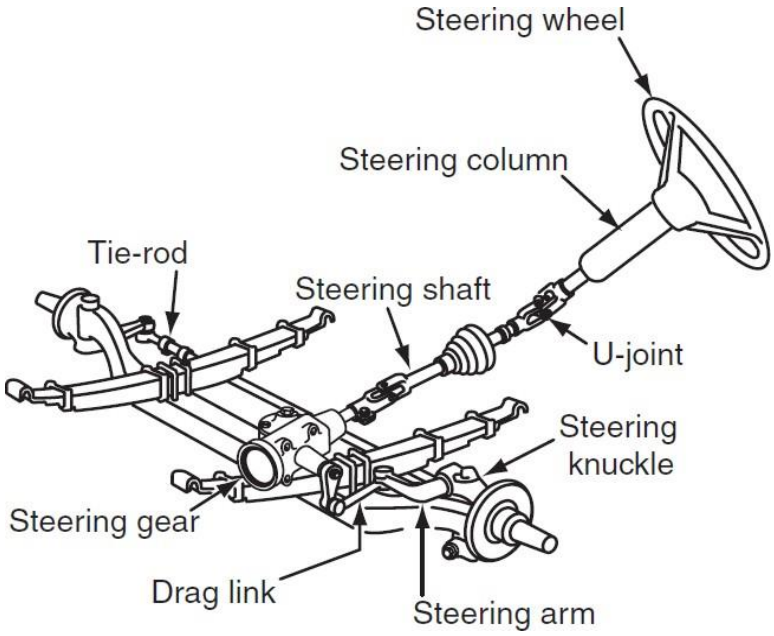

Figure 3.1: Recirculating ball steering system [23]

3.1.1 Steering Wheel

Driver applies effort on a wheel of the vehicle known as the steering wheel/hand wheel so as to provide the directional control to the vehicle. In steering column, torque is generated due to the effort applied by the driver on the hand wheel. It acts as the main input for the system. All the newly made HCV's are now equipped with power-assisted steering system which helps in reduces the effort applied by the driver on the steering wheel. Sometimes in case of power assist failure, if the steering wheel diameter is small then large steering effort is required by the driver. Therefore, keeping it under consideration, steering wheel diameter is kept larger as compared to light commercial vehicles or passenger vehicles. Larger steering wheel provides more torque to the steering column compared to the smaller steering wheel for the same amount of effort applied by the driver. Figure 3.2 shows steering wheel-column assembly with various forces and torques on it. Both steering effort and steering time is important parameter in the vehicle. Steering time refers to time period from the start of steering control to the instance when wheels that has been steered reaches the specified steering angle.

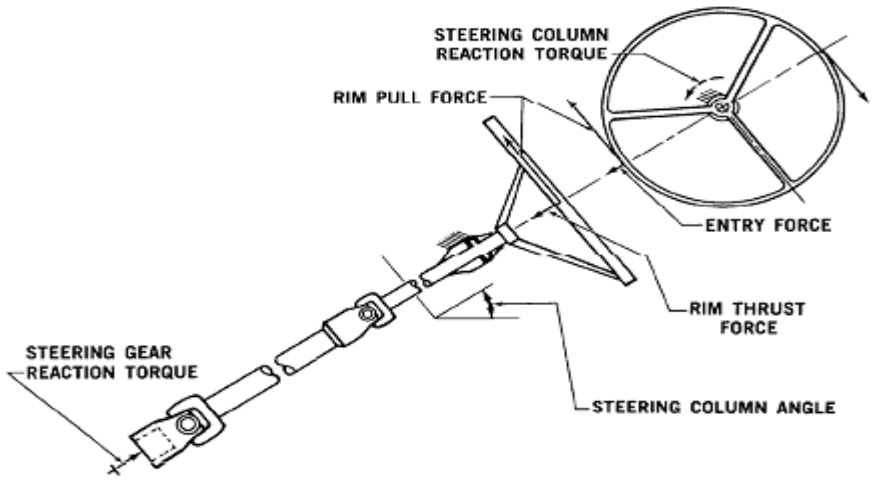

Figure 3.2: Steering wheel-column assembly showing forces & torques [11]

3.1.2 Steering Column Assembly

Steering Column connects the steering gear with the steering wheel. The primary function of the steering column is to transmit torque to the steering gear. It is also used to compensate cabin relative motions in regard to chassis. Figure 3.3 shown below illustrates steering column assembly.

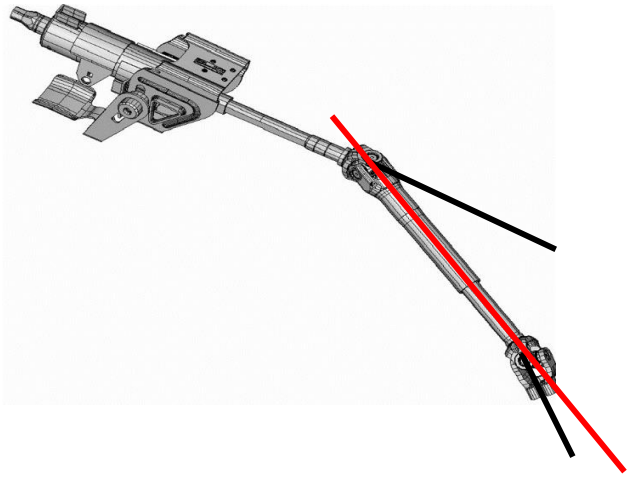

Figure 3.3: Steering column assembly [24]

It comprises of lower & upper shafts, two numbers of universal joints with an intermediate shaft in between those two U-joints. One of the U-joint connects the intermediate and upper shaft while the second U-joint connects the lower shaft and the intermediate shaft. The output velocity may not be same as the input velocity for each of U-joints.

3.1.3 Steering Gear

Steering gear refers to the steering gearbox which is used for multiplication of the steering torque. It also changes the direction of torque applied. There are many types of steering gear boxes available among which recirculating ball steering gears is mostly popular for HCV's. It has worm gear having round thread and when the steering wheel is rotated, metal ball will run in it. Ball nut rack is provided with teeth on a side. These teeth mesh with sector gear and it with sector shaft. Pitman arm is connected to sector shaft. Figure 3.4 shown below represents an overview of steering gear (recirculating ball type). Recirculating balls have an advantage that it decreases the friction and wear in the gear. Moreover, when there is a sudden change in the direction of rotation, they don't allow gears to miss connection. This provides assured steering feel. Hydraulic power aid provided in it works in the same way as in a rack and pinion system. HP (High Pressure) fluid is made to flow to one of the sides of the ball nut rack which provides the power assist. Pressure distribution when steering wheel is in middle, rotated to right and left is illustrated in Figure 3.5, Figure 3.6 & Figure 3.7 respectively.

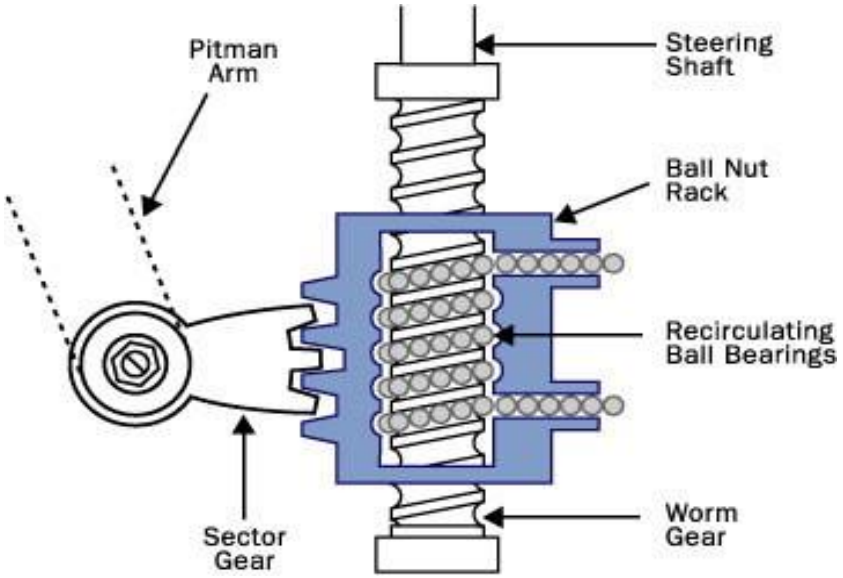

Figure 3.4: Recirculating steering gear box [25]

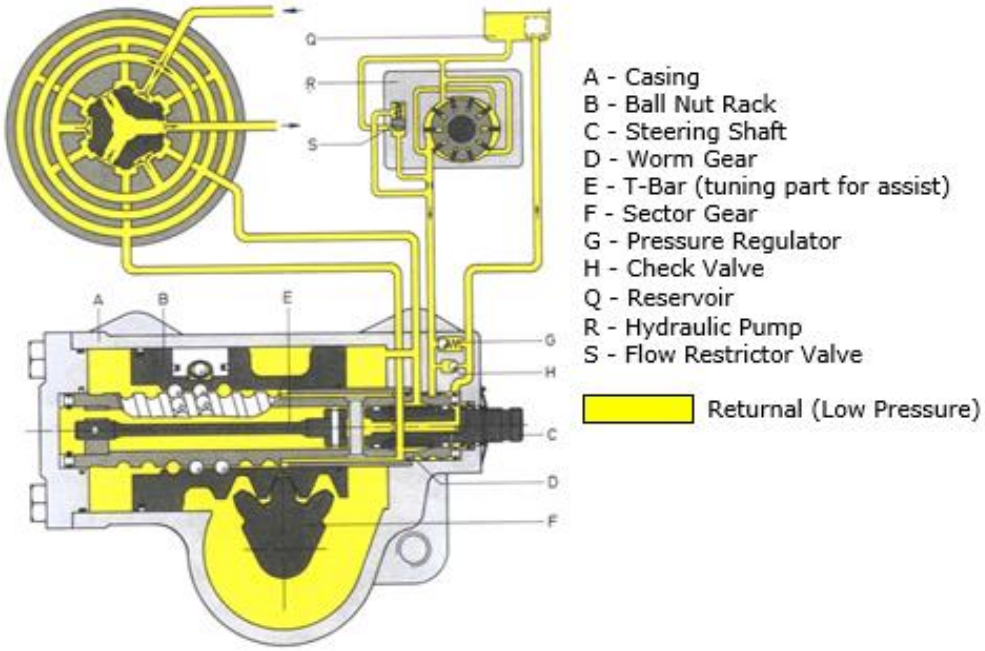

Figure 3.5: Schematic diagram showing pressure distribution within steering gearbox (hand wheel is in middle) [24]

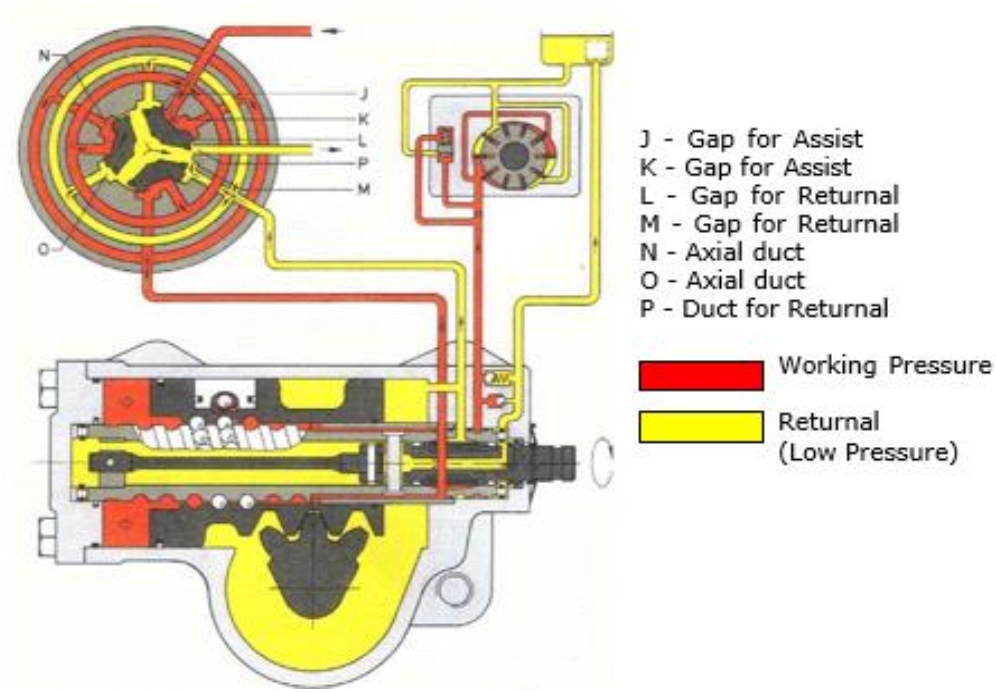

Figure 3.6: Schematic diagram showing pressure distribution within steering gearbox (hand wheel is rotated to right) [24]

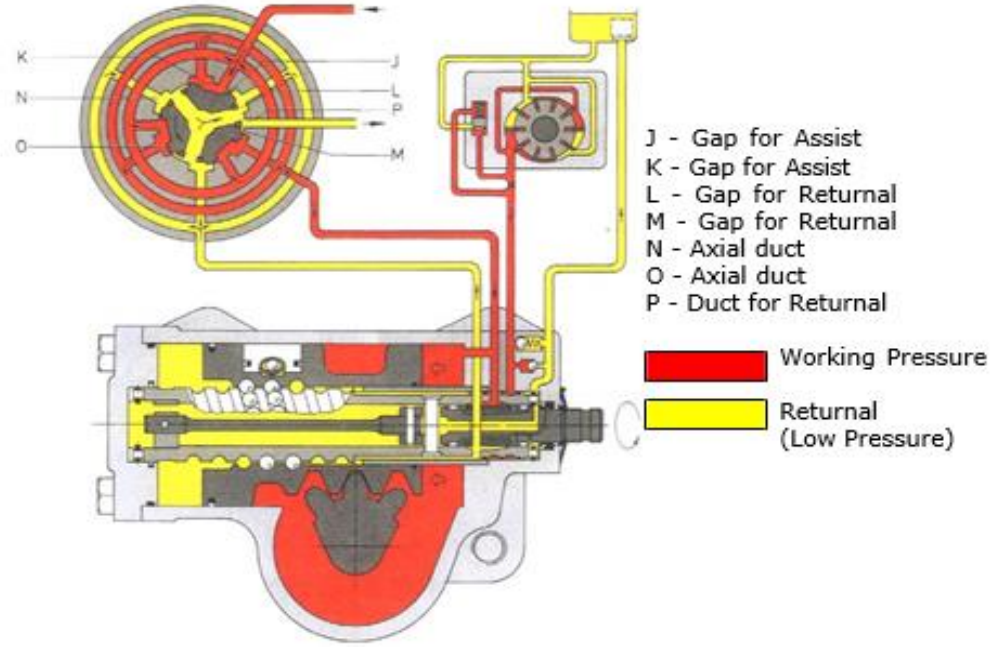

Figure 3.7 Schematic diagram showing pressure distribution within steering gearbox (hand wheel is rotated to left) [24]

3.1.4 Pitman Arm

Pitman arm of the steering system has one of its ends connected to steering gearbox while the other end is connected to drag link. It converts the angular motion (output torque) from the steering gearbox into the linear motion (force) to drag link. The end connected to steering gear has full splines and tapered hole while the one is connected to drag link through a smaller taper hole using ball joint. Pitman arm-to-draglink ball joint is an important hardpoint which has an effect on suspension kinematics and is thus important during linkages optimization. Figure 3.8 illustrates details of pitman arm.

Figure 3.8: Pitman Arm [24]

3.1.5 Draglink

Drag Link is a part of steering linkages that connects the upper steering arm with the pitman arm and is having ball joints at both of its ends. The overall length of the rod can be varied since it is provided with threads on one end to adjust the length. Adjustable length of the draglink helps in centering steering gear box keeping the wheels straight. Draglink-upper steering arm hardpoint plays key role and thus is studied in detail during hardpoint optimization study. Figure 3.9 illustrates the sectional view of partial drag link.

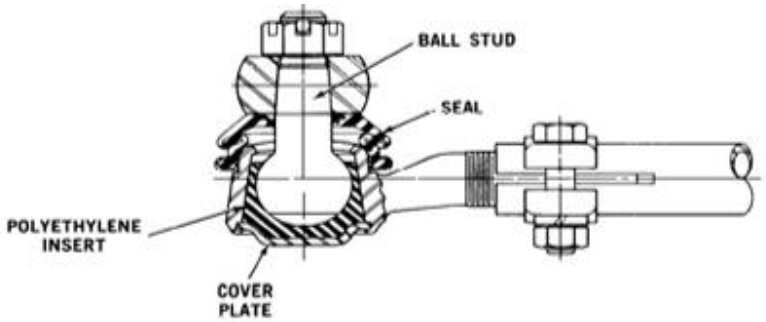

Figure 3.9: Sectional view of a partial drag link [11]

3.1.6 Upper Steering Arm

It is one of the parts of the steering linkages that connects knuckle and draglink. The linear force which has been transferred from the draglink is made to be converted into rotational moment on knuckle and wheels using upper steering arm. During optimization study, area swept by upper steering arm must be studied as it may create packaging hindrances. Upper steering arm length is the distance between upper steering arm-to-knuckle hardpoint & draglink-to-upper steering arm hardpoint. This has influence on steering ratio. Steering ratio refers to ratio of turn angles of the steering wheel to turn angles of the road wheel. Figure 3.10. illustrates an upper steering arm sample showing its connection.

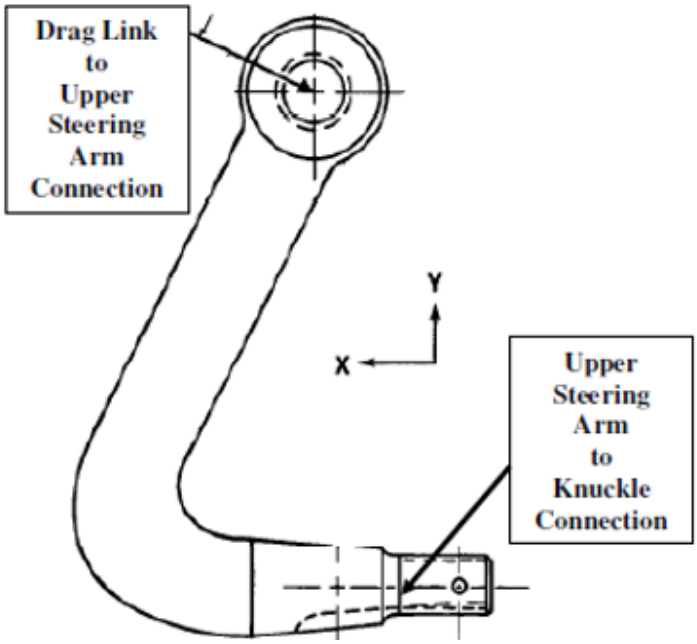

Figure 3.10: Upper steering arm sample showing its connection [11]

3.1.7 Knuckles

Driver side knuckle is rotated due to the torque which is transferred by the upper steering arm, thus this in turn causes front wheel to rotate around the kingpin axis. Kingpins, radial and axial bearings provide connection of knuckles with the front axle and this in turn provides required degree of freedom. Figure 3.11 shows the components within the knuckle using a sectional view. Steering characteristics is mainly affected by knuckle friction and kingpin inclination angle. Axial and radial bearings affect knuckle friction. Axial and radial bearings cast-off in the knuckle subsystem are generally of two different types and thus

they provide different friction performances. Table 3.1 shows knuckle friction values for different bearing combinations.

Table 3.1: Knuckle friction values for different bearing combinations[24]

Combinations / Bearings	*1*	*2*	*3*	*4*
Radial Bearings	Bronze	Needle	Needle	Bronze
Axial Bearings	Contact	Roller	Contact	Roller
Approximate Knuckle Friction (N.m)	250	20	30	120

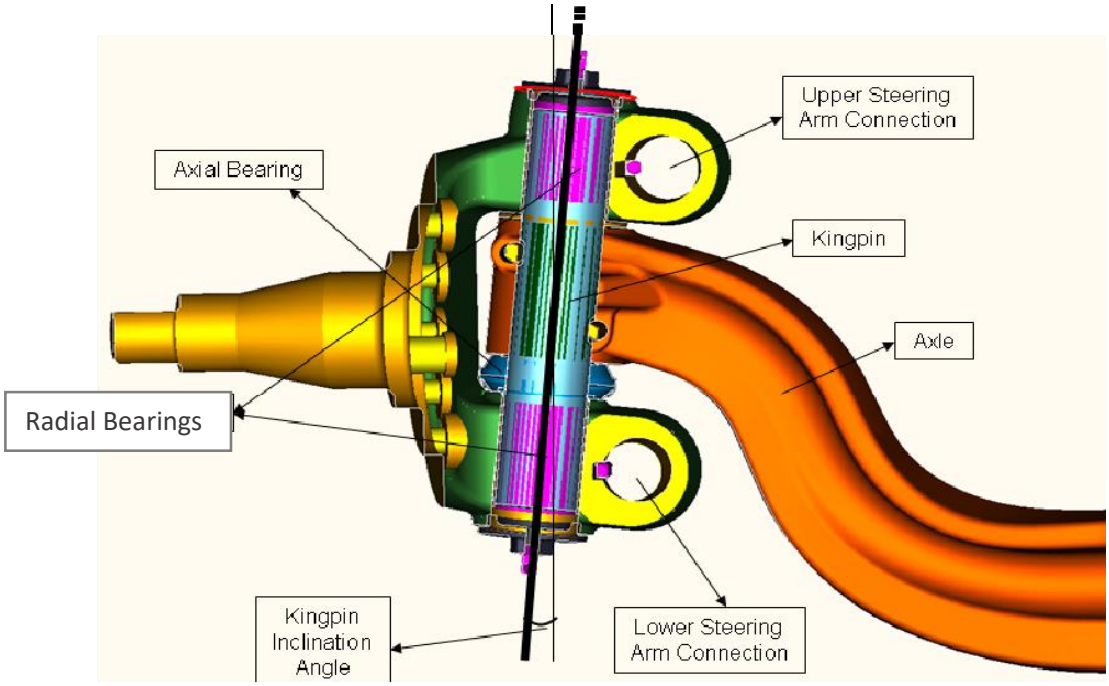

Figure 3.11: Sectional view of knuckle [24]

3.1.7.1 Needle Roller Bearing

These are bearings provided with cylindrical rollers. Diameter of rollers are small even though its load carrying capacity is quite high. This can be used in bearing arrangements when the space available (radial space) is limited. Cross section of a needle roller bearing is shown in Figure 3.12 below.

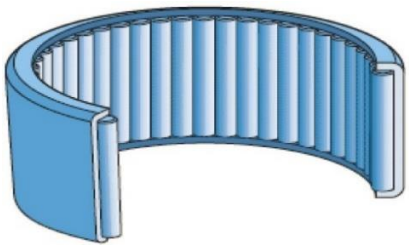

Figure 3.12: Cross-section of needle roller bearing [26]

3.1.7.2 Bronze Bearing

Figure 3.13 illustrates a sample bronze bearing. It is used in operation with no maintenance. Bronze bushings are hard & strong and also have longer life.

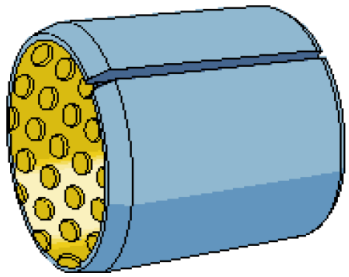

Figure 3.13: Bronze bearing [26]

3.1.7.3 Tapered Roller Thrust Bearings

This is an axial bearing having tapered inner. It is provided with tapered rollers in between outer ring raceways. The lines which are projected from all the surfaces (tapered), they all cut each other at a point. This point lies on the bearing axis. It is suitable for using under combined loads i.e. both radial and axial. It is illustrated in the Figure 3.14.

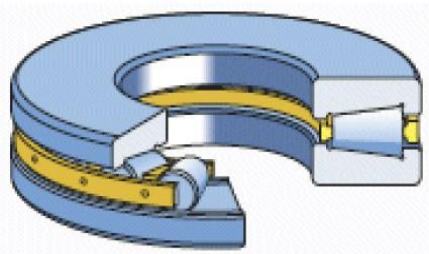

Figure 3.14: Tapered roller thrust bearing [26]

3.1.7.4 Axial Plain Bearings

These are journal bearings which can predominantly carry axial loads. An axial plain bearing which is generally used in between axle and knuckles is shown in Figure 3.15.

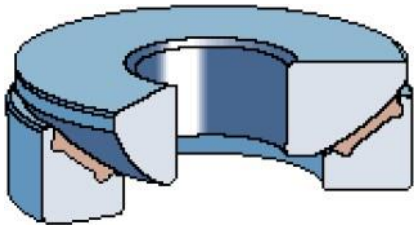

Figure 3.15: Axial plain bearing [26]

3.1.8 Lower Steering Arms

These are parts that are either casted or forged and is connected on both sides to knuckles. It's responsible to affect the Ackerman geometry of front axle. Thus, to decrease the Ackerman during hardpoint optimization study, lower steering arm-to-tie rod hardpoint is closely looked after. Figure 3.16 illustrates a sample of lower steering arm.

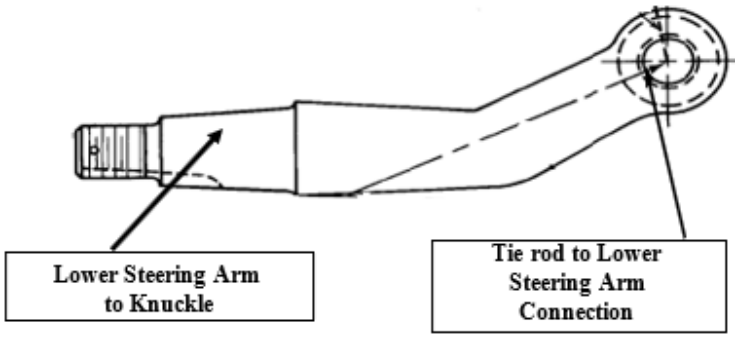

Figure 3.16: Lower steering arm [11]

3.1.9 Tie Rod

Tie rod are the steering linkages part which is provided at the end with two ball joints as illustrated in Figure 3.17. It connects lower steering arms of both sides (left & right) thus transferring the rotational motion of the right wheels to left wheels (in Right Hand drive vehicle) and left wheels to right wheels (in Left Hand drive vehicle). During the hardpoints optimization study, area swept by the tie rod & lower steering arm must be looked after to check packaging feasibility.

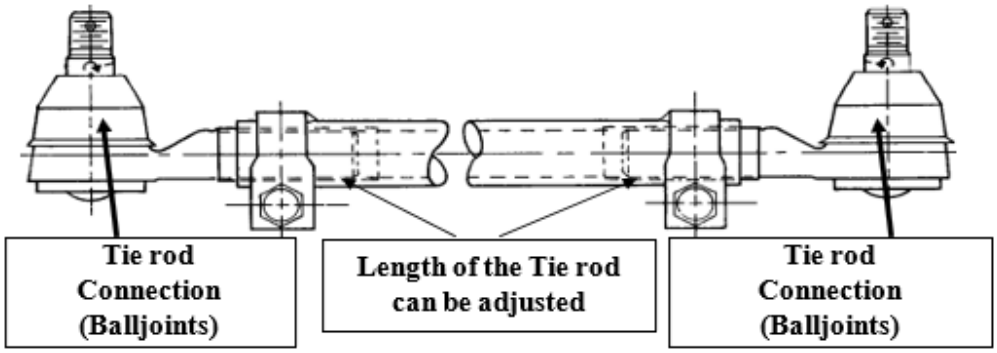

Figure 3.17: Tie rod [11]

3.2 Steering Kinematics of a Heavy Commercial Vehicle

Type of suspension system and steering system plays a key role in the steering kinematics of a heavy commercial vehicle. Therefore, it is very important to perform design optimization between suspension and steering system in order to have better/desired steering characteristics of the vehicle. For this, kinematic characteristics need to be evaluated in detail so that very fast and accurate optimization study could be performed. List of the major kinematic characteristics which are identified as the major contributors to total vehicle steering has been listed and is explained in details below.

- Bump steer- change in the steer angle due to bump (vertical wheel travel)
- Roll steer- change in the steer angle due to suspension roll (cornering)
- Longitudinal compliance (brake steer) and wind-up steer- change in the steer angle (braking) because of longitudinal forces
- Lateral compliance steer- change in the steer angle due to lateral forces
- Roll camber- Due to suspension roll, there is change in the camber angle called roll camber (cornering)
- Maximum wheel angle
- Ackermann geometry

3.2.1 Bump Steer

When the suspension undergoes compression or undergoes rebound from its normal ride height then the front wheels experiences either the toe-out or toe-in which causes the wheel to steer known as bump steer. Due to this unwanted steer, driver have to frequently correct the steering input in order to maintain the straight-ahead movement of the vehicle. Thus, it

is very important to minimize bump steer in HCV's so that the drivers can experience better and smooth driving performance. The vital parameter in its optimization is the arc created by travel of ball joint of drag link-to-upper steering arm & instantaneous center of this arc. Figure 3.18 shown below represents the phenomenon of bump steer during vertical wheel travel.

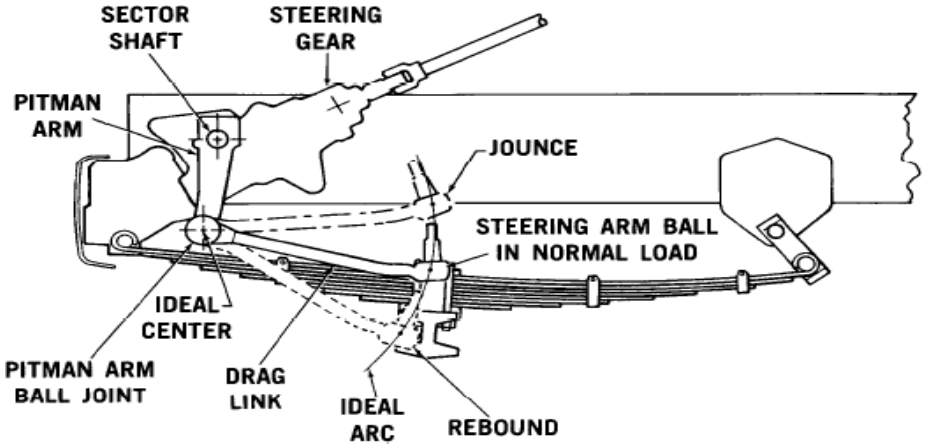

Figure 3.18: Arc created by travel of upper steering arm when the wheel travels in vertical direction [11]

Because of the packaging constraint it is quite difficult to realize this ideal arc. When the wheel travel takes place in the vertical direction, the arc created by the upper steering arm ball joint must analogous to arc realized by axle spring connection to have the minimum bump steer. Else, there is possibility of front wheel to rotate in parallel which affects controllability for the straight-ahead performance of vehicle. Figure 3.19 shown below illustrates the steer of front wheel.

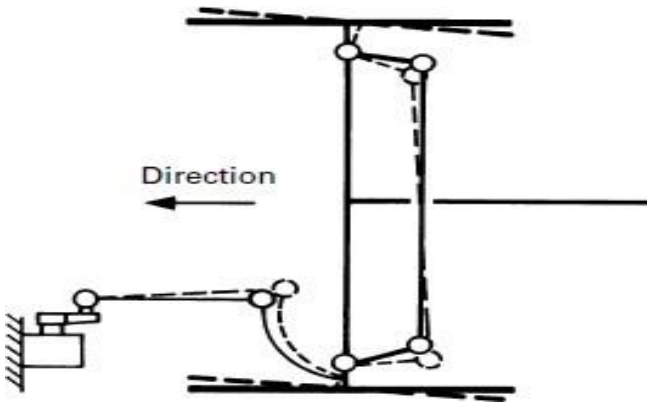

Figure 3.19: Steer of front wheels due to vertical wheel travel [27]

Performance of bump steer mainly depends on the hardpoints of the front suspension which are listed as;

- Front eye bushing hardpoint,
- Pitman arm-to-drag link hardpoint,
- Axle spring hardpoint
- Drag link-to-upper steering arm hardpoint.

3.2.2 Roll Steer

Steer angle change of front wheels when a body roll during a cornering or due to asymmetrical potholes and bumps is termed as roll steer. The stability performance as well as the handling performance of the vehicle is very much affected by the roll steer. Variation in gradient of steer angle during cornering results in changeable handling characteristics. During the optimization study of the roll steer, front eye bushing hardpoint needed to be imparted special attention and is tried to keep as nearby as possible to centerline of the main leaf else there will be asymmetric in the kinematics of right and left leaf springs and roll steer will appear. Figure 3.20 & Figure 3.21 illustrates roll view phenomena for a solid axle front suspension.

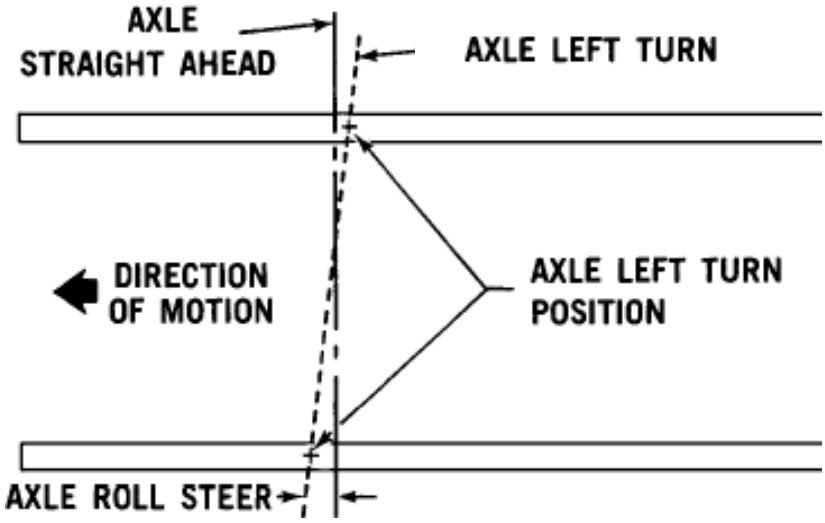

Figure 3.20: Top view of front axle during roll [11]

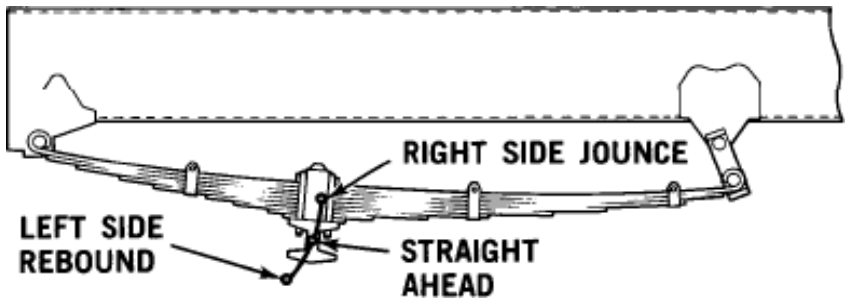

Figure 3.21: Side view of front axle during roll steer [11]

Roll steer performance is dependent on below highlighted hardpoints;

- Front eye bushing hardpoint,
- Axle Spring hardpoint.

3.2.3 Lateral Compliance Steer

During cornering, lateral force is generated at contact patch which anticipates the wheel to rotate. The cause/reason behind it is the softer bushings that has been used in the steering and suspension systems. If a front suspension is having a forward yaw center, then lateral compliance steer will cause an understeer while rearward yaw center causes oversteer. Figure 3.22 shows yaw center – understeer and oversteer relationship. Lateral compliance steer is best studied by examining K & C analysis of the vehicle.

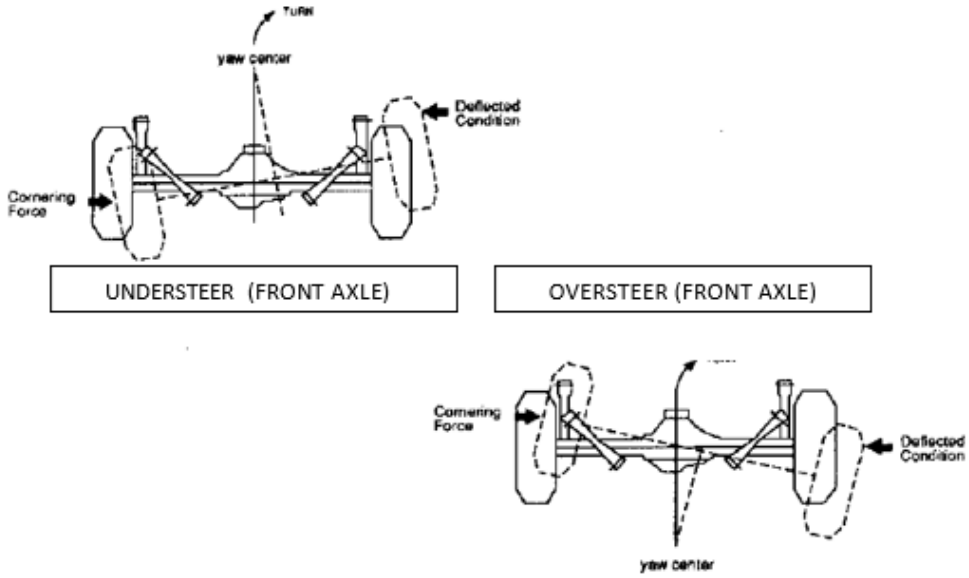

Figure 3.22: Yaw center - U/O steer relationship [28]

3.2.4 Longitudinal Compliance & Wind-up Steer

Change in the steer angle due to braking and acceleration is termed as longitudinal compliance steer. As it is directly related with the torque steer performance and braking stability, it is therefore an important design parameter of the vehicles. Wind up steer does take place during braking since the leaf spring tends to wind-up during braking as the load transfer takes place from rear to front end during braking. This wind-up effect could be decreased or eliminated when draglink-to-upper steering arm ball joint is made to lie on the leaf spring center of rotation at the time of braking. Figure 3.23 shown below illustrates the wind-up steer effect which is resulted due to leaf spring rotation and draglink-to-upper steering arm hardpoint. This is most importantly considered in steering and suspension design optimization.

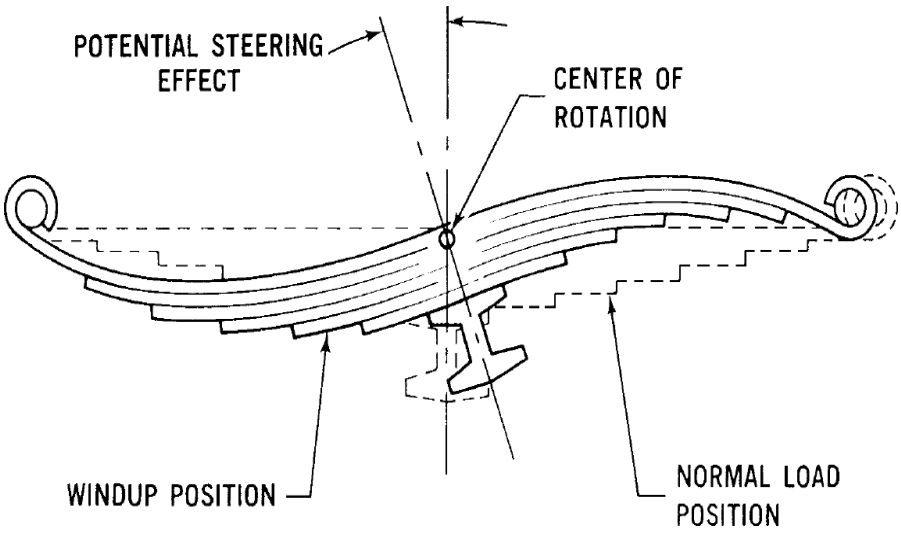

Figure 3.23: Steering effect of wind-up steer [11]

3.2.5 Roll Camber

It is defined as the change in the camber angle during vehicle cornering. Lateral force is produced on a wheel due to the effect of camber angle. This force (lateral) generated due to camber is known as camber thrust. When a vehicle undergoes cornering with change in the camber angle, much less lateral force is developed which generates slip angles.

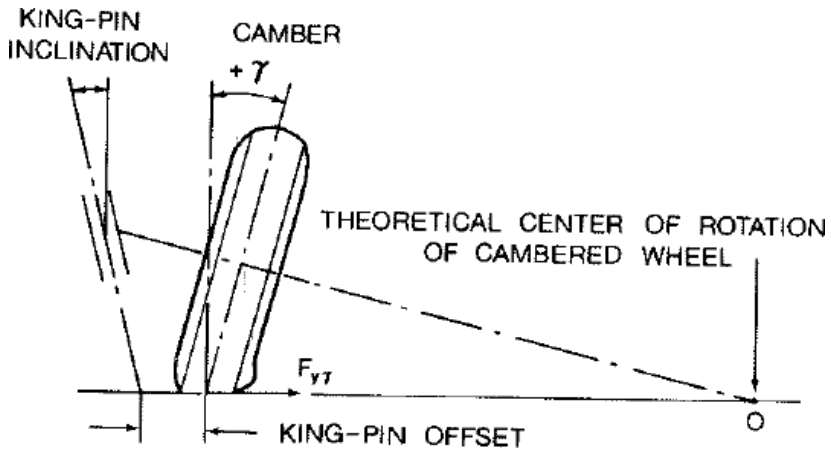

Figure 3.24: Camber thrust phenomena [29]

3.2.6 Ackermann Geometry

Ackermann geometry refers to steering linkages geometric arrangement which in turn will help outside and inside wheel of the vehicle to rotate at different angles at the time of cornering. Inside wheel during cornering follows smaller radius while larger radius is followed by the outer wheel. This is illustrated in the Figure 3.25 below.

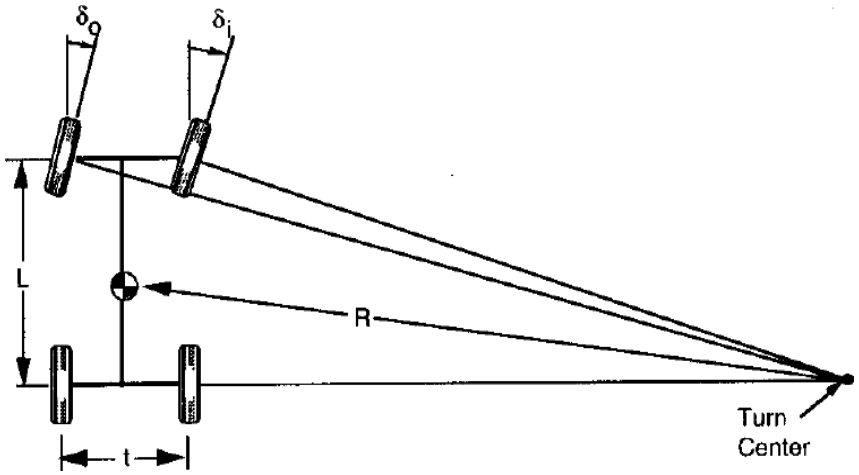

Figure 3.25: Outer & inner wheels angles (where $\delta_i > \delta_o$) during cornering [28]

Ackermann geometry provides true rolling conditions to the vehicle mainly at three conditions viz. one when vehicle is moving straight, and the other two are when the vehicle is negotiating turn with correct angles in left and right side. Excluding these conditions there will always be a difference known as an Ackerman error. Figure 3.26 illustrates three conditions for pure rolling.

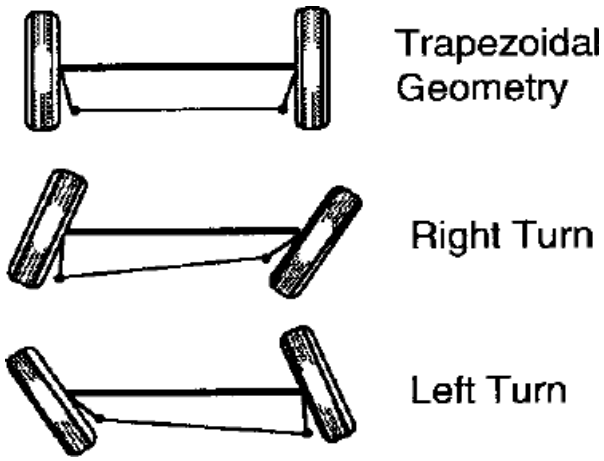

Figure 3.26: Three conditions for pure rolling [28]

It is calculated as;

Ackermann Error (Left/Right) = Steer Angle (Left/Right) – Ideal Steer Angle (Left/Right)

3.2.7 Maximum Wheel Angle

Maximum steering wheel lock position is reliant on packaging constraint as well as the linkages kinematics. Minimum TCD and maneuverability of the vehicle is directly dependent on the maximum wheel lock angle. Thus, it's an important parameter for the drivers. During steering system design (new) and hardpoint optimization, maximum wheel angle is wisely taken into consideration for meeting TCD requirement.

CHAPTER 4

METHODOLOGY

For a New Vehicle Development (NVD), “modularity in design” or “modular design” approach is used. In this concept, whole vehicle is divided into smaller parts. These smaller parts are termed as modules or skids. Each of them can be created independently and they can also be used in different vehicles. This concept helps in reduction of cost, flexibility in design, augmentation & exclusion. Methodology going to be followed in this project are divided into three phases and is visualized in the Figure 4.1 shown below.

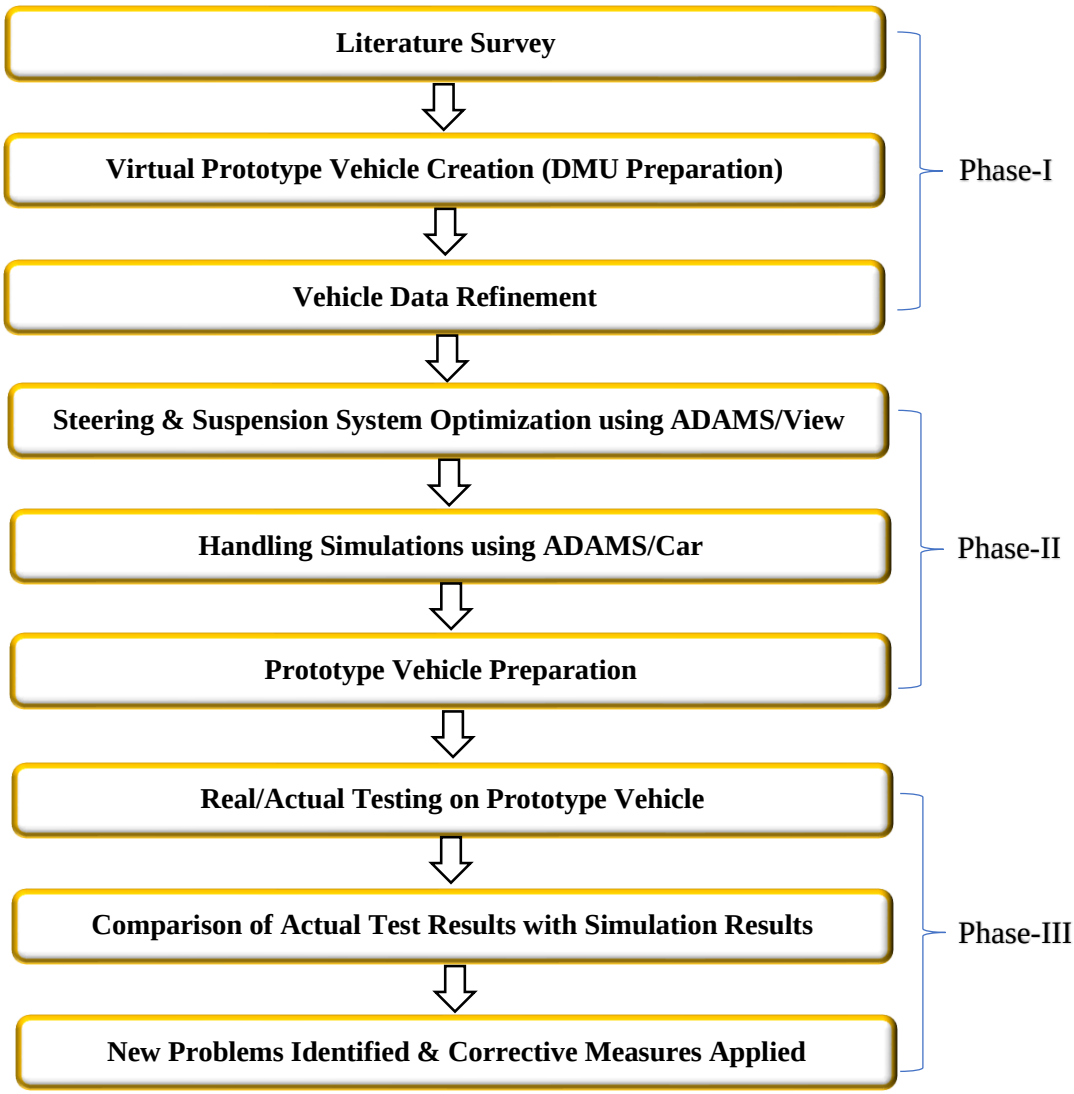

Figure 4.1: Methodology being followed in this project

4.1 Phase-I

In this phase, the first stage is the literature survey and concept development. It mainly focusses on the type of the vehicle needed to be developed, such as truck, tipper, tractor trailer etc., configuration, engine type, driveline etc. Literature survey also refers to the study of the regulations & norms set up by the government for each type of vehicle. Recently in the month of July, 2018 government has revised the regulation for load carrying capacity of the vehicles. Based on the new regulations, for the same configuration of the vehicle, load carrying capacity has been increased thus the vehicle requires certain major modification in the design of axle, suspension, steering system & load body otherwise there will be chances of the breakdown of the vehicle or decrease in the performance of the vehicle. Another step in the new vehicle development is preparation of CAD model of the vehicle known as Digital Mock Up (DMU). In this base vehicle will be chosen and using the identified change content in the base model vehicle, new vehicle development will be done.

The advantages of creating a DMU can be summarized as:

- It helps in identifying all the potential issues during the design process which in turn reduces time-to-market.
- It helps to minimize the number of prototypes being built which in turn reduces total development costs of the product.
- It helps in the investigation of many design possibilities before choosing a final design which in turn will help in increasing the product quality.

After the preparation of the DMU, vehicle design will be validated to check whether the proposed new vehicle design as well as its performance is within the standard result or not for which data refinement of vehicle will be needed. In this detail calculation such as axle reaction calculation, C.G. height of the vehicle, chassis height of the vehicle, position of hard points of steering system & suspension system etc. need to be made available as input for the handling simulations.

4.2 Phase-II

In this phase, steering system optimization and vehicle handling behavior is studied using multibody simulation software (ADAMS) where inputs are feed based on the data collected in Phase-I. Two type of simulations will be performed. One using ADAMS/View in which

optimization of the steering and suspension system design will be done and on the other hand using ADAMS/Car handling behavior of the vehicle is studied. After that final design is proposed based on which an offer drawing will be modified and then prototype vehicle will be made for actual/real testing.

4.3 Phase-III

In this phase, the vehicle will be tested on real conditions and the results will be generated. These results will then be compared with the simulated results. One of the advantages that can be achieved through this project is that it would help to recognize to what extent simulated data could be trusted in future to avoid real testing. This will thus help to cut down lead time of testing & cost saving for the industry so that they can automate/computerize the testing of the proto vehicle based on simulation in future with or without using a correction factor for the simulated results.

CHAPTER 5
MODELING AND SIMULATIONS

Trucks are commercial vehicles, which are sometimes subjected to harsh conditions. Design of steering and suspension system is very important as it plays a key role in vehicle's handling performance during cornering, breaking, bump etc. Driver's comfort during ride depends a lot on the proper design of steering and suspension system. Therefore, considering all the important parameters like break, bump, pitman-draglink toggle, Ackerman error etc. design optimization of steering and suspension linkage is done. After its optimization, designing of parts/linkages will be done. Then, a virtual full vehicle model is prepared on which various test related to handling, ride, fuel economy etc. is simulated based on the requirement of the vehicle. The present work in this thesis can be explained as:

5.1 Modeling of Front Suspension and Steering System in ADAMS/View

Modeling includes building a model that will have movable/rigid parts, its joints and flexible connections with forces being applied on it. In the first part of modeling and simulation, design optimization of front suspension and steering system is done. Modeling of which can be done in two ways in ADAMS:

a) Building a new template (Working from the scratch).
b) Modifying the existing template based on the requirement.

Building a new template in ADAMS requires deep knowledge of modeling and is time consuming. Each part, joints and connections should be accurately modeled to get results close to the tests done on real vehicle. An existing versatile template has been used for modeling of front suspension and steering system of our vehicle. For modeling of our vehicle, we need to identify the inputs required for the modification of the existing template. Inputs includes hardpoints of steering and suspension linkages, load on each axle, forces on the linkages etc. which has been presented in Appendix with its detail calculation. Data obtained through calculation is then made to feed into ADAMS which automatically creates the model.

Figure 5.1 & Figure 5.2 represents the model of front suspension and steering system of the vehicle modeled in ADAMS/View in which existing template has been modified based on data (inputs) obtained in phase-I either by calculation or from DMU of the vehicle.

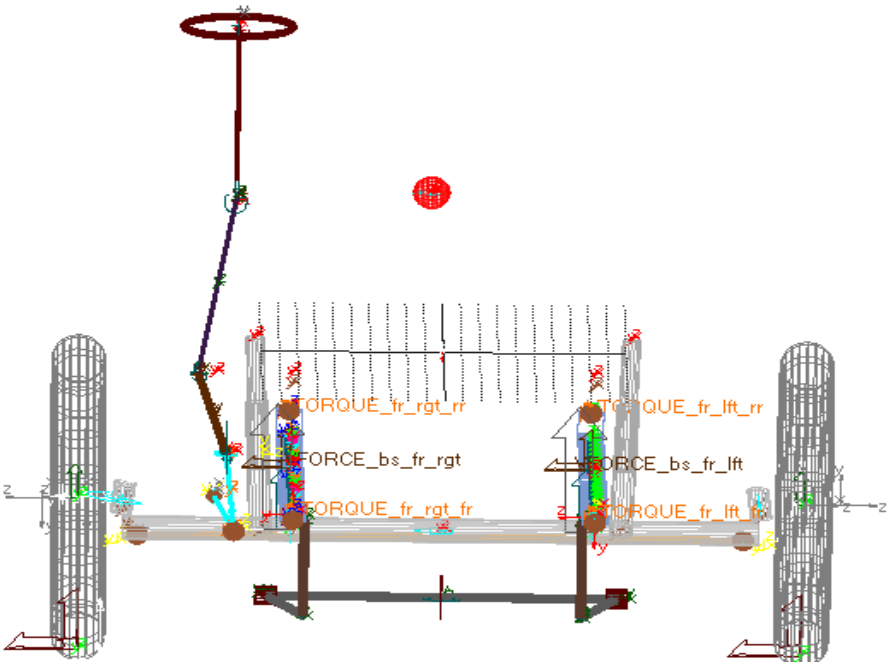

Figure 5.1: Front view of modelled front suspension and steering system

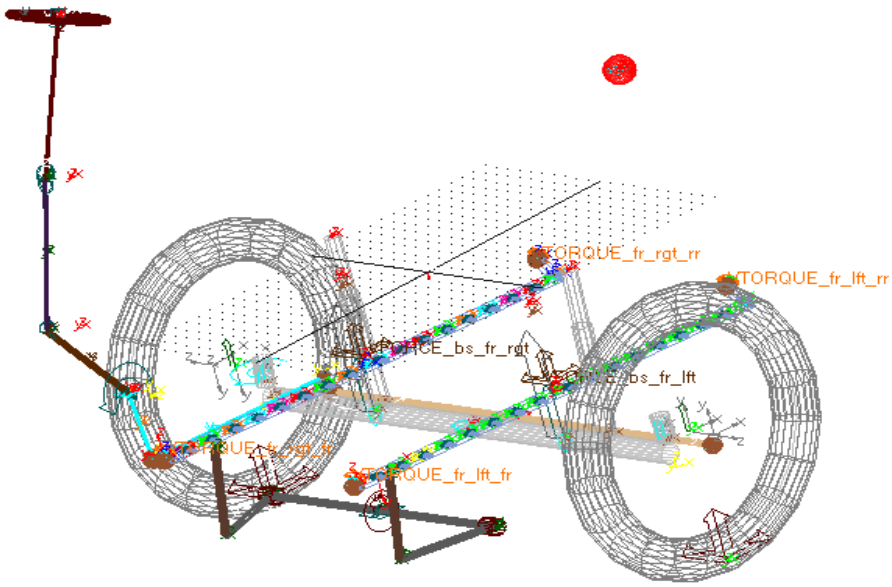

Figure 5.2: Isometric view of modelled front suspension and steering system

All the parts will be majorly connected with either the front chassis or the front axle so it's important to illustrates the parts linked with these aggregates along with the connectors used

to connect those parts. Figure 5.3 & Figure 5.4 shown below illustrates the graphical topology for the front axle and front chassis respectively.

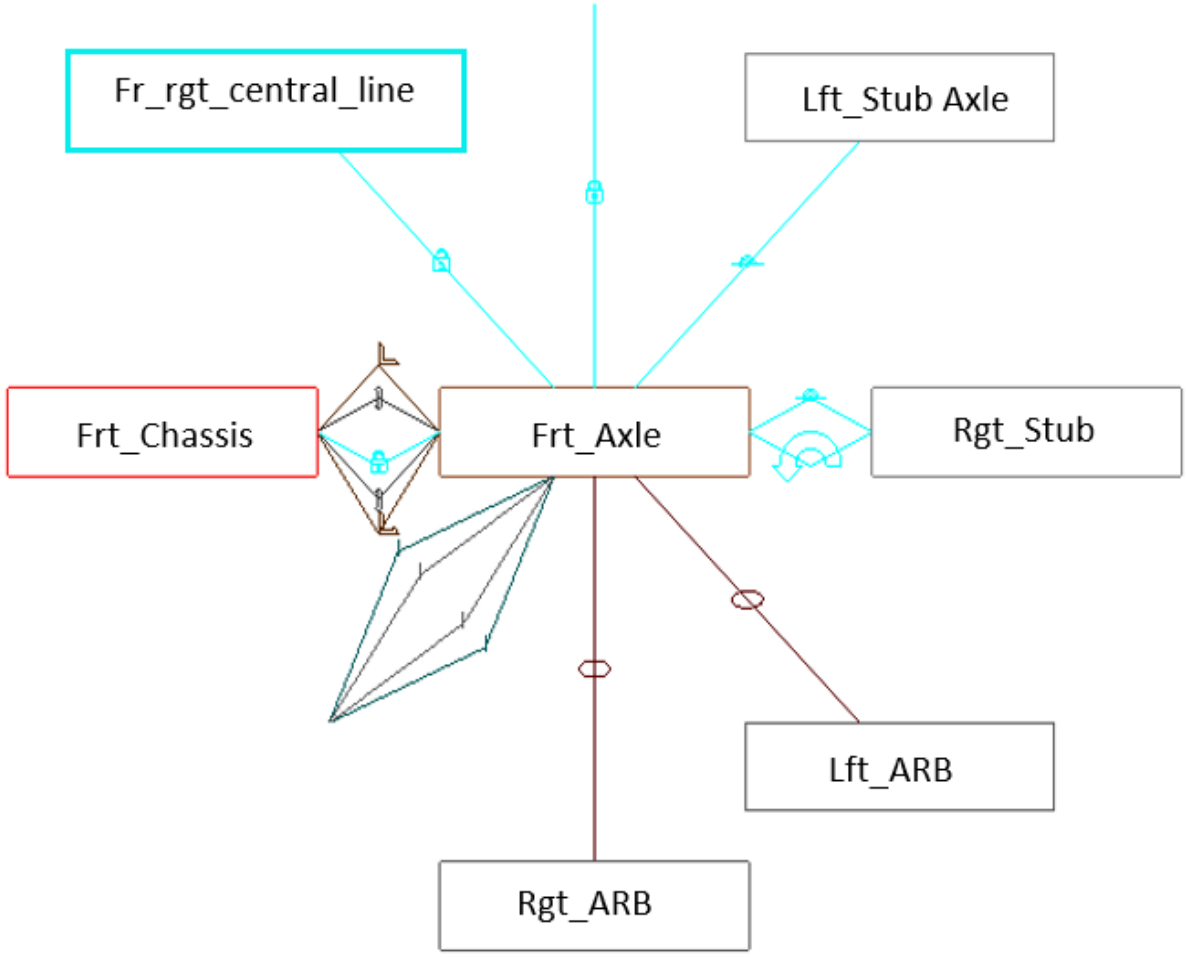

Figure 5.3: Graphical topology of front axle

After modeling of the system, it is very important to check the feasibility of the data, parts modeled, connectors for the parts etc. in order to ensure proper completion of modeling. Then hardpoints influencing the parameters of test needed to be identified. Since in optimization of front suspension and steering system major parameters evaluated are Ackermann error, Brake Steer, Bump Steer and Pitman Arm-Drag Link Toggle, hardpoints affecting these are first identified and process of optimization is started.

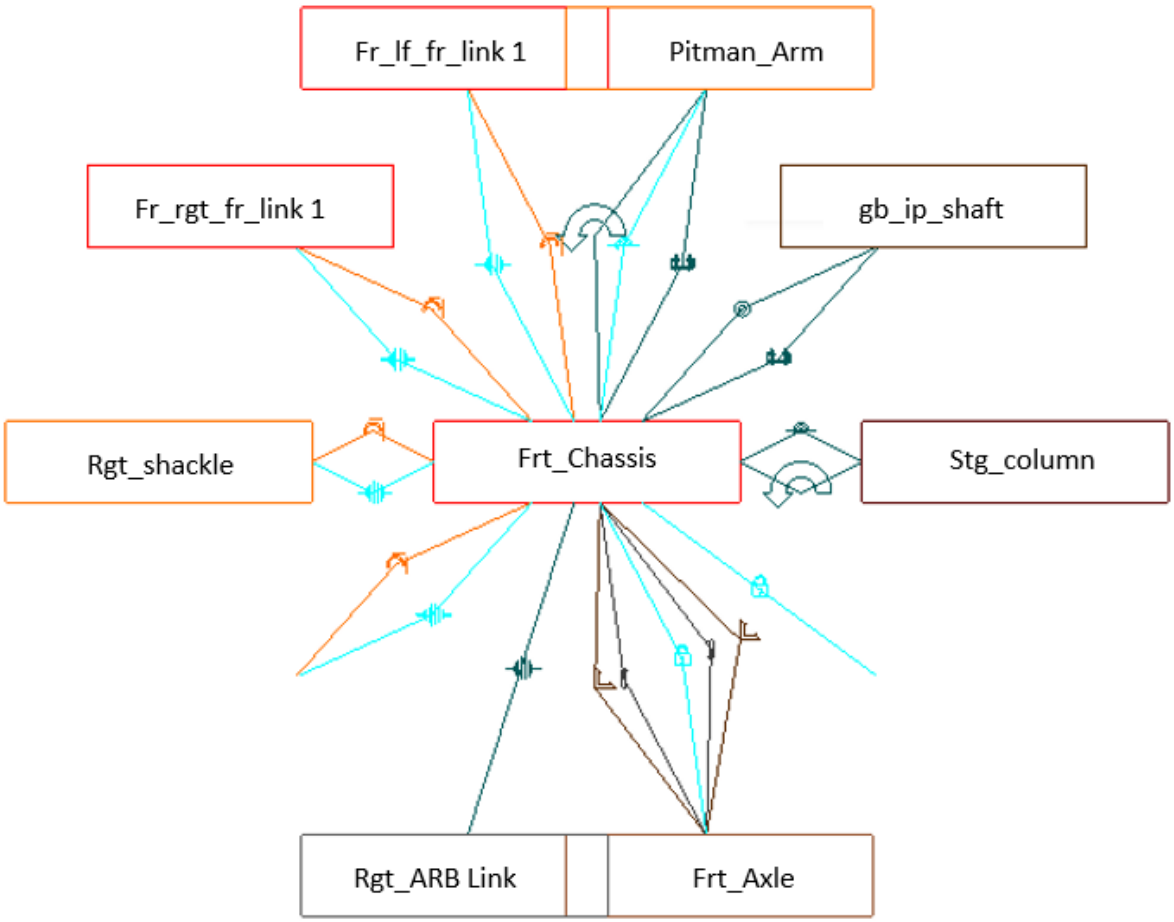

Figure 5.4: Graphical topology of front chassis

5.2 Simulation for Optimization of Front Suspension and Steering System Linkages in ADAMS/View

The major hard points that plays key role in brake and bump steer includes;

a) Pitman Arm-Drag Link Hard Point,
b) Front Eye Bushing Hard Point,
c) Draglink-Steering Arm Hard Point,
d) Axle Spring Hardpoint

These points need to be studied separately first for its effect on brake and bump steer. For same changes made in hardpoints of different vehicles having non similar steering and suspension linkages, test will show different variation in the value of brake and bump steer. Thus, for each

case (different steering and suspension linkages) individual analysis should be done. Sensitivity study of each hardpoint will give clear idea of the importance of each hardpoint on vehicle and will act as a helpline that will reduce unwanted iterations during the optimization process. Initially, existing steering and suspension hardpoint data is collected which can be noted as the base hardpoint & it is collected from DMU. Then, each hardpoint is changed separately in X-direction (along vehicle length) & in Z-direction (along vehicle height) to study its effect on brake and bump steer. Sensitivity study results* has been shown in the Table 5.1 to Table 5.4.

(*Note: keeping in consideration confidentiality of industry data below tabulated data for sensitivity analysis has been modified. Modified values = Actual Value * Manipulation Factor)

Table 5.1: Pitman arm-to-drag link hard points results

Pitman Arm-to-Drag Link Hard Points Results				
Condition		Change in Hardpoints Value	Laden	
			Bump Steer (deg)	Brake Steer (deg/m)
Z-Direction	20mm Up	20	2.36	0.3378
	15mm Up	15	2.5	0.1364
	10mm Up	10	2.64	0.4242
	Original Hardpoints Data	0	2.92	0.5106
	10mm Down	-10	3.2	0.597
	15mm Down	-15	3.34	0.6402
	20mm Down	-20	3.48	0.6835
	30 mm Down	-30	3.76	0.77
X-Direction	30 mm Forward	30	2.97	0.5233
	20mm Forward	20	2.95	0.5192
	10mm Forward	10	2.94	0.515
	Original Hardpoints Data	0	2.92	0.5106
	10mm Behind	-10	2.94	0.5061
	30 mm Behind	-30	2.86	0.4969

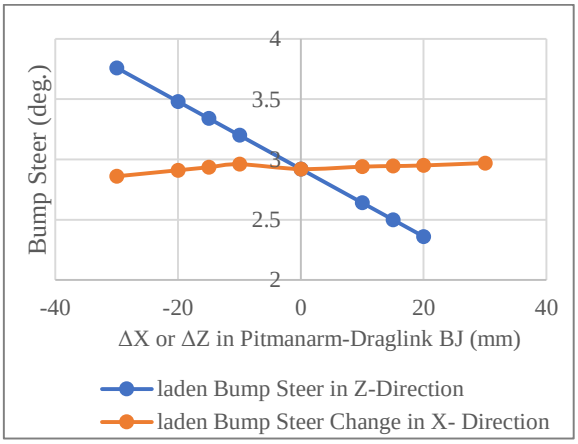

(a) Bump Steer vs Pitman Arm-Draglink BJ

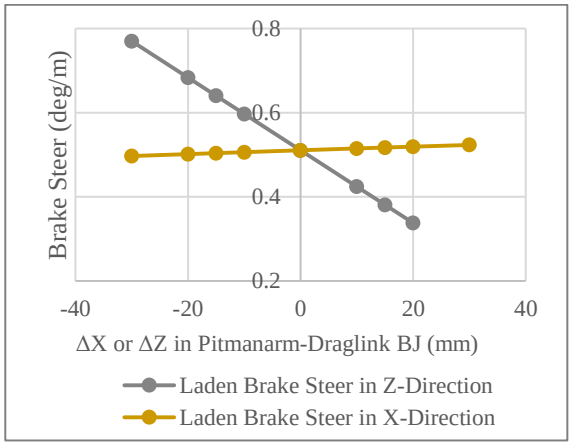

(b) Brake Steer vs Pitman Arm-Draglink BJ

Figure 5.5: Graphs (a) & (b) representing bump and brake steer sensitivity with pitman arm-draglink BJ

Summary of sensitivity analysis for pitman arm-to-draglink ball joint hardpoint are:

i. When we shift the hard point of pitman arm-draglink ball joint there will be noticeable variation in the value of brake steer and bump steer.

ii. Shifting point up, it will improve brake steer as well as bump steer while shifting it down will worsen both brake & bump steer.

iii. Shifting point in front direction will also improve brake & bump steer while shifting in opposite direction it worsens.

iv. Sensitivity is more visible in Z-direction then in X- direction. Thus, vertical shift of this point plays key role while designing steering system.

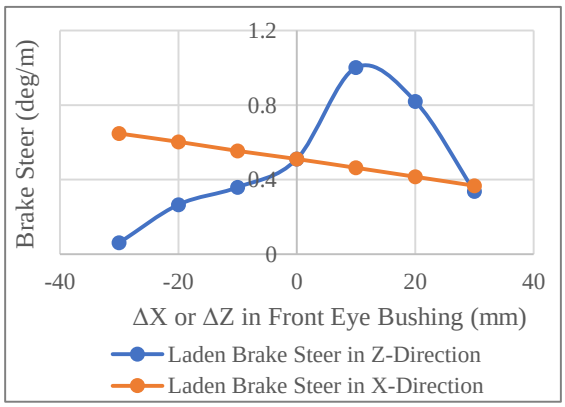

(c) Brake Steer vs Front Eye Bushing

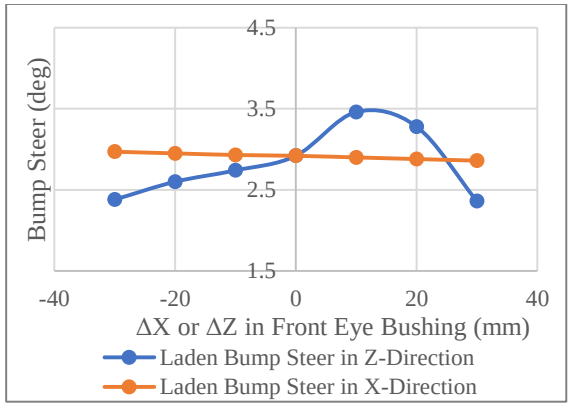

Fig. (d) Bump Steer vs Front Eye Bushing

Figure 5.6: Graphs (c) & (d) representing brake and bump steer sensitivity with front eye bushing

Table 5.2: Front eye bushing hard points results

Front Eye Bushing Hard Points Results				
Condition		Change in Hard Points Value	Laden	
			Bump Steer (deg)	Brake Steer (deg/m)
Z-Direction	30mm Up	30	2.36	0.3378
	20mm Up	20	3.28	0.8202
	10mm Up	10	3.46	1.0016
	Original Hardpoints	0	2.92	0.5106
	10mm Down	-10	2.74	0.3588
	20mm Down	-20	2.6	0.2657
	30 mm Down	-30	2.38	0.061
X-Direction	30 mm Forward	30	2.86	0.3673
	20mm Forward	20	2.88	0.4155
	10mm Forward	10	2.9	0.4633
	Original Hardpoints	0	2.92	0.5106
	10mm Behind	-10	2.93	0.5542
	20mm Behind	-20	2.95	0.6028
	30 mm Behind	-30	2.97	0.6475

Summary of sensitivity analysis for front eye bushing hardpoint

i. When we shift the hard point of front eye bushing pivot there will be noticeable variation in the value of brake steer and bump steer.
ii. Shifting point up, it will worsen both bump & brake steer and after then shows improvement theoretically. However, practically it's not observed due to space limitation between front eye bushing bracket and frame while shifting it down will improve both brake & bump steer.
iii. Shifting point in rear direction will also improve brake & bump steer & vice versa.
iv. Sensitivity is more visible in Z-direction then in X- direction. Thus, vertical shift of this point plays key role while designing steering system.

Table 5.3: Drag link-to-steering arm hard points results

Drag Link-to-Steering Arm Hard Points Results				
Condition		Change in Hard Points Value	Laden	
			Bump Steer (deg)	Brake Steer (deg/m)
Z-Direction	50mm Up	50	4.39	-0.1329
	30mm Up	30	3.79	0.1282
	20mm Up	20	3.5	0.2569
	10mm Up	10	3.52	0.3843
	Original Hardpoints	0	2.92	0.5106
	10mm Down	-10	2.63	0.7039
	30 mm Down	-30	2.07	0.8822
	50 mm Down	-50	1.52	1.1239
X-Direction	50 mm Forward	50	2.87	0.5802
	30 mm Forward	30	2.89	0.5511
	20mm Forward	20	2.9	0.5371
	10mm Forward	10	2.91	0.5237
	Original Hardpoints	0	2.92	0.5106
	10mm Behind	-10	2.92	0.4978
	20mm Behind	-20	2.93	0.4855
	30 mm Behind	-30	2.94	0.4734
	50 mm Behind	-50	2.96	0.4504

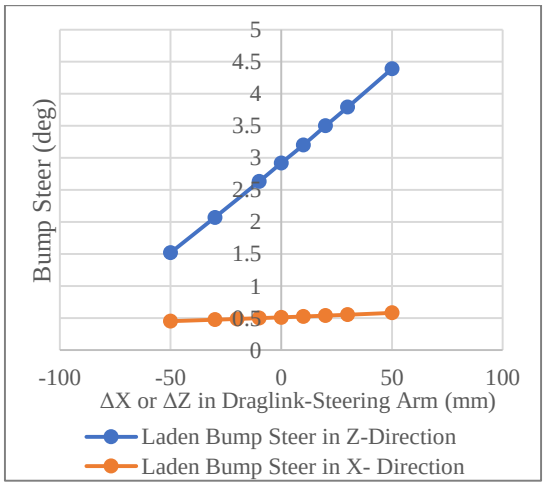

(e) Bump Steer vs Drag Link-Steering Arm

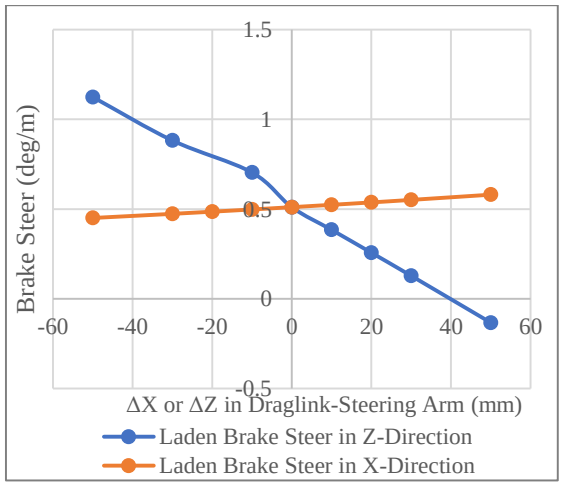

(f) Brake Steer vs Drag Link-Steering Arm

Figure 5.7: Graphs (e) & (f) representing bump and brake steer sensitivity with draglink-steering arm

Summary of sensitivity analysis for draglink-steering arm hardpoint

i. Brake & bump steer has high sensitivity in Z-direction than in X-direction.
ii. Brake steer is slightly sensitive in X-direction while bump steer is very less sensitive in X-direction variation.
iii. Shifting point vertically down will improve bump steer but worsen the brake steer.

Table 5.4: Axle spring hard points results

Axle Spring Hard Points Results				
Condition		Change in Hardpoints Value	Laden	
			Bump Steer (deg)	Brake Steer (deg/m)
Z-Direction	20mm Up	20	2.92	0.5145
	10mm Up	10	2.92	0.5126
	Original Hardpoints	0	2.92	0.5106
	10mm Down	-10	2.92	0.5085
	20 mm Down	-20	2.92	0.5082
	50 mm Down	-50	2.92	0.5004
X-Direction	50 mm Forward	50	2.9	0.6432
	30 mm Forward	30	2.91	0.5974
	10mm Forward	10	2.91	0.5397
	Original Hardpoints	0	2.92	0.5106
	10mm Behind	-10	2.92	0.4813
	30mm Behind	-30	2.92	0.4224
	50 mm Behind	-50	2.93	0.3636

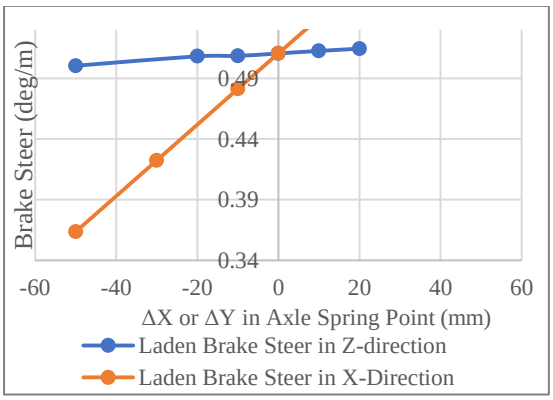

(g) Brake Steer vs Axle Spring

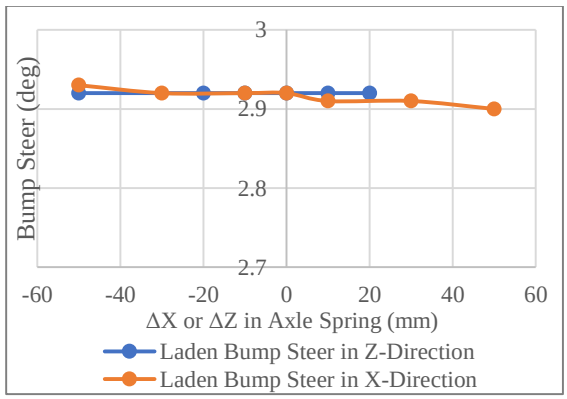

(h) Bump Steer vs Axle Spring

Figure 5.8: Graphs (g) & (h) representing brake and bump steer sensitivity with axle spring

Summary of sensitivity analysis for axle spring

i. Bump steer are not very sensitivity for the variation of point in Z-direction & X-direction.
ii. Brake steer is slightly sensitive in Z-direction but is very much sensitive in X-direction variation.
iii. Shifting point in rear direction will improve brake steer & vice-versa.

Axle Spring point change will have effect on other hardpoints as well because the axle position will be altered. Hence, only axle spring point variation study is not sufficient in real practice. After studying the effect of each hardpoint separately on brake and bump steer multiple changes of the hardpoints are then considered. Many numbers of iterations are then made and finally optimized hardpoints are proposed. Based on these hardpoints, design of linkages of steering and suspension system takes place and final design is released for prototype vehicle. Table 5.5 to Table 5.10 shown below illustrates some of important iterations made during optimization of linkages hardpoints.

* Note:	RED	Not Acceptable	YELLOW	At Par	GREEN	Acceptable

Table 5.5: Results of iteration 1 on base design (Before optimization)

Iteration 1 Base design (Before optimization)			
	Unladen	Laden	Overladen
Ackermann Error	At 0 deg., wheel steer angle = 0.13 deg.		
	At -35.5 deg., right wheel steer angle = 5.7 deg.		
	At 48 deg., right wheel steer angle = 3.9 deg.		
Bump Steer (deg)	40	39	38
Brake Steer (deg/m)	-3.6	-2.01	-1.04
	-3.7	-3.3	-2.5
	0.1	1.29	1.46
Pitman Arm Rotation (deg)	Unladen & Laden: 37° 43°, Overladen: 32° 48°		
PADL Toggle (deg)	150	151	180

First iteration was performed using the hardpoints of base. Draglink-to-steering arm ball joint hardpoint was located above steering arm. Results obtained after simulation shows that bump steer for all condition (unladen, laden and overladen) is very high and not acceptable. Similarly, Brake steer is higher in laden and overladen case and pitman arm-draglink toggle value for overladen case is also not acceptable. Based on sensitivity analysis study which shows there is improvement in brake steer when draglink-to-steering arm hardpoint is shifted vertically down

so for second iteration it is considered that draglink-to-steering arm hardpoint is shifted down by taking draglink ball joint from bottom of steering arm.

Table 5.6: Results of iteration 2 draglink-to-steering arm hardpoint shifted 96 mm down from base

Iteration 2. Drag link-to-steering arm hardpoint is shifted down by 96mm from base			
	Unladen	Laden	Overladen
Ackermann Error	At 0 deg., wheel steer angle = 0.13 deg.		
	At -35.5 deg., right wheel steer angle = 5.7 deg.		
	At 48 deg., right wheel steer angle = 3.9 deg.		
Bump Steer (deg)	8.7	7.3	6.7
Brake Steer (deg/m)	-0.29	0.63	1.11
	-0.53	-0.4	-0.3
	0.24	1.03	1.41
Pitman Arm Rotation (deg)	Unladen & Laden: 42° 44°, Overladen: 56° 44°		
PADL Toggle (deg)	150	151	180

Based on the second iteration. It is observed that bump steer has improved and obtained value is under the acceptable range. Brake steer and toggle optimization have to be done. Study of first and second iteration shows that the optimized hardpoint for the brake steer lies in between the above two points. For third iteration, considering steering arm to be shifted up by 33mm which in turn shifts draglink-to-steering arm point up by 33mm, we get the following results.

Table 5.7: Results of iteration 3 draglink-to-steering arm shifted 33mm up from iteration 2

Iteration 3 Draglink-to-steering arm hardpoint shifted 33mm up from iteration 2			
	Unladen	Laden	Overladen
Ackermann Error	At 0 deg., wheel steer angle = 0.13 deg.		
	At -35.5 deg., right wheel steer angle = 5.7 deg.		
	At 48 deg., right wheel steer angle = 3.9 deg.		
Bump Steer (deg)	18	17	16
Brake Steer (deg/m)	-1.38	-0.21	0.42
	-1.57	-1.31	-1.06
	0.19	1.1	1.48
Pitman Arm Rotation (deg)	Laden: 45° 44°,		
PADL Toggle (deg)	144	145	165

Shifting up draglink-to-steering arm hardpoint again worsen bump steer but studying both iterations, Y1 value changes from negative to positive and current value is nearer to zero value.

Table 5.8: Results of iteration 4 draglink-to-steering arm shifted 96 mm down & pitman arm moved by 20mm in X-direction from base

Iteration 4 draglink-to-steering arm shifted 96 mm down & pitman arm moved by 20mm in X-direction from base			
	Unladen	Laden	Overladen
Ackermann Error	At 0 deg., wheel steer angle = 0.13 deg.		
	At -35.5 deg., right wheel steer angle = 5.7 deg.		
	At 48 deg., right wheel steer angle = 3.9 deg.		
Bump Steer (deg)	9.5	8.5	7.6
Brake Steer (deg/m)	-0.36	0.62	1.11
	-0.5	-0.4	-0.3
	0.14	1.02	1.41
Pitman Arm Rotation (deg)	Unladen & Laden: 45º 46º, Overladen: 40º 45º		
PADL Toggle (deg)	140	141	159

It improved both bump steer and brake steer in comparison to base. Moreover, changing pitman arm in X-direction helped to improve toggle.

Table 5.9: Results of iteration 5 draglink-to-steering arm shifted 66 mm down & pitman arm moved by 20mm in X-direction from base

Iteration 5 draglink-to-steering arm shifted 66 mm down & pitman arm moved by 20mm in X-direction from base			
	Unladen	Laden	Overladen
Ackermann Error	At 0 deg., wheel steer angle = 0.13 deg.		
	At -35.5 deg., right wheel steer angle = 5.7 deg.		
	At 48 deg., right wheel steer angle = 3.9 deg.		
Bump Steer (deg)	8.6	7.8	7
Brake Steer (deg/m)	-0.3	0.67	1.15
	-0.5	-0.4	-0.3
	0.2	1.07	1.45
Pitman Arm Rotation (deg)	Unladen & Laden: 45º 46º, Overladen: 40º 45º		
PADL Toggle (deg)	140	141	163

Iteration 5 is the combination of change of hardpoints of iteration 3 and iteration 4. After several more iterations complete optimization of steering and suspension linkages taking into considerations brake steer, bump steer, pitman arm-to-draglink toggle etc. was achieved. Below tabulated result in Table 5.10 shows the final iteration result and is used to propose the optimized steering and suspension design.

Table 5.10: Results of final iteration for optimized hardpoints of steering and suspension linkages

Final iteration for optimized hardpoints of steering and suspension linkages			
	Unladen	Laden	Overladen
Ackerman Error	At 0 deg., wheel steer angle= 0.03 deg.		
	At -35.5 deg., right wheel steer angle= 3.8 deg.		
	At 48 deg., right wheel steer angle= 5.67 deg.		
Bump Steer (deg)	1.7	2.4	3.8
Brake Steer (deg/m)	0.28	0.19	0.04
	0.13	0.08	0.02
	0.15	0.11	0.02
Pitman Arm Rotation (deg)	Laden: 42.7° 45.2°,		
PADL Toggle (deg)	139	144	162

Bump and brake Steer both are optimized. Moreover, the PADL toggle value in overladen is at par condition but can be accepted. Major changes in the suspension leads to the change in hardpoint of bracket front pivot, spring shackle, axle spring. Change in front axle design and tire changed kingpin center, kingpin ground intersection point & axle spring. Variables like flat to bump, flat to rebound, flat to unladen, flat to laden and flat to overladen also changed.

Figure 5.9 to Figure 5.16 shown below illustrates the graph generated in ADAMS/View during front suspension and steering system optimization. Only graphs for first iteration (base design) and final iteration (optimized design) has been illustrated below.

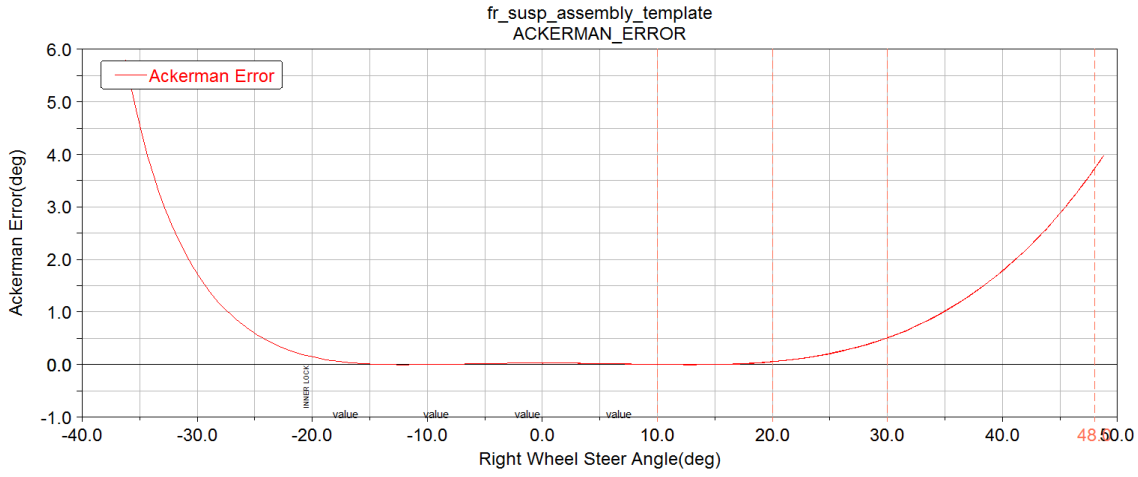

Figure 5.9: Ackerman error (Base design)

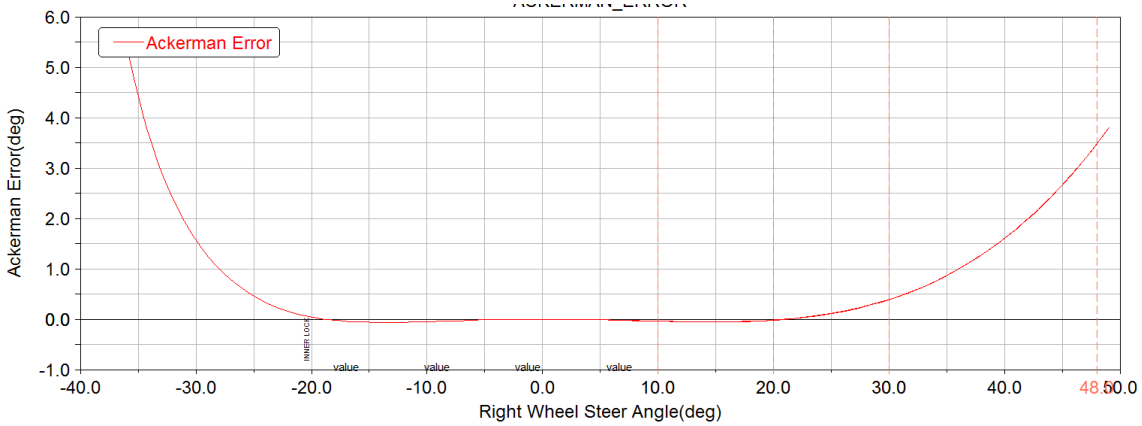

Figure 5.10: Ackerman error (Optimized design)

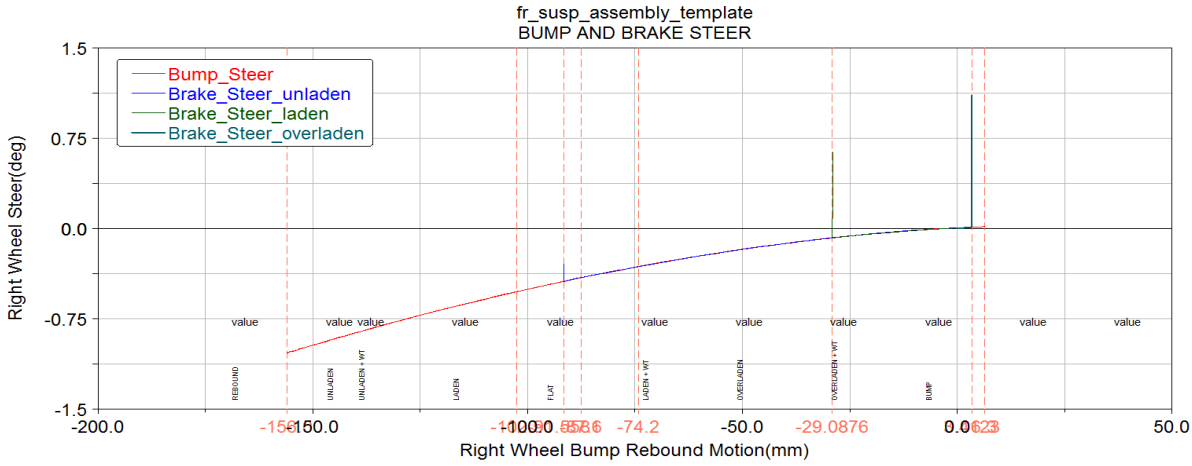

Figure 5.11: Bump and brake steer (Base design)

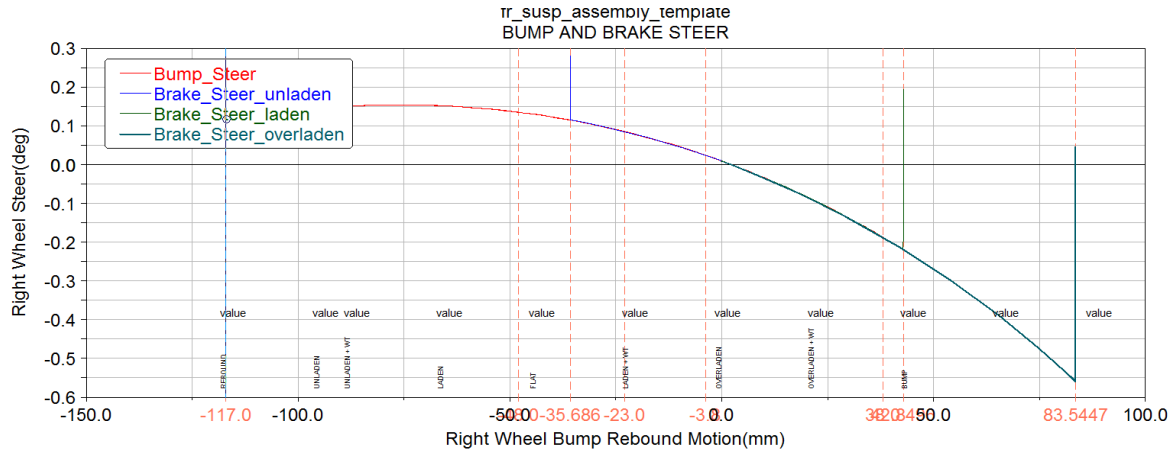

Figure 5.12: Bump and brake steer (Optimized design)

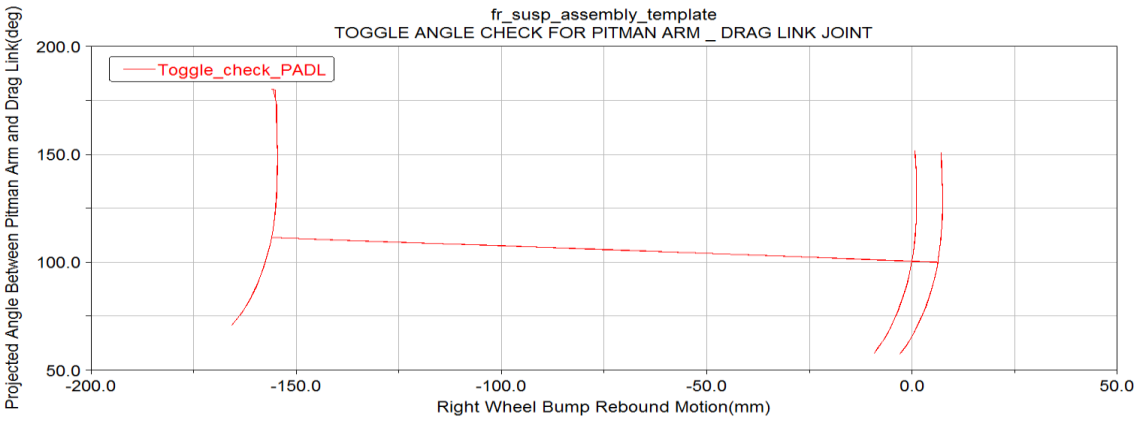

Figure 5.13: Toggle angle check for pitman arm drag link joint (Base design)

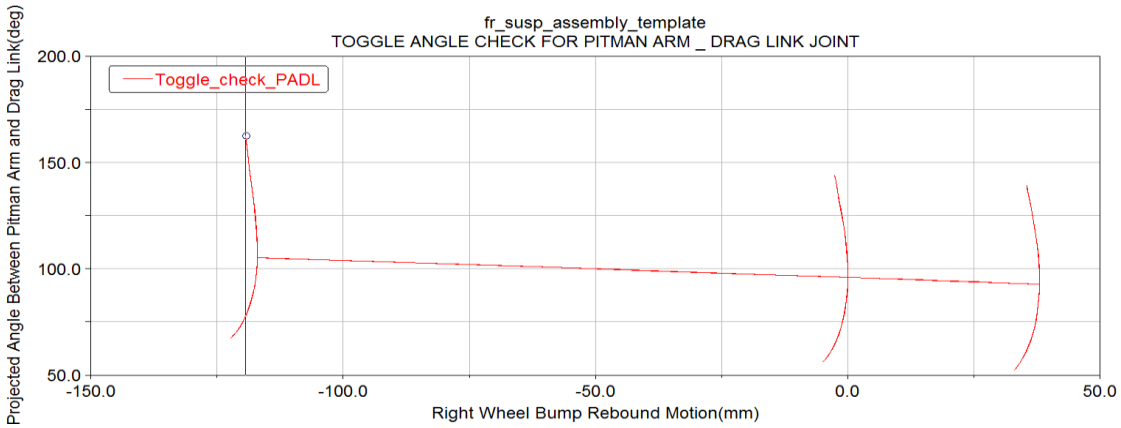

Figure 5.14: Toggle angle check for pitman arm drag link joint (Optimized design)

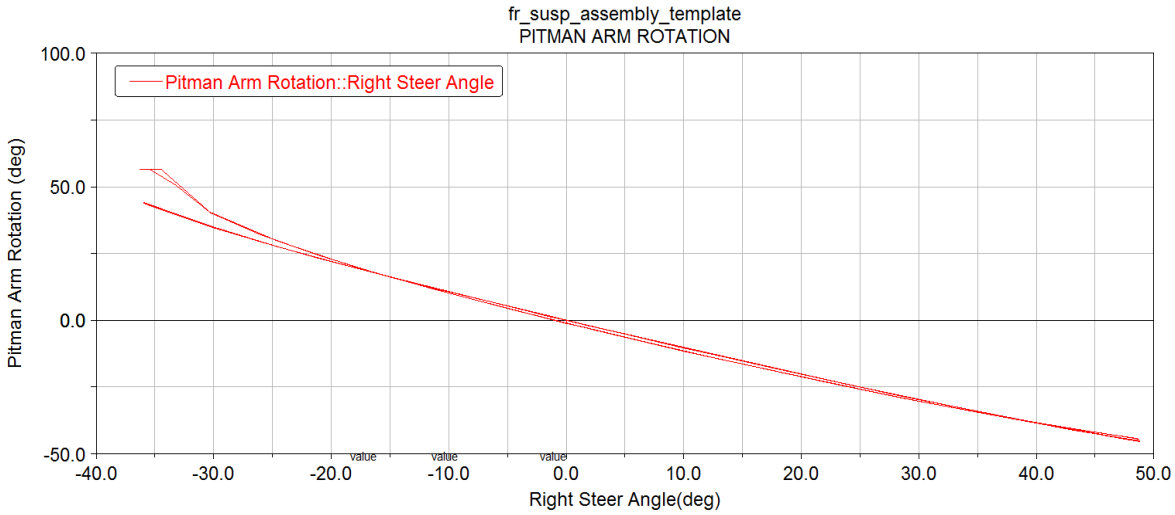

Figure 5.15: Pitman arm rotation (Base design)

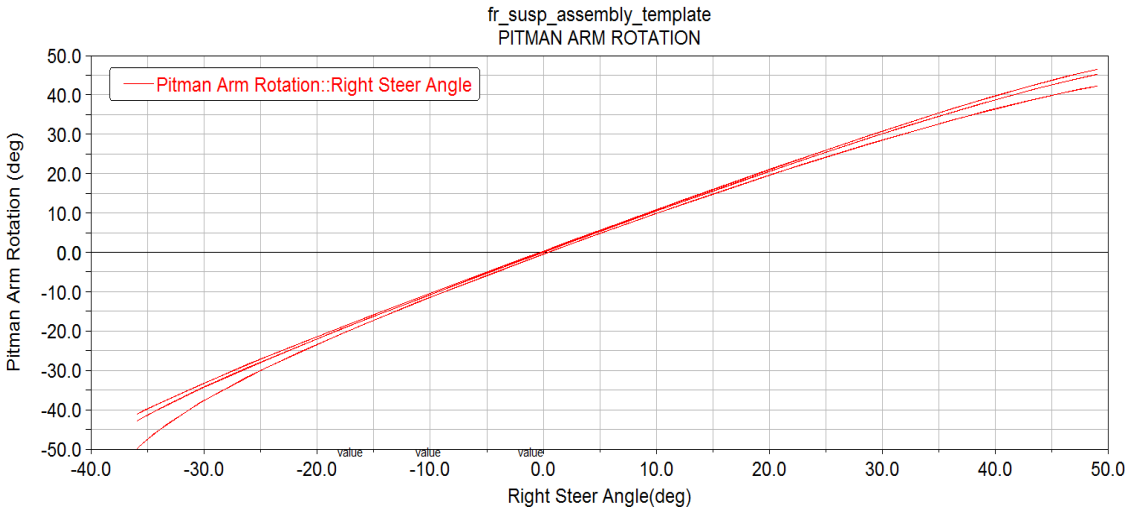

Figure 5.16: Pitman arm rotation (Optimized design)

After the optimization process of the steering and front suspension hardpoints, design of the steering system and front suspension begins. Figure 5.17, Figure 5.18 & Figure 5.19 represents the comparison of old design with new design of front suspension system, steering system and assembly of front suspension and steering system respectively. Comparison of design has been represented using tricolor where red represents old design while green represents the new design components and blue color represents the common overlapping parts.

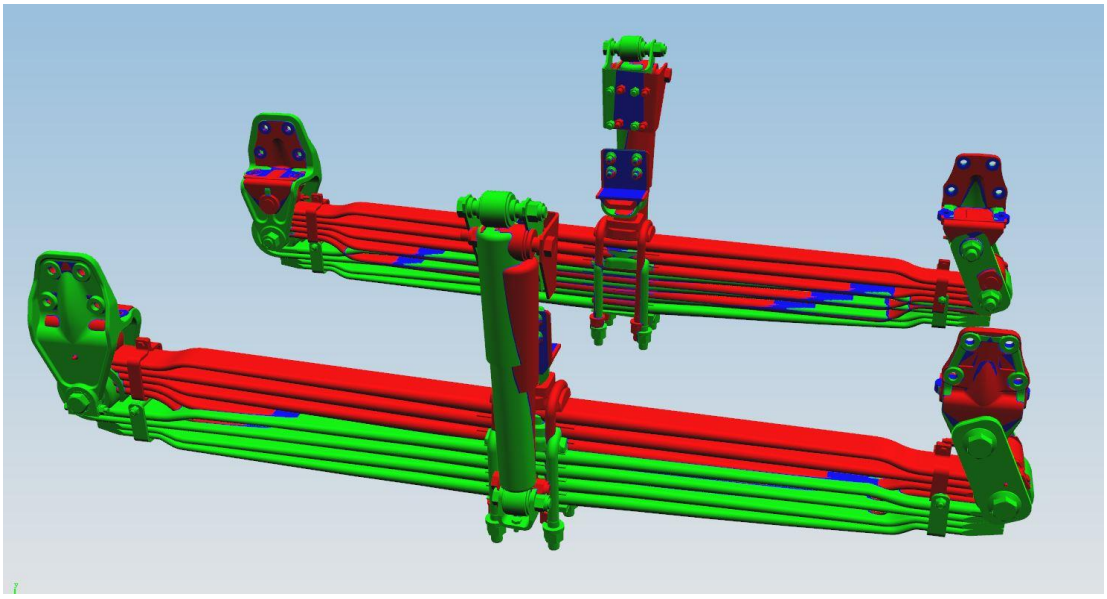

Figure 5.17: Design comparison of new suspension system with old suspension system

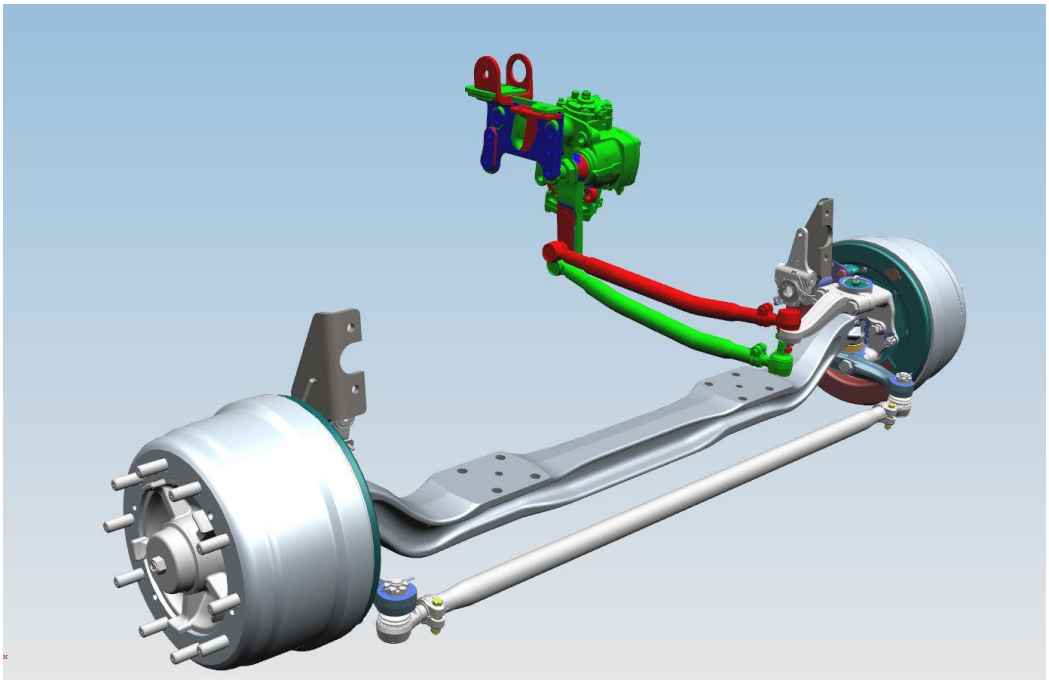

Figure 5.18: Design comparison of new steering system linkages with old steering system linkages

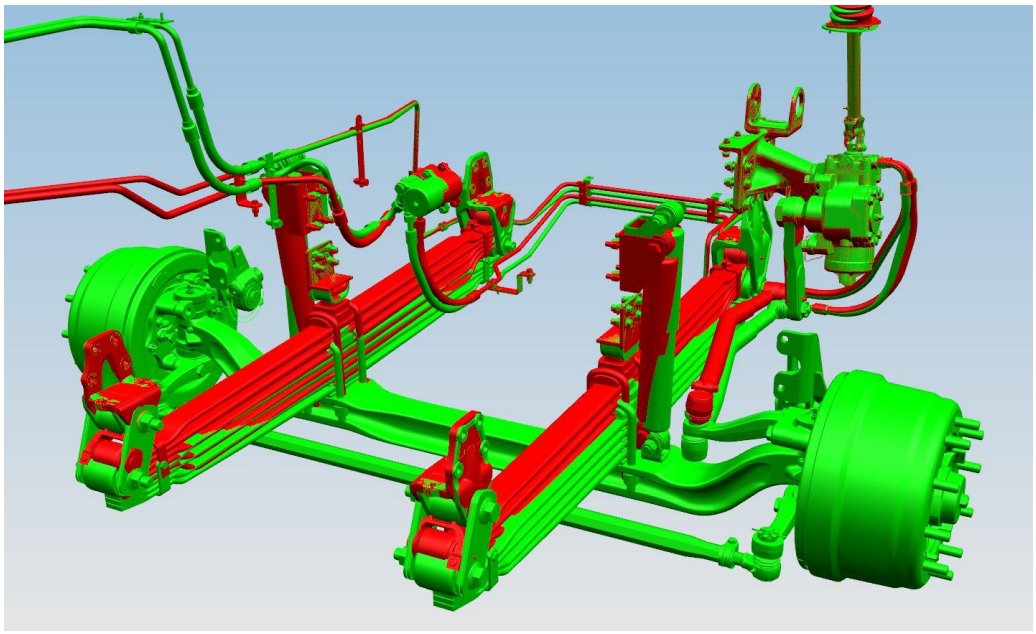

Figure 5.19: Comparison of new suspension and steering system design with old design

5.3 Modeling of Full Model Vehicle in ADAMS/Car

ADAMS, which is abbreviated as Automatic Dynamics Analysis of Mechanical Systems, is used for all types of vehicles from heavy commercial to light commercial vehicles and is also used for all passenger vehicles. Virtual prototyping of a vehicle in ADAMS includes following processes which are highlighted in below flow chart in Figure 5.20.

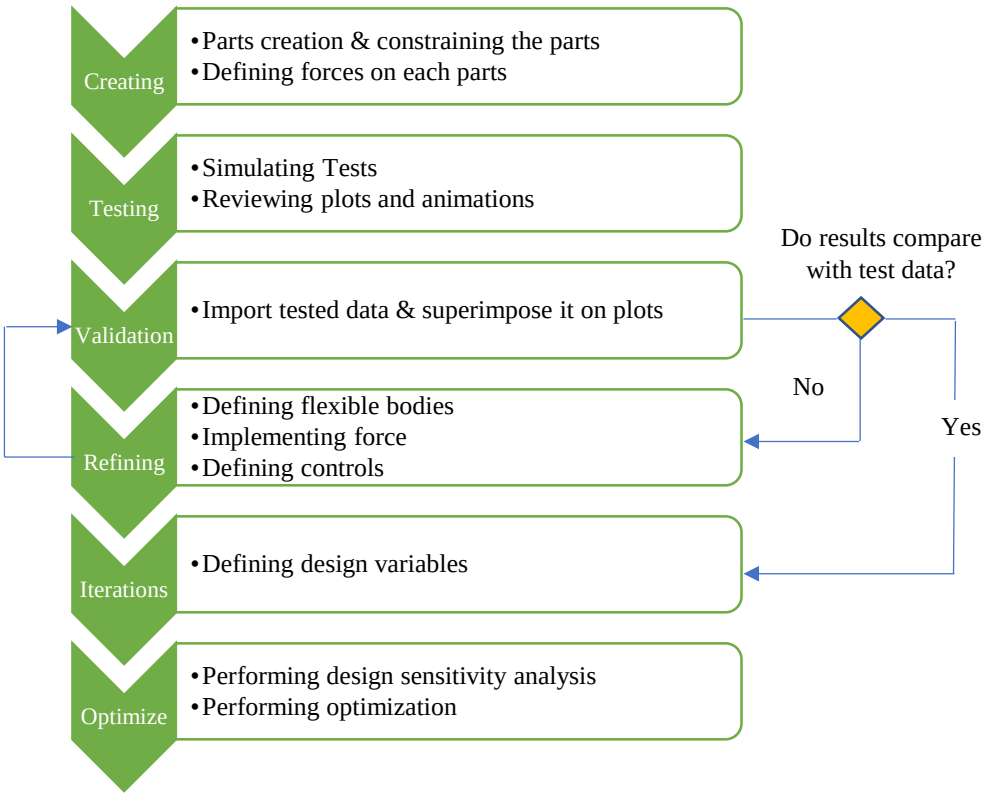

Figure 5.20: Flowchart showing virtual prototyping process

Full vehicle can be modelled in ADAMS/Car either using the built-in templates or by creating new templates. Built-in templates are easy to use since only the required data have to be modified in the template and the software automatically will constructs the subsystem models as well as full vehicle assemblies. While creating new templates requires core knowledge of modelling & is time consuming. Based on the comparison of built-in templates with the real vehicle subsystems, it is made sure that existing build-in template can be used or not. In the present study, built-in template has been used.

Real vehicle has following main subsystems; Steering system, chassis frame, front suspension, rear suspension, cabin, cabin suspension and wheels and tires. For other subsystems an overview information is provided.

5.3.1 Front Suspension

Vehicle is provided with rigid axle type front suspension. Some of its major components includes; leaf springs, knuckles, axle etc. which has been illustrated in the figure below. It has been made in Creo Parametric 3.0. Various suspension data is required which is made to fed in during modeling. Making use of graphical topology, a feature of ADAMS/Car, modelling process for the front suspension can be presented where all joints & connectors on a part is visible.

5.3.2 Front axle

All the various parts of the front suspension are connected to axle. Axle is modelled as rigid element. Figure 5.21 shown below illustrates the various parts and the joints that has been connected to the front axle.

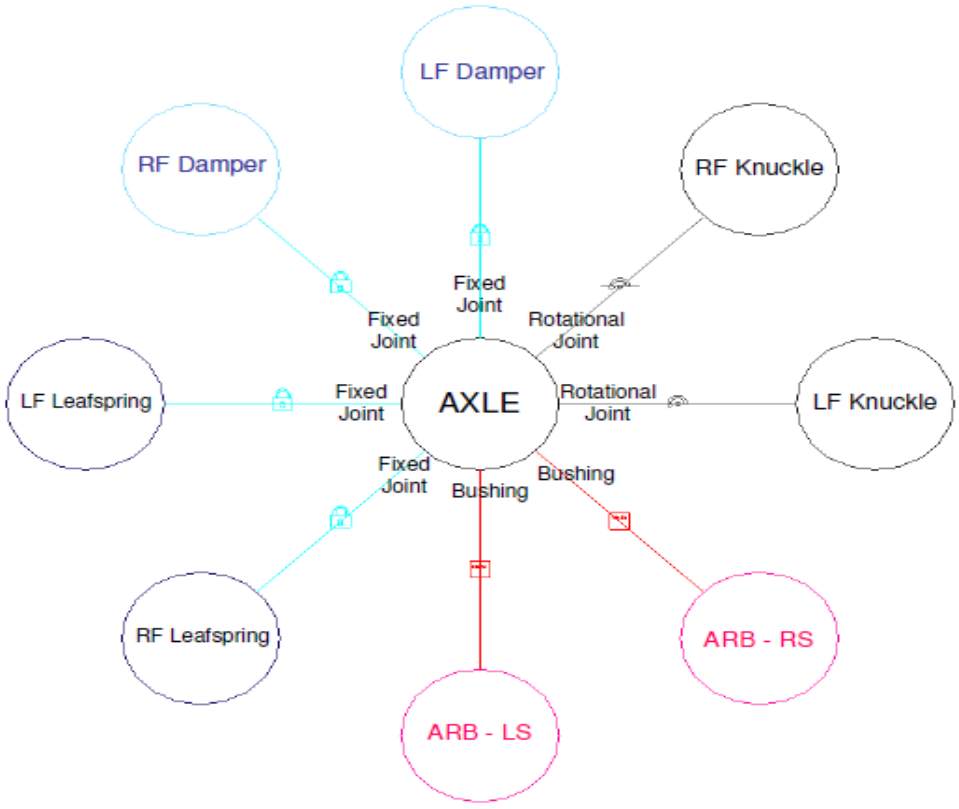

Figure 5.21: Graphical topology of front axle.

5.3.3 Leaf Spring

Front Suspension leaf springs is modelled as beam-elements. Data such as leaf spring geometry at its free position & bushing rates are needed so that to have an accurate modeling of leaf spring. These mentioned data are fed to the Leaf spring Pre-Processor for its modeling in ADAMS. Using 3 identical bushings leaf springs are made to connect to the chassis. One is at the front known as front eye bushing, second will be in rear between leaf springs and shackles while the third one is between chassis and shackles. Physical data and stiffness data will be then updated in the model. Figure 5.22 shown below illustrates the local coordinate system using which data are made to be input. Below graphs shown in Figure 5.23 to Figure 5.26 are used as input data for modeling of leaf spring.

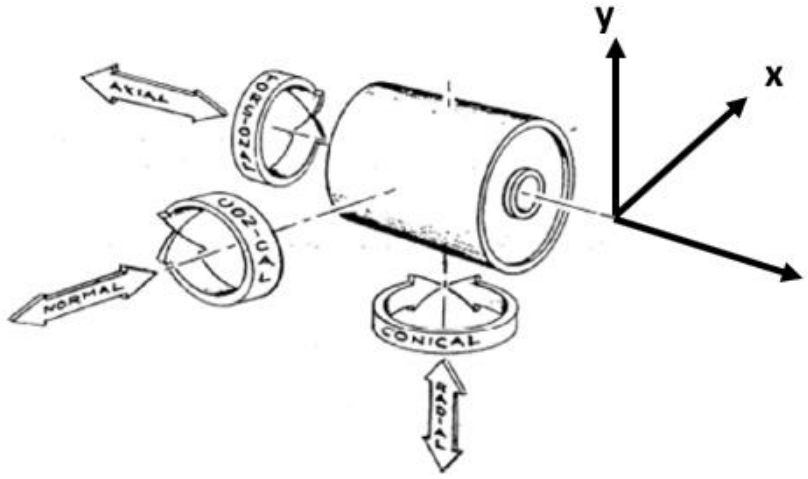

Figure 5.22: Local coordinate system for bushing [25]

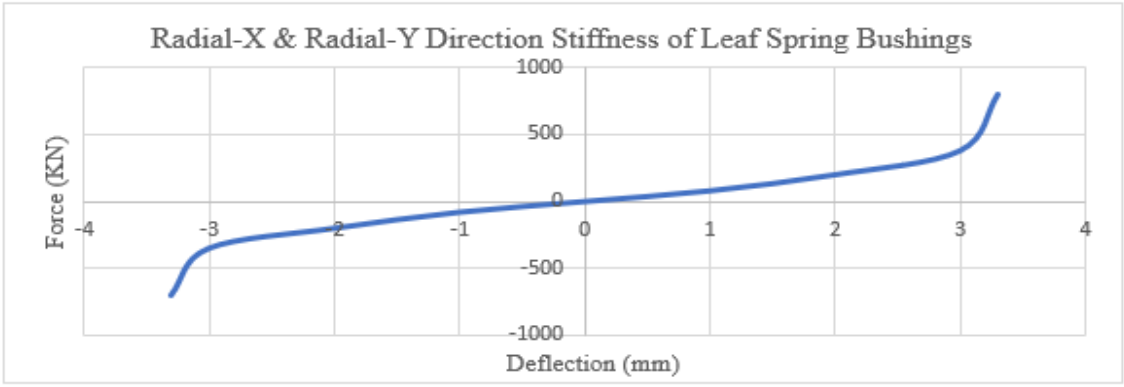

Figure 5.23: Leaf spring bushing radial – X direction & radial- Y direction stiffness plots

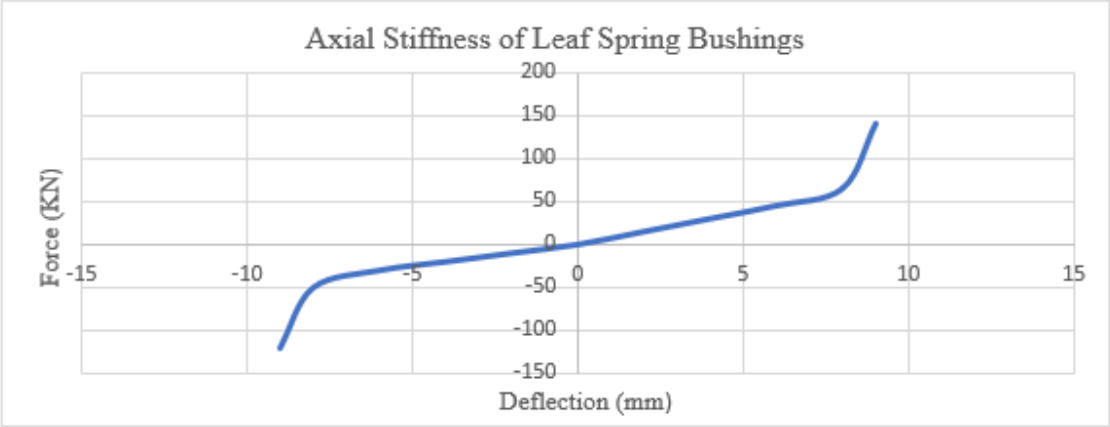

Figure 5.24: Leaf spring bushing axial stiffness plot

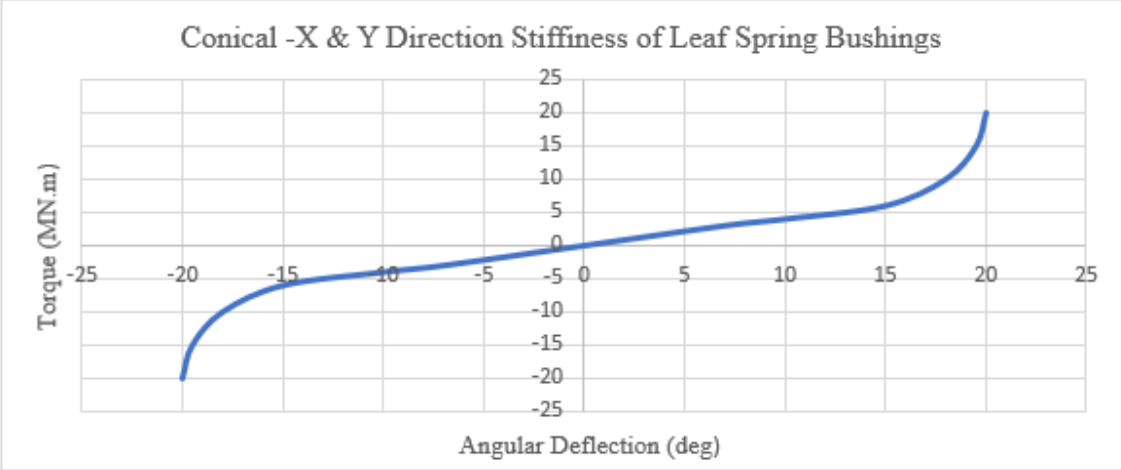

Figure 5.25: Leaf spring bushing conical – X direction & conical – Y direction stiffness plot

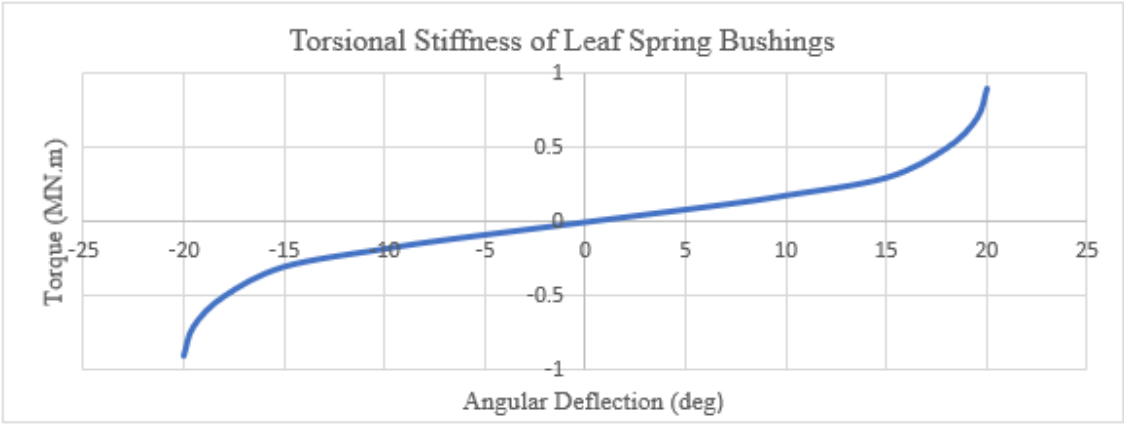

Figure 5.26: Leaf spring bushings torsional stiffness plot

5.3.4 Steering System

Major components of a steering system of a vehicle includes; a steering wheel, a steering column (translational joint), steering gear box (recirculating ball type), a pitman arm, draglink, upper (1 no.) & lower (2 no's) steering arms & a tie rod. 3D CAD model of a steering system of a commercial vehicle has been illustrated in the Figure 5.27.

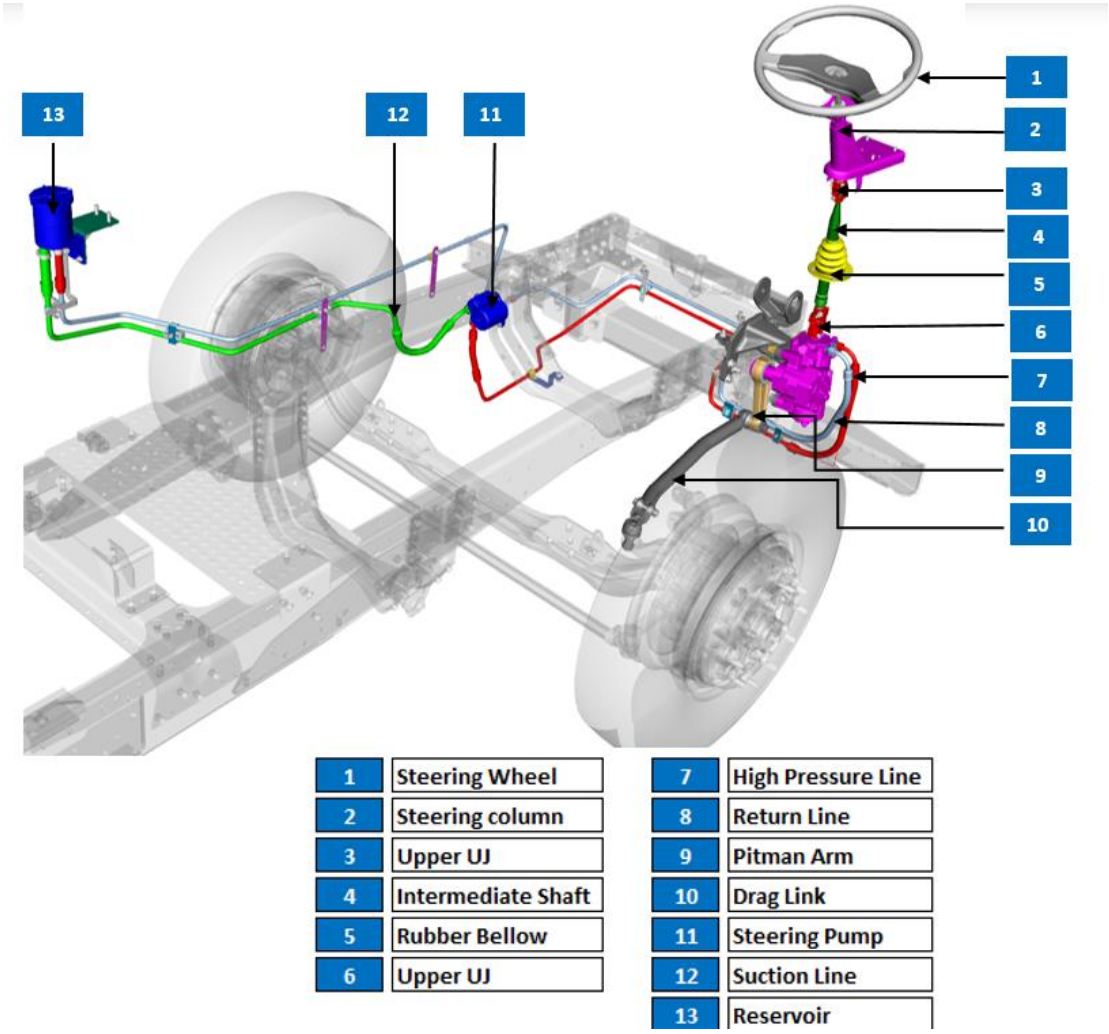

Figure 5.27: 3D CAD drawing of steering system of commercial vehicle

5.3.4.1 Steering Wheel

Steering wheel used in this vehicle is having the diameter of 470mm, which is having a playing a key role in driver applied efforts.

5.3.4.2 Steering Column

It consists of 2 universal joints provided with an intermediate shaft with translational joint which helps in compensating the cab movement with respect to the chassis.

5.3.4.3 Steering Gear Box

Steering Gear Box which has been used in this vehicle is having steering ratio of 26.4:1. In this steering ratio doesn't changes with respect to steering wheel angle.

5.3.4.4 Steering Linkages

Steering linkages includes lower steering arms, upper steering arm, draglink, tie-rod & pitman arm which defines kinematic characteristics of the system. Linkages design most be optimized for better handling, ride & ergonomics. Hardpoints optimized using ADAMS/View will be provided as an input.

Figure 5.28 shown below illustrates various linkages and its joints used in modelling of the steering system.

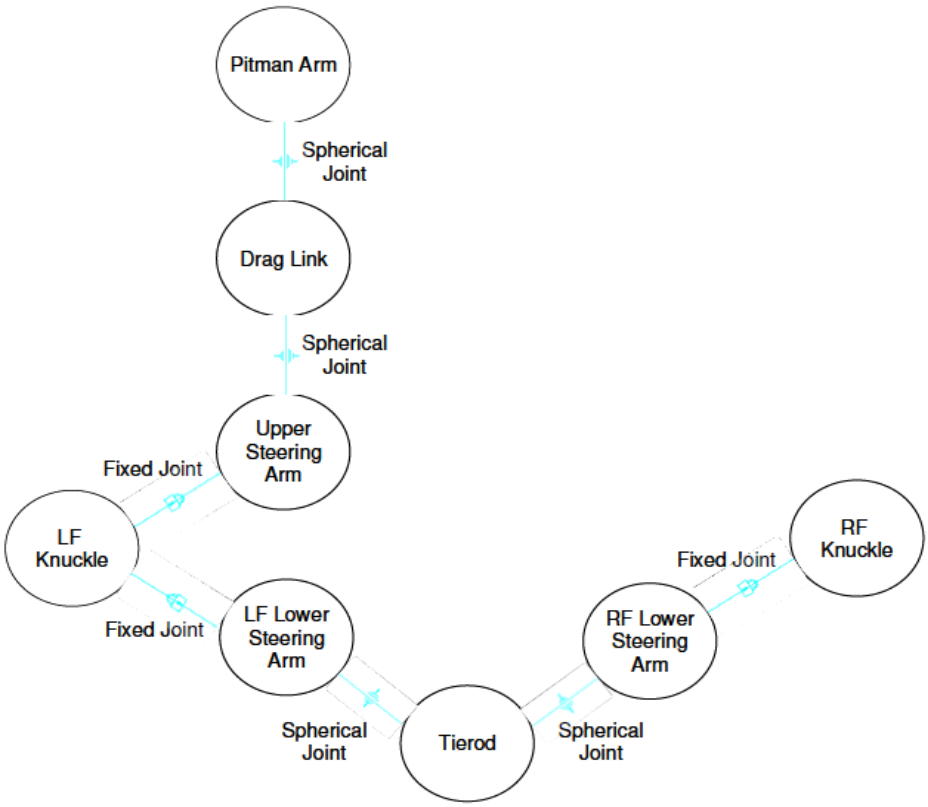

Figure 5.28: Graphical topology of the steering system

5.3.5 Rear Suspension

Vehicle is provided with rigid axle type rear suspension. Following mentioned are the major components that are needed to be modelled; Air spring, Tandem Leaf Springs & hubs. Figure 5.29 shown below illustrates the rear suspension of the vehicle which has been created in Creo Parametric 3.0. Suspension data such as stiffness, camber, toe angle etc. for the rear suspensions is fed. Figure 5.30 shown below illustrates the lift axle suspension of the vehicle.

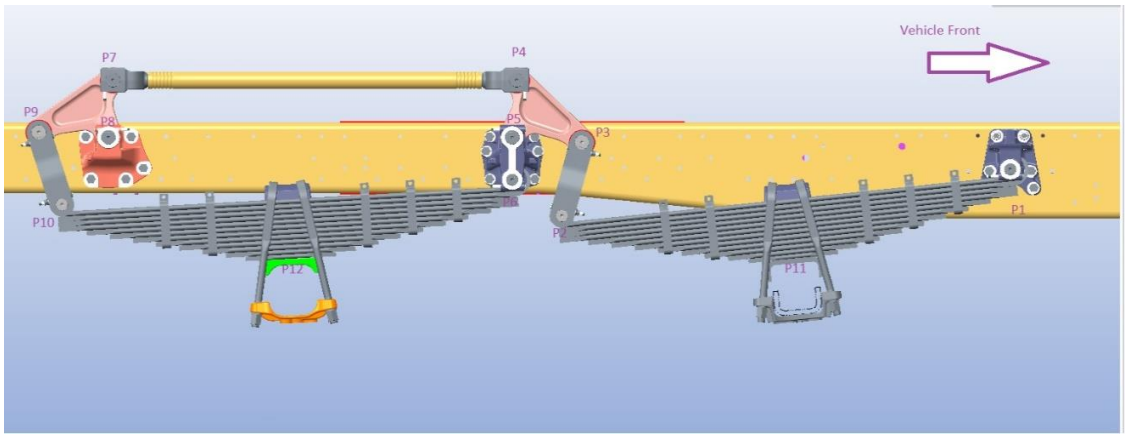

Figure 5.29: 3D CAD model of rear suspension with hardpoints (P1, P2…., P12)

Figure 5.30: 3D CAD model of lift axle suspension [30]

Mass of propeller shaft, differential and hubs (unsprung mass) will be modelled as lumped mass. Load-deflection measurements of air spring (adiabatic) are fed into the model. Figure shown below illustrates various data that has been used for model building or rear suspensions. Trim load of air springs are then adjusted to get required axle reaction at pusher axle. V-rod is connected to chassis frame at one end while another end is connected to differential. It has been modeled as rigid and its stiffness value is then fed.

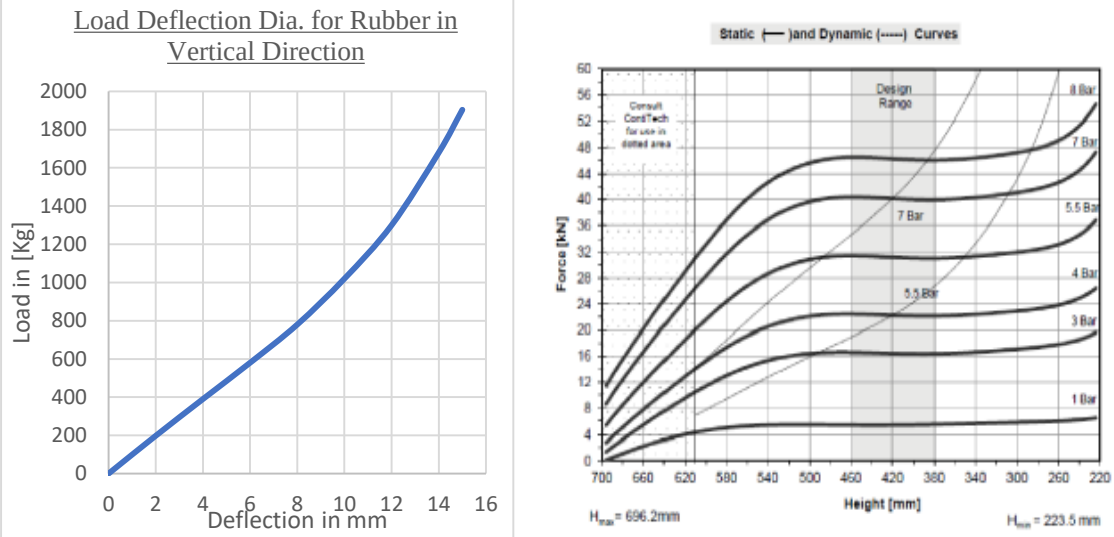

(a) Load vs Deflection (b) Force vs Height

Figure 5.31: Input data of lift axle for (a) Load vs Deflection, (b) Force vs Height

5.3.6 Chassis Frame

One of the main components of the vehicle on which almost all subsystems & parts are connected is the chassis frame which is modeled as a rigid part. Figure 5.32 shown below shows parts and joints which are connected to chassis frame.

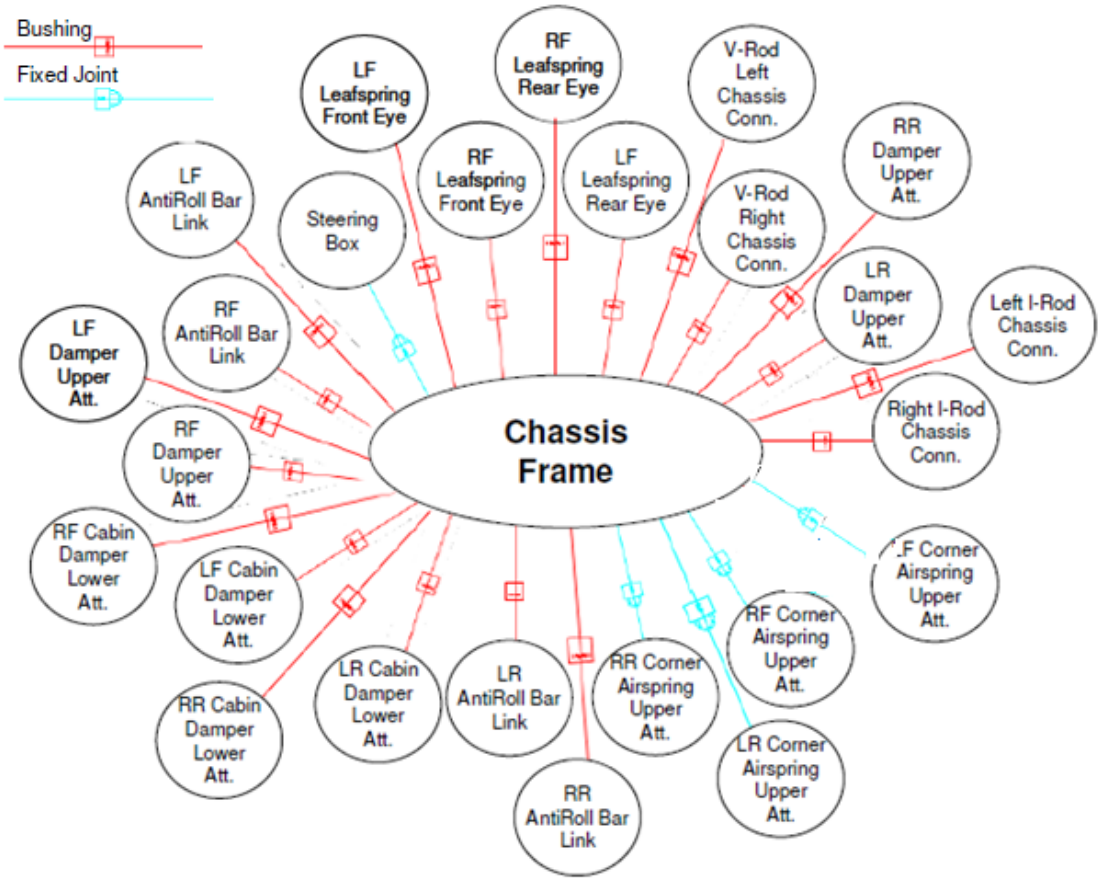

Figure 5.32: Graphical topology of the chassis frame

5.3.7 Wheel & Tires

For front and rear tires, the force and moment characteristics provided by the suppliers is used & entered in ADAMS during its modeling.

5.3.8 Cabin and its Suspension

Cabin suspension is modeled for spring-damper. Damping coefficient is feed while modeling of cabin suspension. Similarly, moment of inertial and center of gravity height for the cabin is modeled as lumped mass.

Other useful data such as axle loads, sprung and unsprung mass, C.G. height, moment of inertias etc. have to be correctly calculated (refer appendices for calculation method) and then feed into the system while modelling. Figure 5.33 shown below represents a full vehicle model of the vehicle modeled in ADAMS/Car.

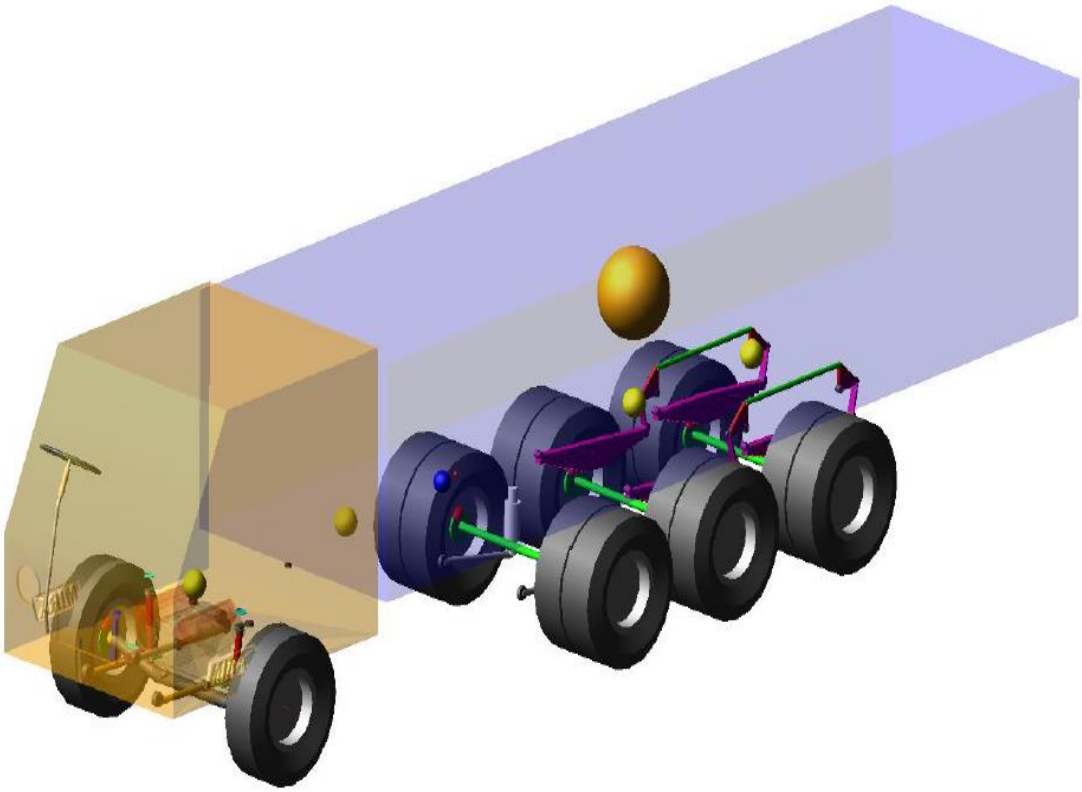

Figure 5.33: Full vehicle model prepared in ADAMS/Car

5.4 Simulation for Vehicle Handling Performance in ADAMS/Car

The 3D model of the vehicle prepared in ADAMS/Car is now used to analyze the handling behavior of the concept vehicle. Vehicle handling refers to the way how vehicle will respond to the inputs from a driver or how will it move along a road or track. It is evaluated by performing cornering, acceleration and braking & directional stability test in steady state condition.

Various test used for the evaluation of the vehicle handling performance are listed below;

i. Steady State Circular Test
ii. Transient Test
iii. Double Lane Change Test
iv. Shalom Test Weave Test

Steady state circular test is selected in this thesis for evaluating handling performance of concept vehicle. Simulation is carried out at a circular radius of 33m. Graphs for linear roll gradient, linear hand wheel angle (HWA) gradient & tire side slip angles obtained after simulations are illustrated below.

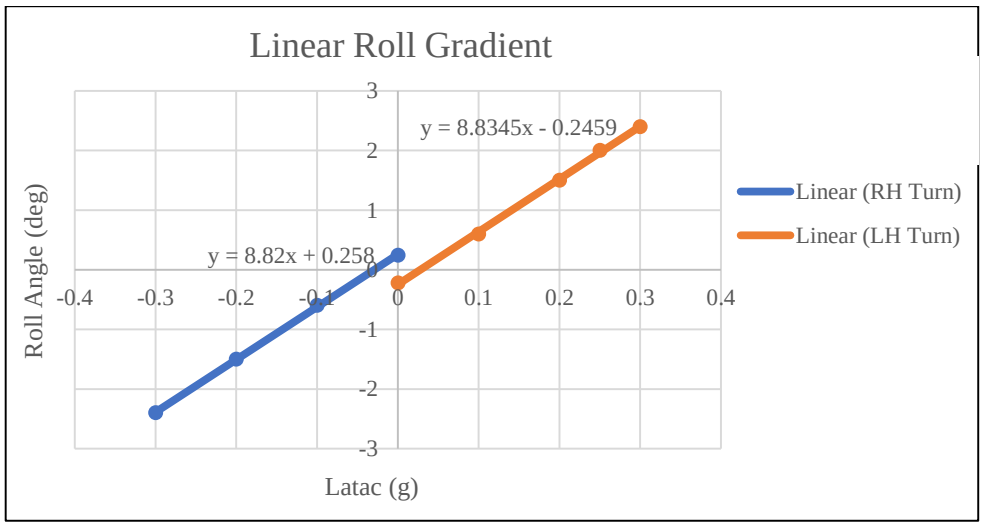

Figure 5.34: Linear roll angle (deg) vs Lateral acceleration (g)

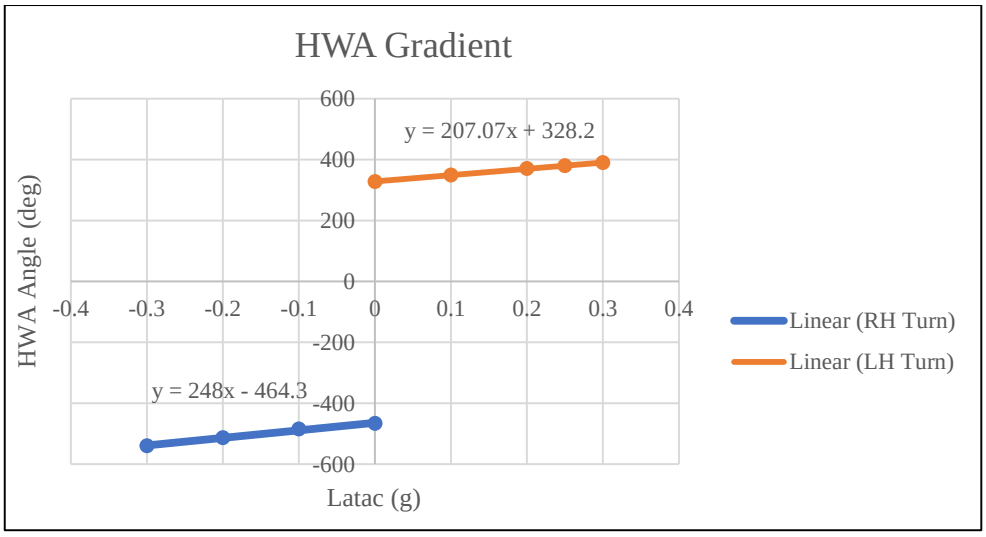

Figure 5.35: Hand wheel angle (deg) vs Lateral acceleration (g)

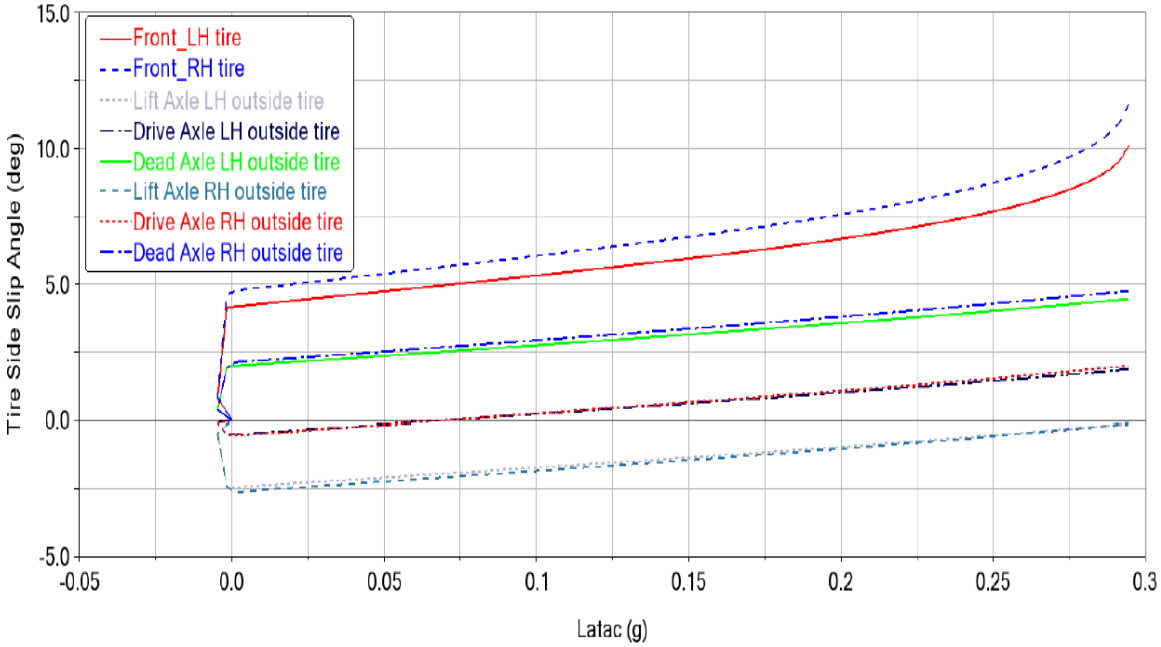

Figure 5.36: Tire side slip angle (deg) vs Lateral acceleration (g)

Consolidated result is tabulated below.

Table 5.11: Result of handling simulation

Steady state circular test at R=33m circle for proposed vehicle			
Parameters	Vehicle	Target	Remarks
Max. Speed (km/h)	32.65	NA	Beyond this speed, the wheel lift can occur at lift axle.
Max. Latac (g)	0.3		
Linear Roll Gradient (deg/g)- LH / RH	8.83/8.82	<11	Higher roll stiffness of lift axle because of stiff pivot bushing resulted in lower roll gradient.
Linear HWA gradient (deg/g) +ve value means understeer	207.1/248	50<G<180 (Understeer)	Higher front axle roll steer and more front tire slip leading to higher understeer

Handling Simulation Summary

- With the uniformly distributed load, the axle reaction at front axle is less than the rated load. In addition, the lift axle is seen to be lowering the axle reaction at drive axle.
- While steady state circular test simulation at R=33m circle, it is observed that lift axle wheels will be lifted after 0.3g lateral acceleration.
- Roll gradient of the vehicle is 8.83 deg/g. The roll of the vehicle is mainly restricted by lift axle, which have very high roll stiffness due to stiff pivot bushings.
- The vehicle exhibits highly understeer behavior. The higher front axle roll steer and higher tire slip at front axle resulted in highly understeer vehicle behavior.

CHAPTER 6
RESULTS AND DISCUSSION

Full-body 3D model of the concept vehicle was modeled in ADAMS/Car and then simulation for the handling behavior was carried out. Based on which, it was predicted that the vehicle will exhibit highly understeer behavior due to lateral forces on wheels of lift axle which will oppose the vehicle trajectory at time of cornering at low and high speed. After the development of the prototype vehicle, tests were performed on it and the highly understeer behavior was also observed on the real vehicle. Highly understeer behavior also causes problem for the vehicle to meet the TCD norms. Some of the major problem identified on the prototype vehicle are highlighted below:

1. Not meeting TCD requirement norms.
2. Highly understeer behavior.
3. Self-centering minimum requirement not meeting.

6.1 TCD Issue and Highly Understeer Behavior

Turning circle diameter of a vehicle mainly depends on the wheel lock angle, wheelbase & wheel track. Decision on what should be value of maximum wheel lock angle for the steering system is taken in the beginning during kinematics simulation i.e., while performing optimization of the steering system. If wheel lock angle is changed it will affect other parameters that depends on the steering wheel lock angle. Increasing wheel lock angle will improve TCD but there is a constraint over the enhancement of TCD by this method as certain limit lateral stiffness tire scrubbing starts and it increases tire wear[19]. Wheel track is fixed and therefore we can't play on this parameter. Wheelbase plays a decisive role in determining the TCD. We all have been familiar with the general expression of TCD for simple two axle vehicle having rigid rear axles and steerable front axle. Ellis[15] have recommended a method which states equivalent action of tandem axle bogie can be achieved using single equivalent axle placed midway between tandem spread with an assumption that shared load is equal between tandem axles and the cornering stiffness of all the tires being same. Equivalent wheelbase expression has been proposed which explains the equivalent wheelbase is dependent on the load on each axle and cornering stiffness of the tires. The actions taken to overcome the issue of meeting TCD requirements were

1. Steer by brake
2. Lift axle lifting/deployment control based on requirements
3. Caster steer sale (self-steerable axle)

6.1.1 Steer by Brake

It is method using which turning circle diameter of a commercial vehicle is tried to be reduced without making any changes in its geometry. Synchronization of the braking system with steering system is done for the enhancement vehicle low speed turning ability. In this selective breaking is done and steer is achieved by pivoting the table. The concept of torque vectoring has been used where controlled biased torque (differential torque) is distributed to the outer and inner wheel of the live axle which creates differential speed during cornering. It incorporates an electronic, a pneumatic and a torque distribution unit. Figure 6.1 shown below illustrates Controller-Electronic unit layout.

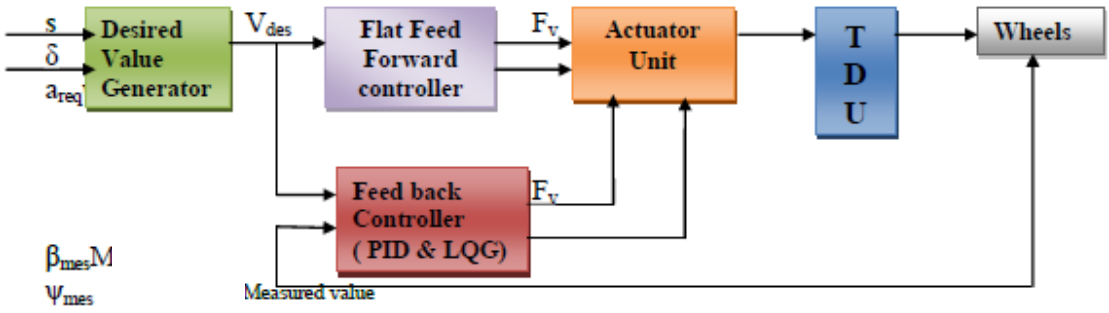

Figure 6.1: Controller-Electronic unit layout [21]

Steering angle (δ) from the steering wheel and desired acceleration (a_{req}) using pedal is provided to DVG which produces favored states (yaw rate, velocity & side slip angle). A flat feed forward controller is connected in parallel LQG & PID controller which calculates desired force along the vehicle length and yaw along vertical height of the vehicle. It helps to improve system dynamics. Linear Quadratic Gaussian (LQG) works for reducing lateral errors due to disturbances like side winds & PID controller reduces disturbance along longitudinal direction. Torque Distribution Unit (TDU) transfers requested torque to individual wheel by using pneumatic actuator which actuates torque vectoring differential. Figure 6.2 shown below illustrates schematic representation of operation of pneumatic system (straight ahead).

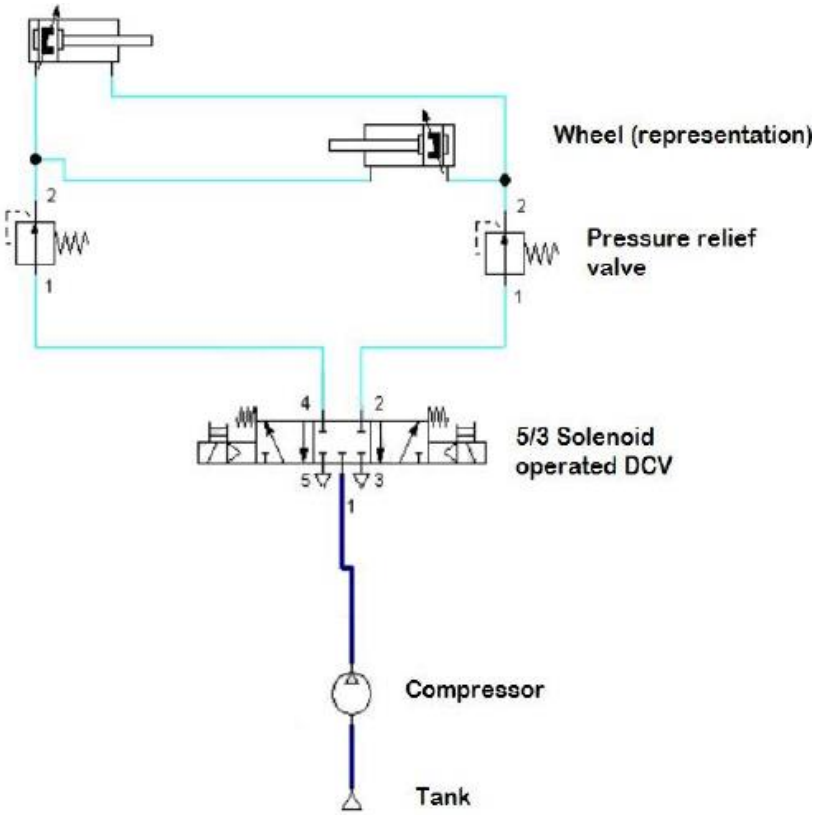

Figure 6.2: Schematic representation of operation of pneumatic system (Straight ahead) [21]

When the trial for the steer by brake was done improvement in the TCD was observed but it was not up to the mark as the result obtained from the trial doesn't fall under the target value. (TCD<24m).

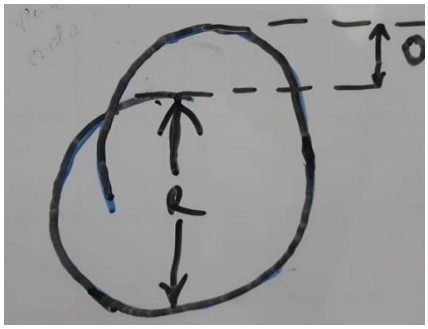

R- Stands for maximum diameter from start point in one turn.

O -Stands for offset observed between start and end point in one turn.

Figure 6.3: Path traced out by vehicle during steer by brake trial

Table 6.1: Result of steer by brake with and without automatic traction controller (ATC)

Parameter	LH	Remarks	Comments
TCD without ATC (R)	(X) m	Test conducted in full lock condition with steering wheel fixed at lock position and speed 7 kmph.	Lateral shift of vehicle observed with instability. Start point and end point for turning circle diameter do not match.
TCD with ATC (R)	(X-9) m	Test conducted in full lock condition with steering wheel fixed at lock position and speed 7 kmph.	Lateral shift of vehicle observed with instability, start point and end point for turning circle diameter do not match. TCD observed with ATC is less compared to without ATC but issue raised of lateral shift still persists.
Offset without ATC (O)	(Y) m	Test conducted in full lock condition with steering wheel fixed at lock position and speed 7 kmph.	Lateral shift of vehicle observed with instability, the start points and end point for turning circle diameter do not match.
Offset with ATC (O)	(Y-0.4) m	Test conducted in full lock condition with steering wheel fixed at lock position and speed 7 kmph.	Lateral shift with instability observed, the start points and end point for TCD do not match. TCD observed with ATC is less compared to without ATC but issue of lateral shift still persists.

6.1.2 Lift Axle Lifting/Deployment Control Based on Requirements

When the vehicle is in the laden case the lift axle will be in the grounded condition (lift axle down) for the uniform distribution of load at each axle. It was observed that the vehicle was facing an issue to meet TCD requirement norms for which a search of an alternative to solve the problem begins. Steer by brake didn't completely solved the problem and thus an algorithm-based controller was built based on which relation between steering lock angle and lift axle dropping and lifting was made. When the steering wheel is rotated it causes the front steerable wheels to steer and when it reaches a set angle while negotiating turn, the sensor senses and sends input to the ECU which further sends signal to controller which makes the lift axle to be lifted and when the steering wheel returns back to the straight ahead condition then ECU again sends the signal to the controller which in turn causes the lift axle wheel to drop to ground. Following are the results obtained from the simulation which shows satisfactory result in terms of meeting TCD norms and it also decreases the understeer behavior of the vehicle as the load on the drive axle and front axle is increased. The main disadvantages of using this technique is that it leads to an abuse loading condition and therefore load/stress at chassis long member and cross member

increases. Following are the simulation-based results which illustrates differences in the TCD of the vehicle when lift axle is grounded & lifted up.

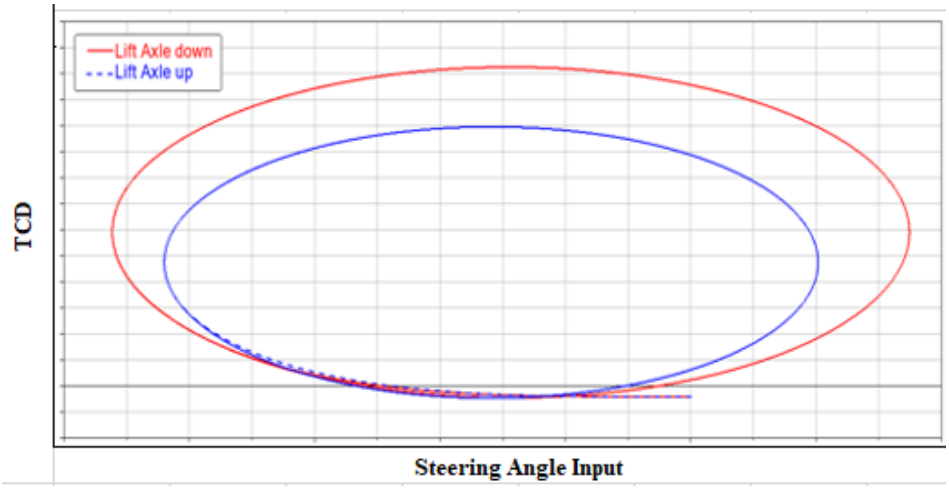

Figure 6.4: TCD of the vehicle for 1000 deg steering wheel angle input in lift axle up & lift axle down condition

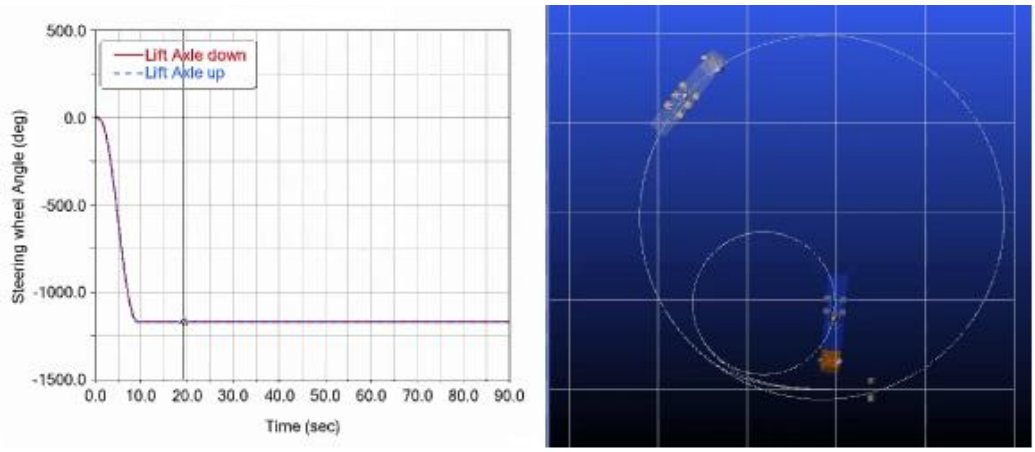

Figure 6.5: Position of a vehicle in both lift axle down and up condition taking circular turn after time duration, t=20 sec

Table 6.2: TCD value of vehicle in lift axle up & down condition

Condition of Vehicle	Lift Axle Down	Lift Axle Up
TCD for 1000 deg. SWA input	"X" m	"X-6.71" m
TCD for wheel lock angle input	"Y"	"Y-22.88" m

6.1.3 Caster Steer Axle

Self-steerable axle is known as caster steer axle. Caster steer axle align itself straight while having straight ahead motion & it starts to steer itself to left or right depending on the vehicle negotiating left or right turn respectively. The design of the steerable lift axle is different from the rigid lift axle. This idea is under the development stage having twin tires for the company. Steerable lift axle having single tires on each side of the axle has already been developed and validated. Steerable lift axle directly affects handling performance which has been already analyzed by Winkler[16], [17] with Pacejka's handling diagram. Following important facts regarding handling performance has been summarized[19]

- Vehicle tends to become oversteer i.e. handling quality starts to degrades with a rigid axle is replaced by a self-steered loaded auxiliary axle.
- As load is increased on self-steered auxiliary axle vehicle response tends to be more unstable.

General equations have been derived in literature [18] by Williams and Nhila based on which, vehicle which is having any number of axles & any number of non-steerable and steerable axles, understeer gradient & equivalent wheelbase of the vehicle can be calculated. Applying the concept used in literature[16]–[18], equations for equivalent wheelbase and understeer gradient for four axles vehicle having auxiliary axle in between first and third axle have been deduced and is listed below.

Equivalent Wheelbase for four axle vehicles =

$$\frac{\begin{aligned}[& C1{,}0C2{,}0N1N2(l-t-d)\text{^}2 + C1{,}0C3{,}0N1N3(l-t)\text{^}2 + C1{,}0C4{,}0N1N4l\text{^}2 + \\ & C2{,}0C3{,}0N2N3d\text{^}2 + C2{,}0C4{,}0N2N4(t+d)\text{^}2 + C3{,}0C4{,}0N3N4t\text{^}2\ ]\end{aligned}}{C1{,}0C2{,}0N1N2(l-t-d) + C1{,}0C3{,}0N1N3(l-t) + C1{,}0C4{,}0N1N4l}$$

Where,

Ci,0 = nominal side force coefficient on i^{th} axle

N*i* = actual normal load on i^{th} axle

l = geometric wheelbase

t = tandem spread

d = distance between 2nd axle and 3rd axle

Understeer Gradient for four axle vehicles =

$$\frac{-No[\,(C1,0-C2,0)N1N2(l-t-d)+(C1,0-C3,0)N1N3(l-t)+(C1,0-C4,0)N1N4l+(C2,0-C3,0)N2N3d+(C2,0-C4,0)N2N4(t+d)+(C3,0-C4,0N3)N4t\,]}{g\,[\,C1,0C2,0N1N2(l-t-d)+C1,0C3,0N1N3(l-t)+C1,0C4,0N1N4l\,]}$$

If 2nd axle is made caster steer then $C2,0 = 0$ and above equation could be further simplified.

Below mentioned results refers to simulation result for caster steer auxiliary axle. It clearly shows that the understeer behavior will degrade and this will lead to improve in handling characteristics compared to non-steerable lift axle. Moreover, TCD is improved as compared to result of non-steerable lift axle.

Table 6.3: Handling result after updating vehicle with self-steerable lift axle

Parameter	Target	Value
Roll gradient (LH / RH)- deg/g	< 11	9.3 / 9.27
HWA gradient (LH / RH)- deg/g	50 G < 180	116.3 / 123.4

6.2 Self-Centering Minimum Requirement Not Meeting.

For the identification of the cause behind not meeting self-centering minimum requirement, the frictional force distribution for steering linkages was done and its result has been shown in Table 6.4.

Table 6.4: Frictional force distribution for steering linkages

	LH (kgf)	%	RH (kgf)	%
Total Force	2.729	100%	3.773	100%
Tie rod	0.620	39%	0.953	25%
Drag Link	1.056	23%	0.670	18%
Steering Gearbox	0.748	27%	1.636	43%
Steering Column	0.305	11%	0.515	14%
Existing Self Centering	62.6%		64.4%	
Target Self Centering	70.0%		70.0%	

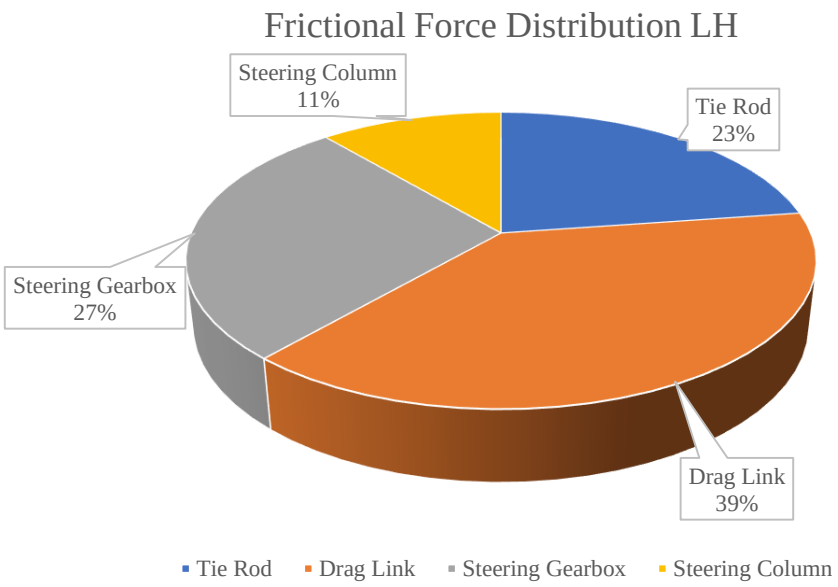

Figure 6.6: Frictional force distribution in left hand side of steering system

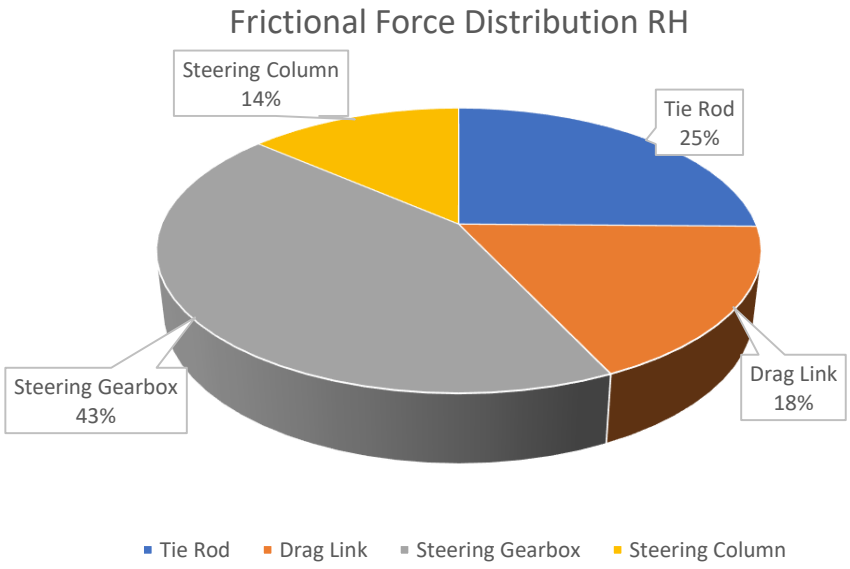

Figure 6.7: Frictional force distribution in right hand side of steering system

To improve self-centering, greaseable tie rod which was already modified in final design was replaced on the vehicle with proper greasing and drag links were replaced. After that self-centering measurement were repeated to understand the improvements. Self-centering target (>70% within 3 seconds) was achieved. Its result has been illustrated below in Table 6.5.

Table 6.5: Self-Centering for LH & RH cut after modification on vehicle

Particular	% Self Centering	Average % Self-Centering	Target	Remarks
LH Cut	70.25	71.32	70% within 3 sec	Self-Centering Laden
	70.10			
	73.60			
RH Cut	69.15	70.56		
	70.63			
	71.90			

The graph generated during experimentation of self-centering i.e. before and after modification that has been made in the vehicle to solve self-centering issue has been presented below.

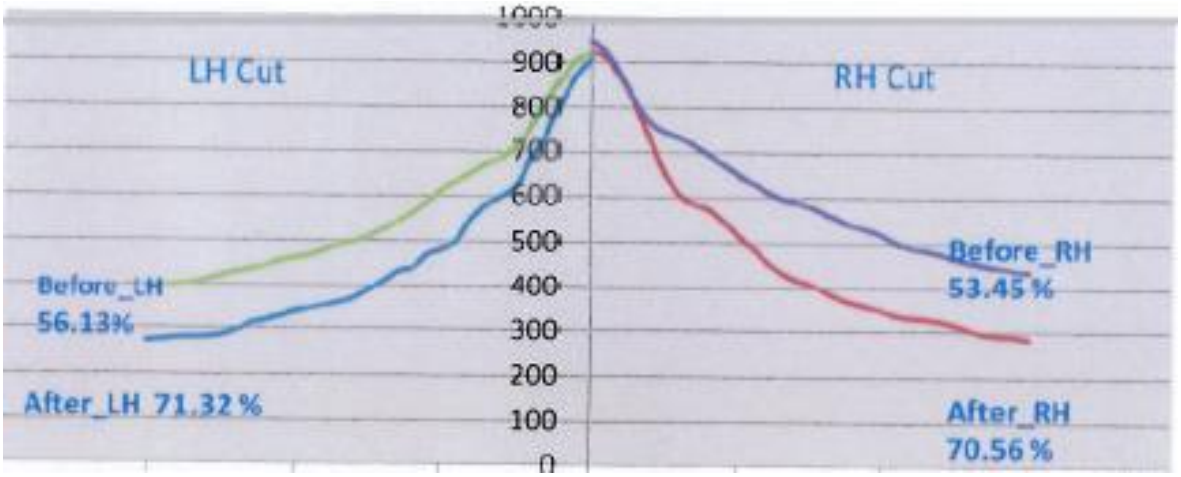

Figure 6.8: Graph for self-centering before vs after modification on vehicle

.

CHAPTER 7
CONCLUSION

During the development of previous generation of heavy-commercial vehicles, all the focus was given on performance, economy and durability (PED) which is just not enough these days to attract the customers. Other vehicle attributes such as steering, braking, NVH, cost of ownership, ride and comfort, ergonomics etc. has also been considered by the customers, while choosing a vehicle.

After IAL regulation implementation, major changes in the design of front axle, suspension & chassis has been proposed in order to provide provision of higher payload. Using these changes, DMU is created and hardpoints are taken i.e. known as base design hardpoints. Values of bump steer & brake steer in laden condition while PADL toggle in overladen condition for base design were 39 deg., 1.29 deg/m & 180 deg. respectively that were not acceptable therefore is reduced to 2.4 deg., 0.11 deg/m & 162 deg respectively in final iteration based on the changes made that has been highlighted in Appendix. Handling behavior is studied considering steady state circular test of radius 33m using optimized steering and suspension linkages. Maximum speed, maximum lateral acceleration & linear roll gradient (RH) were found to be 32.65 km/h, 0.3g & 8.82 deg/g respectively. Linear hand wheel gradient (RH) is 248 deg/g which means vehicle is highly understeer. During outdoor testing on real prototype vehicle, TCD requirement not meeting target, highly understeer vehicle behavior and self-centering issues were identified as the major problems. First corrective measure that is taken to solve TCD requirement is steer by brake concept which doesn't come up as a complete solution. Secondly, use of electronically controlled lift axle wheel is used which decreased TCD by 22.88m but also causes the load on front and rear wheels to exceed than rated load which is the case of an abuse loading. Finally, the concept of self-steerable lift axle is evaluated through simulation that helped to achieve TCD target & also solved highly understeer issue. Physical validation of self-steerable lift axle is planned as per design and development timeline. To solve self-centering issue, greaseable tie rod is modified in the final design and replaced on the vehicle with proper greasing which improved the self-centering of the vehicle and met the target of greater than 70% within 3 seconds. Thus, to conclude, both subjective evaluation and objective measurements show that the vehicle dynamics performance optimization study has been successful and will provide better straight-ahead controllability and handling experience as a result of which customers expectation will be met with the optimized design.

CHAPTER 8
SCOPE OF FUTURE WORK

As a next step, study for decreasing the number of iterations (simulation run), cutting down the timings of simulation and use of statistical approaches in order to evaluate brake and bump steer characteristic in the optimization study can be made. These three improvements when considered will definitely improve the optimization study efficiency and will decrease development as well as testing timings.

Future investigations are required to work on the optimization of the steering linkages design giving emphasis on the parameters like caster angle, camber angle, toe angle, kingpin inclination etc. which has direct effect on the vehicle's tire life. Increase in the tire life will help to attract more customers, as tire is one of the most expensive aggregate of a vehicle, and is thus need to be studied in detail separately. Similarly, transient handling trials should be studied for better vehicle handling performance.

TCD improvement using only steer by brake concept didn't gave satisfactory result thus steer by brake concept in association of ABS can be further studied which assists in decreasing vehicle TCD and thus may help in achieving TCD norms in our vehicle.

References

[1] MoRTH, *Revision of Safe Axle Weights for Transport Vehicles and Enforcement thereof.* 2018.

[2] V. A. Upadhyay, K. Gopalakrishna, and A. R. Kshirsagar, "A Simple, Cost Effective, Method of Evaluating Bump Steer and Brake Steer, and Achieving Correlation with ADAMS Analysis," in *SAE Technical Paper Series*, 2008, vol. 1, pp. 1–9.

[3] R. P. Rajvardhan, S. R. Shankapal, and S. M. Vijaykumar, "Effect of Wheel Geometry Parameters on Vehicle Steering," *SAS Tech J.*, vol. 9, no. 2, pp. 592–597, 2010.

[4] G. Rane and K. M. Narkar, "Steering System Optimization for Vehicle Drift," in *International Journal on Mechanical Engineering and Robotics (IJMER)*, 2014, vol. 2, no. 5,2014, pp. 16–20.

[5] U. Kulkarni, M. M. H. Gowda, and H. K. Venna, "Effect of Tie Rod Length Variation on Bump Steer," in *SAE Technical Paper Series*, 2016, vol. 1.

[6] T. S. Sonawane and S. D. Kachave, "Method of Assessing Bump Steer and Brake Steer, and Accomplishing Link with ADAMS," *Int. Adv. Res. J. Sci. Eng. Technol.*, vol. 3, no. 7, pp. 104–107, 2016.

[7] A. S. Ansara, A. M. William, M. A. Aziz, and P. N. Shafik, "Optimization of Front Suspension and Steering Parameters of an Off-road Car using Adams/Car Simulation," *Int. J. Eng. Res. Technol.*, vol. 6, no. 09, pp. 104–109, 2017.

[8] A. Gupta, B. Ghosh, A. Balasubramanian, S. Patil, and C. Raval, "Reducing Brake Steer Which Causes Vehicle Drift During Braking," in *SAE Technical Paper Series*, 2019, vol. 1, pp. 1–12.

[9] J. Agrawal, "Analysis of Spring Wind-up and Brake Steer in Heavy Commercial Vehicles," in *SAE Technical Paper Series*, 2015, vol. 1.

[10] M. Shridhare, S. Sonar, M. Ranawat, and A. K. Jindal, "Estimation and Reduction of Lateral Deviation (Brake Pulling) of a Vehicle due to Difference in Left and Right Wheel Brake Force," in *SAE Technical Paper Series*, 2017, vol. 1.

[11] J. W. Durstine, “The Truck Steering System from Hand Wheel to Road Wheel,” in *SAE Technical Paper Series*, 1973, vol. 1.

[12] S. Hasagasioglu, K. Kilicaslan, O. Atabay, and A. Güney, “Vehicle Dynamics Analysis of a Heavy-Duty Commercial Vehicle by Using Multibody Simulation Methods,” in *International Journal of Advanced Manufacturing Technology*, 2012, vol. 60, no. 5–8, pp. 825–839.

[13] A. C. C. Alvarez, E. Corte, L. Garbin, and V. de Almeida Lima, “Vehicle Dynamics Simulation at Commercial Vehicle Development,” in *SAE Technical Paper Series*, 2012, vol. 1.

[14] K. Hussain, W. Stein, and A. J. Day, “Modelling Commercial Vehicle Handling and Rolling Stability,” in *Proceedings of the Institution of Mechanical Engineers, Part K: Journal of Multi-body Dynamics*, 2005, vol. 219, no. 4, pp. 357–369.

[15] J. R. Ellis, “The Steering Characteristics of Multiple Axle Bogie Systems,” *Veh. Syst. Dyn.*, vol. 5, no. 4, pp. 221–238, 2007.

[16] D. E. Williams, “On the Equivalent Wheelbase of a Three-Axle Vehicle,” *Veh. Syst. Dyn.*, vol. 49, no. 9, pp. 1521–1532, 2011.

[17] D. E. Williams, “Generalised Multi-Axle Vehicle Handling,” *Int. J. Veh. Mech. Mobil.*, vol. 50, pp. 149–166, 2012.

[18] D. Williams and A. Nhila, “Handling Comparison of Vehicles with Steerable Auxiliary Axles,” *SAE Int. J. Commer. Veh.*, vol. 6, no. 2, pp. 281–287, 2013.

[19] C. A. Vichare, A. Gupta, G. Bandaru, and S. Palanivelu, “Evaluation of the Tire Wear Possibility due to Non-Steerable Twin Tire Lift Axle on Heavy Commercial Vehicle,” in *SAE Technical Paper Series*, 2019, vol. 1, pp. 1–6.

[20] J. Shukla, A. Grinspan, and J. Subramanian, “Design and Analysis of Lifting Pusher Drop Axle for Heavy Commercial Vehicle,” *SAE Int. J. Commer. Veh.*, vol. 10, no. 1, pp. 8–17, 2017.

[21] A. k Alex, R. Sasikumar, P. V Vijomon, R. Vishnu, and D. M. Shanmugharaj, “Design and

Analysis of Brake Assisted Torque Steering System for Heavy Commercial Vehicle to Reduce Turning Circle Diameter," *Int. J. Innov. Res. Sci. Eng. Technol.*, pp. 1–6, 2017.

[22] V. Upadhyay, A. Pathak, A. Kshirsagar, I. Khan, and K. Nandkeolyar, "Development of Methodology for Steering Effort Improvement for Mechanical Steering in Commercial Vehicles," in *SAE Technical Paper Series*, 2010, vol. 1.

[23] S. Bennett, *Heavy Duty Truck Systems*. 2011.

[24] B. Ozan, "Steering System Optimization of a Heavy Commercial Vehicle to Improve Straight Ahead Controllability Using Kinematics & Compliance," Istanbul Technical University, 2012.

[25] URL-1, [Online]. Available: http://auto.howstuffworks.com/steering3.htm.

[26] URL-2, [Online]. Available: http://www.skf.com/portal/skf/home.

[27] J. Reimpell, H. Stoll, and J. W. Betzler, "The Automotive Chassis: Engineering Principles," *Butterworth-Heinmann, Oxford*, 2001.

[28] T. D. Gillespie, "Fundamentals of Vehicle Dynamics," *Society of Automotive Engineers*. Society of Automotive Engineers, Warrendale.

[29] J. Y. Wong, "Theory of Ground Vehicle." John Wiley & Sons, New York, ISBN 0 471 52496 4., 2001.

[30] URL-3, Available: https://reycogranning.com/suspensions-cat/lift-axle-suspension/.

APPENDIX-I Calculation for Axle Reaction and C.G. Height

Note: Data's have been changed. Following data are just to illustrate the method followed to obtain datas that will be used as inputs during simulations in ADAMS.

Reactions at each axle & C.G. Calculation										
		Total Weight on Vehicle			Distance from Vehicle Cordinate System			Moment		
	Aggregates	Weight(Kg) [A]	Quantity [B]	Weight on Vehicle [C] = AXB	X-Distance From VCS [D]	Y- Distance (Vehicle Width Centre Line) [E]	Z-Direction (From Long Member Top) [F]	Distance from FACL (Front Axle Centre Line) [G] = C-0	Moment in X-direction at FACL [H] = C X G	Moment in Z-direction at LM Top [I] = C X F
Sprung Mass	Cab	800	1	800	-450	0	1000	-450	-360000	800000
	Engines with Flywheel Housing	500	1	500	-85	0	-203.7	-85	-42500	-101850
	Radiator Assembly	45	1	45	-820	0	55	-820	-36900	2475
	Air Filter Assembly	25	1	25	-1100	-613	-125	-1100	-27500	-3125
	Engine mount RH on chassis side	20	1	20	480	286.5	-125	480	9600	-2500
	Clutch	80	1	80	480	0	-229.5	480	38400	-18360
	Gearbox & Clutch housing	200	1	200	540	0	-317	540	108000	-63400
	GSL linkages + Mtg bkt on Engine+GSL Hand Lever	15	1	15	540	0	-317	540	8100	-4755
	Clutch Booster Assembly+ Kit Piping Clutch+Clutch Control Assembly with Foot Rest+Clutch Master Cylinder	15	1	15	480	0	-229.5	480	7200	-3442.5
	Acc. Pedal unit + mtg bkt+assly stopper	5	1	5	-830	0	55	-830	-4150	275
	Frame Assly	900	1	900	300	0	-145	300	270000	-130500
	Assly FUPD	70	1	70	-1100	0	-525	-1100	-77000	-36750
	Asly RUPD	30	1	30	7800	0	-470	10593	317790	-14100
	Assly SUPD	30	1	30	3000	0	0	3000	90000	0
	Front Spring hanger mtg bkt	25	1	25	-900	433.2	-315.5	-900	-22500	-7887.5
	Front Spring hanger mtg bkt-RH	40	1	40	980	434.39	-267	980	39200	-10680
	Rear sp hanger mtg bkt -RH	15	1	15	5500	497	0	5500	82500	0
	Rear sp hanger mtg bkt -RH	20	1	20	7000	506.5	0	7000	140000	0
	Rear sp hanger mtg bkt-RH	20	1	20	8100	494.5	0	8100	162000	0
	Fuel tank assly	450	1	450	1400	816	-300	1400	630000	-135000
	Spare wheel + carrier assy	120	1	120	7000	-639.5	-411.5	7000	840000	-49380
	Battery Assembly	100	1	100	3700	-801	-147	3700	370000	-14700
	Electrical Aggregates Weight	30	1	30	5300	0	-142.5	5300	159000	-4275
	Air tank assly	35	1	35	4000	783	-150	4000	140000	-5250
	Assly APU	10	1	10	3000	270	-200	3000	30000	-2000
	Purge tank	5	1	5	3000	-315	-200	3000	15000	-1000
	Spring brake actuator on drive axle	20	1	20	4800	355	-592	4800	96000	-11840
	Spring brake actuator on dummy axle	20	1	20	6300	355	-600	6300	126000	-12000
	Spring brake actuator on Lift axle	20	1	20	3500	355	-400	3500	70000	-8000
	Front Axle Relay Valve + Modulator with Mtg Bkt	6	1	6	1500	0	-150	1500	9000	-900
	Rear Relay Valve + Modulator with Mtg Bkt + Relay Valve for Parking + Lift Axle Relay	7	1	7	6000	0	-150	6000	42000	-1050
	Pnumatic Bunch + Metal Piping Compressor	10	1	10	4500	450	-285	4500	45000	-2850
	Exhaust system	44	1	44	3500	180	-450	3500	154000	-19800
	Urea tank assly	65	1	65	2500	-750	-350	2500	162500	-22750
	Propeller shaft (1)	25	1	25	1900	0	-285	1900	47500	-7125
	Propeller shaft (2)	30	1	30	3200	0	-285	3200	96000	-8550
	Propeller shaft (3)	50	1	50	5400	0	-490	5400	270000	-24500
	Lift Axle valves	35	1	35	6750	0	-150	6750	236250	-5250
	Tools	10	1	10	-1000	-300	0	-1000	-10000	0
	Steering System	250	1	250	-100	450	-200	-234	-58500	-50000
	Miscellaneous	150	1	150	5421.2	0	567	5421.2	813180	85050
	Load body (without load)	2000	1	2000	5421.2	0	567	5421.2	10842400	1134000

Unsprung Mass	Front Axle Assy-F1(with Brake drums)	480	1	480	0	0	-560	0	0	-268800
	Wheel Rim & Tyre Front	120	2	240	0	-1042	-560	0	0	-134400
	Front Spring Assembly	300	1	300			-460	0	0	-138000
	Wheel Rim & Tyre Rear (Rear Front)	120	4	480			-550	5485	2632800	-264000
	Wheel Rim & Tyre Rear (Rear Rearward)	120	4	480			-550	6915	3319200	-264000
	Rear Forward Axle Assembly (Axle+Stubaxle+Hub+Wheel Assy etc) + Rear Suspension partial load	750	1	750			-552	5390	4042500	-414000
	Rear Rearward Axle Assembly + Rear Suspension Partial Load	450	1	450			-560	6820	3069000	-252000
	Rear Front Springs Assembly	300	1	300			-330	5390	1617000	-99000
	Rear Rear Springs Assembly	280	1	280			-365	6820	1909600	-102200
Lift Axle Assly	Lift Axle Assembly Sprung Wts(i.e. Side Rail, Structural Parts)	350	1	350			-280	4040	1414000	-98000
	Lift Axle Assembly Unsprung Wts.(i.e. Axle Assly with Lower Links)	500	1	500			-545	4040	2020000	-272500
	Wheel rim & Tyre Lift Axle (Unsprung)	120	4	480			-545	4040	1939200	-261600

Total Weight with Load body (Sum of aggregates weight)	11437	Kg	GVW	40500	Kg
Total Weight without Load body	9437	Kg	Payload	29063	Kg

Weight of Load Body with Payload	31063	1	31063
Moment of Load Body with Payload (WeightX C.G. distance of Load Body and Payload)	31063 X 5421.2 =	168398735.6	

Input			
FOH	1379	mm	Input
F1-Lift Axle	4040	mm	Derived
Lift Axle -R1	1350	mm	Input
R1-R2	1430	mm	Input
ROH	2868	mm	Derived
Total Vehicle Length	11067.4	mm	Derived
Loadbody Start From FACL	1154	mm	Input
Loadbody Length	8534.4	mm	Derived
Loadbody Length	28	feet	Input
Load body CG in X-direction from VCS	5421.2	mm	Derived
% of Rear Overhang	46.98	mm	Derived
Wheel Base	6105	mm	Input

Output			
Pusher Axle Grounded			
Load at Lift Axle Pusher (12.5 T)	12500	Kg	Fixed
Reaction at Rear Axle	23726	Kg	Derived
Load at Front Axle (F1)	4274	Kg	Derived
C.G in X-direction w.r.toFront Axle C/L	4823.4	mm	Derived
Pusher Axle Lifted Up			
Load at Lift Axle Pusher (12.5 T)	0	Kg	Fixed
Reaction at Rear Axle	31998	Kg	Derived
Load at Front Axle (F1)	8502	Kg	Derived
C.G in X-direction w.r.to Front Axle C/L	4823.4	mm	Derived

Sprung Mass	7084.5
CG in X-direction	2653.4
Cg in Y-direction	0.0
Cg in Z- direction	137.5

		Axle 1	Axle 2	Axle 3	Axle 4
	Unsprung Mass	870	1006.3	1406.3	1070.0
	CG in X-direction	0	4037.3	5395.3	6862.6
(Assumed)	Cg in Y-direction	0	0.0	0.0	0.0
	Cg in Z- direction	-542.8	-540.8	-443.8	-530.0

Using calculation for chassis height (Refer Appendix-II)				
Chassis Height	1055	1067	1073	1080
C.G. Z from ground	512.2	535.5	636.7	566.8

APPENDIX-II **Chassis Height Calculation Under Various Loading Conditions**

Inputs										
Common Inputs for various load conditions										
Unsprung Mass for front Axle	870	Kg	Stiffness of Front Forward spring (F1)	Assumed value to demonstrate the process for calculation of chassis height	60	Kg/mm	DIMN(Flat Load) for Front Spring	Assumed value to demonstrate the process for calculation of chassis height	570	mm
Unsprung Mass for Rear Forward Axle	1406	Kg	Stiffness of Rear Forward spring (R1)		125	Kg/mm	DIMN(Flat Load) for R1 Spring		550	mm
Unsprung Mass for Rear Rearward Axle	1070	Kg	Stiffness of Rear Rearwardspring (R2)		125	Kg/mm	DIMN(Flat Load) for R2 Spring		565	mm
Unsprung Mass for Lift Axle (Pusher)	1006	Kg	Axle Drop of front forward Axle		75	mm	SLR for Front Forward Tyre		493	mm
Distance between Front Axle and C/L of Rear Axle	6105	mm	Per Spring Load (Flat Load for F1)		7100	Kg	SLR for Lift Axle Tyre		493	mm
Distance between front Axle and Lift Axle	4040	mm	Per Spring Load (Flat Load for R1)		7400	Kg	SLR for Rear Forward Tyre		493	mm
Spacer (Front)	0	mm	Per Spring Load (Flat Load for R2)		7400	Kg	SLR for Rear Rearward Tyre		493	mm
Inputs for different load conditions (Refer Appendix-I to calculate axle reaction under various conditions)										
Unladen Condition				**Laden condition (8X2)**				**Laden condition (6X2)**		
		UDL			**Rated**	**UDL**				**UDL**	
Front Forward Axle Weight	-	5247	Kg	Front Forward Axle Weight	7000	4274	Kg	Front Forward Axle Weight	-	8502	Kg
Lift Axle Weight	-	0	Kg	Lift Axle Weight	12500	12500	Kg	Lift Axle Weight	-	0	Kg
Rear Forward Axle Weight	-	3095	Kg	Rear Forward Axle Weight	10500	11863	Kg	Rear Forward Axle Weight	-	15999	Kg
Rear Rearward Axle Weight	-	3095	Kg	Rear Rearward Axle Weight	10500	11863	Kg	Rear Rearward Axle Weight	-	15999	Kg
GVW	-	11437	Kg	GVW	40500	40500	Kg	GVW	-	40500	Kg
Results										
Unladen Condition				**Laden condition (8X2)**				**Laden condition (6X2)**		
		UDL			**Desired**	**UDL**				**UDL**	
Load on Front axle spring		4377	Kg	Load on Front axle spring	6130	3404	Kg	Load on Front axle spring		7632	Kg
Load on Lift axle		0	Kg	Load on Lift axle	11494	11494	Kg	Load on Lift axle		0	Kg
Load on R1 axle spring		1689	Kg	Load on R1 axle spring	9094	10457	Kg	Load on R1 axle spring		14593	Kg
Load on R2 axle spring		2025	Kg	Load on R2 axle spring	9430	10793	Kg	Load on R2 axle spring		14929	Kg
Load on each side Front Spring		2188.5	Kg	Load on each side Front Spring	3065	1702	Kg	Load on each side Front Spring		3816	Kg
Load on each side Lift Axle		0	Kg	Load on each side Lift Axle	5747	5747	Kg	Load on each side Lift Axle		0	Kg
Load on each side Rear Forwad Spring (R1)		844.5	Kg	Load on each side Rear Forwad Spring (R1)	4547	5228.5	Kg	Load on each side Rear Forwad Spring (R1)		7296.5	Kg
Load on each side Rear Rearward Spring (R2)		1012.5	Kg	Load on each side Rear Rearward Spring (R2)	4715	5396.5	Kg	Load on each side Rear Rearward Spring (R2)		7464.5	Kg
Deflection (Front Forward Axle)		-81.86	mm	Deflection (Front Forward Axle)	-67.25	-89.97	mm	Deflection (Front Forward Axle)		-54.73	mm
Deflection (Rear Forward Axle)		-52.44	mm	Deflection (Rear Forward Axle)	-22.82	-17.37	mm	Deflection (Rear Forward Axle)		-0.83	mm
Deflection (Rear Rearward Axle)		-51.10	mm	Deflection (Rear Rearward Axle)	-21.48	-16.03	mm	Deflection (Rear Rearward Axle)		0.52	mm
Height of LM top to F1 Centre		576.86	mm	Height of LM top to F1 Centre	562.25	584.97	mm	Height of LM top to F1 Centre		549.73	mm
Height of LM top to Lift axle Centre		598.31	mm	Height of LM top to Lift axle Centre	573.77	577.84	mm	Height of LM top to Lift axle Centre		554.98	mm
Height of LM top to R1 Centre		602.44	mm	Height of LM top to R1 Centre	572.82	567.37	mm	Height of LM top to R1 Centre		550.83	mm
Height of LM top to R2 Centre		616.10	mm	Height of LM top to R2 Centre	586.48	581.03	mm	Height of LM top to R2 Centre		564.48	mm
Chassis Height for F1		1069.86	mm	Chassis Height for F1	1055.25	1077.97	mm	Chassis Height for F1		1042.73	mm
Chassis Height for Lift Axle		1091.31	mm	Chassis Height for Lift Axle	1066.77	1070.84	mm	Chassis Height for Lift Axle		1047.98	mm
Chassis Height for R1		1095.44	mm	Chassis Height for R1	1065.82	1060.37	mm	Chassis Height for R1		1043.83	mm
Chassis Height for R2		1109.10	mm	Chassis Height for R2	1079.48	1074.03	mm	Chassis Height for R2		1057.48	mm
Chassis Height for Rear Tandem Axle Centre Line		1102.27	mm	Chassis Height for Rear Tandem Axle Centre Line	1072.65	1067.20	mm	Chassis Height for Rear Tandem Axle Centre Line		1050.66	mm
Nose Down		32.41	mm	Nose Down	17.40	-10.77	mm	Nose Down		7.92	mm
Critical Ground Clearance at Lift Axle (Pusher)		189.31	mm	Critical Ground Clearance at Lift Axle (Pusher)	NA	NA	mm	Critical Ground Clearance at Lift Axle (Pusher)		145.98	mm

APPENDIX-III Calculation of Load Transfer

			Unladen Condition	Laden Condition	Overladen Condition
Deceleration value	Input	in terms of 'g'	0.6	0.6	0.6
Height of CG from ground	Input	in 'mm'	1085	1645	1688
Wheel base	Input	in 'mm'	6105	6105	6105
GVW of vehicle	Input	in Tons	11.437	40.5	52.65
Static load on each tyre	Input	in Kgs	2623.5	2137	4550
Dynamic radius (rolling radius)	Input	in mm	513	513	513
Wt transfer to the front axle	Derived	Kgs	1219.6	6547.7	8734.5
Wt transfer to each tyre	Derived	Kgs	609.8	3273.8	4367.2
Total Weight on each tyre	Derived	Kgs	3233.3	5410.8	8917.2
FAW	Ff	Kgs	5247	4274	5556.2
GVW	P	Kgs	11437	40500	52650
Deceleration Value	z	in terms of 'g'.	0.6	0.6	0.6
CG from ground	h	mm	1085	1645	1688
Wheelbase	l	mm	6105	6105	6105
Reaction due to braking force	Rf=(Ff +(P*z*h/l	Kgs	6466.6	10821.7	14290.7
Brake force generated at the front axl	Tf=mu * (Rf)	Kgs	5496.6	9198.4	12147.1
Tyre dynamic radius	r	m	0.513	0.513	0.513
Brake torque	Fb	Kg-m	2819.7	4718.8	6231.4
		(per front wheel)	1409.9	2359.4	3115.7

For overladen condition, 30% additional than rated load is considered.

APPENDIX-IV Major Changes Made for Final Iteration in Comparison to Base Design

a) Tires: Changed from 10R20 having SLR 497mm to 295/90R20 having SLR 513mm.
b) Axle design: Delta change in axle drop is 40mm. Drop of new axle is less than old design.
c) Delta change in Hardpoints: Following are the changes in values of hardpoints,

Hardpoints	Delta change compared to base (Final value – Base Value)	Remark
Bracket Front Pivot	ΔZ= -90mm (-ve refers hardpoint shifted down taking chassis as the reference)	Change due to new suspension design
Spring Shackle	ΔZ= -40mm	Change due to new suspension design
Axle Spring	ΔZ= -15mm	Change due to new suspension & front axle design
Kingpin Centre	ΔZ= -75mm	Change due to front axle design and tire.
Kingpin Axis Ground Intersection	ΔX= +22 mm (+ve for front shift) ΔZ= -75mm	Change due to front axle design and tire.
Steering Rod Stubaxle	ΔZ= -70mm	Basic Changes

d) Changes in variables of leaf spring suspension: Following are the changes in values of variables of leaf spring suspension system,

Variables	Delta change compared to base (Final Value – Base Value)
Flat to Bump	31.7 mm
Flat to Rebound	-39 mm
Flat to Unladen	-54.5 mm
Flat to Laden	-64.6 mm
Flat to overladen	70.4 mm

ME Thesis RISHI SHAH

ORIGINALITY REPORT

5%	3%	2%	1%
SIMILARITY INDEX	INTERNET SOURCES	PUBLICATIONS	STUDENT PAPERS

PRIMARY SOURCES

1	polen.itu.edu.tr Internet Source	2%
2	goaonline.gov.in Internet Source	1%
3	Yahya Oz, Berzah Ozan, Eren Uyanik. "Steering System Optimization of a Ford Heavy-Commercial Vehicle Using Kinematic & amp; Compliance Analysis", SAE International, 2012 Publication	<1%
4	Submitted to University of Bradford Student Paper	<1%
5	John W. Durstine. "The Truck Steering System From Hand Wheel to Road Wheel", SAE International, 1973 Publication	<1%
6	Upendra Kulkarni, Monish M. H. Gowda, Hima Kiran Venna. "Effect of Tie Rod Length Variation on Bump Steer", SAE International, 2016	<1%